TURUN
YLIOPISTO
UNIVERSITY
OF TURKU

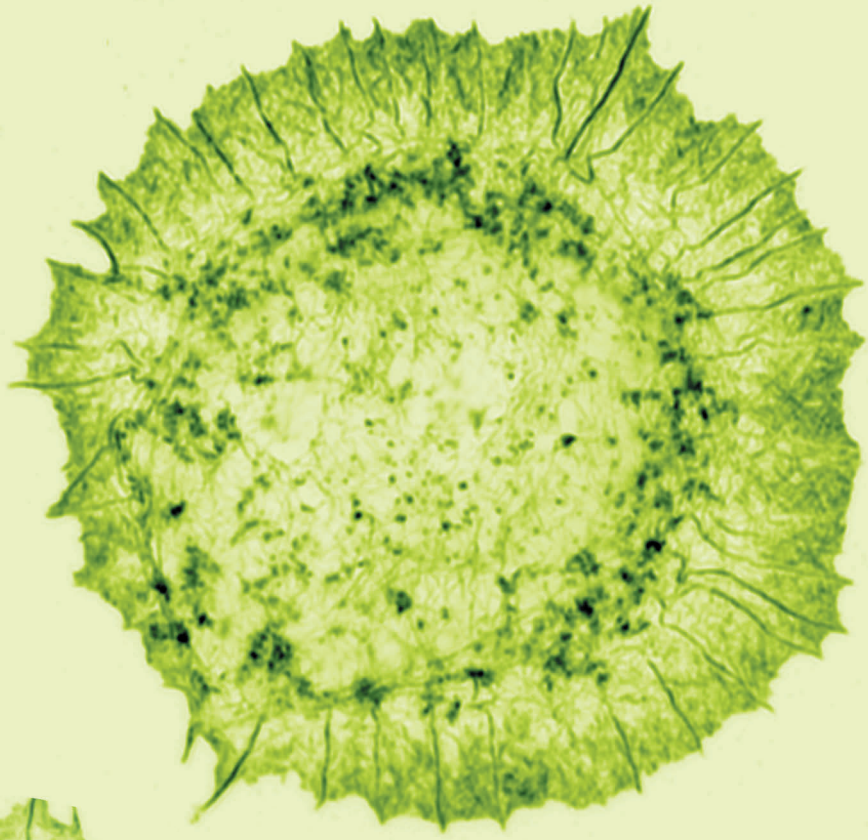

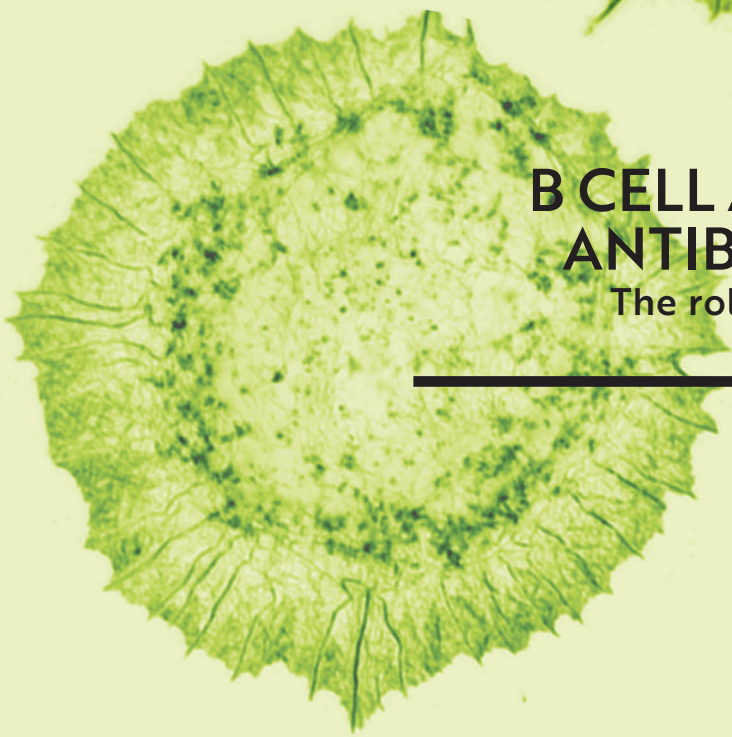

B CELL ACTIVATION AND ANTIBODY RESPONSES

The role of vesicle trafficking and Rab GTPases

Sara Hernández Pérez

TURUN YLIOPISTON JULKAISUJA – ANNALES UNIVERSITATIS TURKUENSIS
SARJA – SER. D OSA – TOM. 1645 | MEDICA – ODONTOLOGICA | TURKU 2022

TURUN
YLIOPISTO
UNIVERSITY
OF TURKU

B CELL ACTIVATION AND ANTIBODY RESPONSES

The role of vesicle trafficking and Rab GTPases

Sara Hernández Pérez

TURUN YLIOPISTON JULKAISUJA – ANNALES UNIVERSITATIS TURKUENSIS
SARJA – SER. D OSA – TOM. 1645 | MEDICA – ODONTOLOGICA | TURKU 2022

University of Turku

Faculty of Medicine
Institute of Biomedicine
Pathology and Immunology
Turku Doctoral Programme of Molecular Medicine (TuDMM)

Supervised by

Docent, Pieta Mattila, PhD
Lymphocyte Cytoskeleton Group
Institute of Biomedicine
University of Turku
Turku, Finland

Reviewed by

Nuria Martínez Martín, PhD
Centro de Biología Molecular Severo Ochoa (CBMSO-CSIC)
Madrid, Spain

Leonardo de Almeida Souza, PhD
Helsinki Institute of Life Science (HiLIFE) University of Helsinki
Helsinki, Finland

Opponent

Balbino Alarcón, PhD
Centro de Biología Molecular Severo Ochoa (CBMSO-CSIC)
Madrid, Spain

The originality of this publication has been checked in accordance with the University of Turku quality assurance system using the Turnitin OriginalityCheck service.

Cover Image: Sara Hernández Pérez

ISBN 978-951-29-8921-8 (PRINT)
ISBN 978-951-29-8922-5 (PDF)
ISSN 0355-9483 (Print)
ISSN 2343-3213 (Online)
Painosalama, Turku, Finland 2022

“Success is not the key to happiness. Happiness is the key to success.
If you love what you are doing, you will be successful.”
- Albert Schweitzer

UNIVERSITY OF TURKU
Faculty of Medicine
Institute of Biomedicine
Pathology and Immunology
SARA HERNÁNDEZ PÉREZ: B Cell Activation and Antibody Responses
Doctoral Dissertation, 190 pp.
Turku Doctoral Programme of Molecular Medicine (TuDMM)
August 2022

ABSTRACT

B lymphocytes are an important part of the adaptive immune system. As one of their main functions, B cells can recognise specific antigens via their B cell receptor and produce antibodies that help clear infections. In T-dependent antibody responses, B cells need to uptake protein antigens and degrade them in specialised and highly regulated intracellular vesicles. The resulting peptides will be loaded onto the Major Histocompatibility Complex II (MHCII) and presented to the T lymphocytes to fully activate the immune response. Hence, precise coordination of vesicular trafficking is essential for antigen processing and presentation. However, how these processes are coordinated remains poorly understood.

This thesis focused on the characterisation of the antigen processing routes in B lymphocytes and the role of the small GTPase Rab8a, a vesicle regulator, in the B cell immune response. First, we followed the traffic of the antigen in mouse B cells and studied its colocalisation with different endosomal markers using high-end microscopy. This allowed us to identify a population of highly dynamic and heterogenous vesicles with degradative capacity. These vesicles, termed early MHCII compartments (eMIIC), also contained MHC II internalised from the cell surface and its chaperone H2-M, indicating that eMIIC could readily process and present uptaken antigens with remarkable efficiency. Second, we developed a specific hybridisation internalisation probe (SHIP) assay that allowed for the precise imaging of internalised antigen in B lymphocytes. Third, we investigated the role of Rab8a in B cell biology for the first time using conditional Rab8a knock out mice. Interestingly, despite of its localization to antigen vesicles, Rab8a deficiency did not alter antigen internalisation, processing or presentation. Instead, it caused increased antibody responses *in vivo*. Our work demonstrates that Rab8a regulates the antibody responses, although the molecular mechanisms remain to be discovered. Overall, this thesis contributes to the understanding of the antigen processing route and the role of an uncharacterised Rab GTPase, Rab8a, in B lymphocytes.

KEYWORDS: adaptive immunity, B cells, BCR signalling, antibody responses, Rab GTPases, Rab8, vesicle traffic, antigen processing, microscopy

TURUN YLIOPISTO
Lääletoeteellinen tiedekunta - Biolääketieteen laitos
Patologia ja Immunologia
SARA HERNÁNDEZ PÉREZ: B-soluaktivaatio ja vasta-ainereaktio – Kalvorakkulaliikenteen ja Rab GTPaasien rooli
Väitöskirja, 190 s.
Turun Molekyylilääketieteen tohtoriohjelma (TuDMM)
Elokuu 2022

TIIVISTELMÄ

B-(lymfosyytti)soluilla on tärkeä tehtävä elimistön mukautuvan immuunijärjestelmän toiminnassa. B-solujen yhtenä päätehtävänä on tunnistaa spesifisiä antigeenejä B-solureseptoriensa (BCR) avulla ja tuottaa vasta-aineita, jotka auttavat parantamaan infektioita. T-soluvälitteisissä vasta-ainereaktioissa B-solut ottavat sisäänsä proteiiniantigeenin ja hajottavat sen erikoistuneissa ja tarkoin säädellyissä solunsisäisissä kalvorakkuloissa. Prosessissa syntyvät peptidit ladataan MHCII-komplekseihin ja esitellään T-soluille täyden immuunivasteen aktivoimiseksi. Siten kalvorakkulaliikenteen tarkalla säätelyllä on merkittävä rooli antigeenin prosessoinnissa ja esittelyssä. Mekanismeja, joiden avulla näitä tapahtumasarjoja B-soluissa säädellään, tunnetaan kuitenkin tällä hetkellä huonosti.

Tämä työ keskittyi karakterisoimaan antigeenin prosessointireittejä B-soluissa sekä selvittämään Rab8-kalvorakkulasäätelijän roolia B-soluvälitteisessä immuunipuolustuksessa. Aluksi seurasimme antigeenin ottamista solun sisälle ja sen paikallistumista erilaisiin kalvorakkuloihin moderneja kuvantamistyökaluja käyttäen. Identifioimme antigeenin erittäin dynaamisissa ja heterogeenisissä kalvorakkuloissa, joilla oli kapasiteettia myös antigeenin hajottamiseen. Nämä nopeasti muodostuvat kalvorakkulat sisälsivät myös solun pinnalta tulleita MHCII kompleksejа, sekä MHCII kompleksin tarvitsemaa esiliina-proteiinia H2-M; tämä tulos viittaa näiden kalvorakkuloiden mahdollisuuteen prosessoida antigeenia esiteltäväksi hyvin nopeasti. Toisessa työssä kehitimme hybridisoituvaa internalisaatio-koetinta käyttävän protokollan, jonka avulla voidaan poistaa solun pinnalla olevan antigeenin taustasignaali ja täten kuvantaa ainoastaan solun sisälle otettua antigeenia. Lopuksi tutkimme Rab8-proteiinin roolia B-soluissa käyttäen konditionaalista Rab8a-poistogeenistä hiirimallia. Työn tulokset osoittivat, että Rab8a lokalisoitui antigeenia sisältäviin kalvorakkuloihin mutta sen puute ei vaikuttanut antigeenin sisään ottamiseen, prosessointiin tai esittelyyn. Sen sijaan Rab8a:n puuttuminen B-soluista lisäsi hiirissä muodostuvaa vasta-ainereaktiota. Työmme osoitti, että Rab8a kontrolloi vasta-ainetuotantoa, mutta molekyylitason mekanismien selvittäminen vaatii vielä lisätutkimuksia. Tämä lopputyö laajentaa ymmärrystämme antigeenien prosessointireiteistä B-soluissa sekä aiemmin karakterisoimattoman Rab GTPaasin, Rab8a:n, roolista.

AVAINSANAT: mukautuva immuniteetti, B-solu, BCR-signalointi, vasta-ainetuotanto, Rab GTPaasit, Rab8, kalvorakkulaliikenne, antigeenin prosessointi, mikroskooppi

Table of Contents

Abbreviations

APC	Antigen-presenting cell
Ag	Antigen
AID	Activation-induced cytidine deaminase
ARC	Antigen-retaining cell
ASC	Antibody-secreting cell
BCAP	B cell adaptor for PI3-kinase
BCR	B cell receptor
BLNK	B cell linker
BM	Bone marrow
Btk	Burton´s tyrosine kinase
CARE	Content-aware image restoration
CatS	Cathepsin S
CD	Cluster of differentiation
CDE	Clathrin-dependent endocytosis
CGG	Chicken gamma globulin
CIE	Clathrin-independent endocytosis
CIIV	Class II vesicles
CR	Complement receptor
CRAC	Calcium release-activated calcium channel
CSR	Class switch recombination
CTV	Cell trace violet
DAG	Diacylglycerol
DAMP	Damage-associated molecular patterns
DC	Dendritic Cell
EE	Early endosome
EF	Extrafollicular
ELISA	Enzyme-linked immunosorbent assay
ELISpot	Enzyme-linked immunospot
eMIIC	early MHC II Compartment
ER	Endoplasmic reticulum
Fab	Fragment antigen-binding

Fc	Ig constant region (fragment, crystallizable)
FcR	Fc receptor
FCS	Fetal calf serum
FDC	Follicular dendritic cell
FHL	Familial Hemophagocytic Lymphohistiocytosis
FIP	Fluorescent Internalisation Probe
FO	Follicular
FoxO	Forkhead box protein O
GAP	GTPase-activating proteins
GC	Germinal centre
GDI	Guanine dissociation inhibitor
GDP	Guanosine diphosphate
GEF	Guanine nucleotide exchange factor
GS	Griscelli syndrome
GTP	Guanosine triphosphate
GTT	Geranylgeranyl transferase
HEL	Hen egg lysozyme
HPS	Hermansky-Pudlak syndrome
IFN	Interferon
IFT	Intraflagellar transport
Ig	Immunoglobulin
Ii	Invariant chain
IKK	IκB kinase
IL	Interleukin
IP_3	Inositol 1,4,5-trisphosphate
IS	Immune Synapse
ITAM	Immunoreceptor Tyrosine-based Activation Motif
KLH	Keyhole limpet hemocyanin
KO	Knock out
LE	Late endosome
LPS	Lipopolysaccharide
MAPK	Mitogen-activated protein kinase
MHC	Major Histocompatibility Complex
mIg	Membrane-bound Ig
MIIC	MHC II Compartment
mTOR	Mammalian target of rapamycin
MZ	Marginal zone
NFAT	Nuclear factor of activated T cells
NFkB	Nuclear factor κ-light-chain-enhancer of activated B cells
NK	Natural Killer

OVA	Ovalbumin
PAMP	Pathogen-associated molecular patterns
PC	Plasma cells
PH	Pleckstrin homology
PI3K	Phosphatidylinositol-3 kinase
PIP_2	Phosphatidylinositol 4,5-bisphosphate
PIP_3	Phosphatidylinositol 3,4,5 trisphosphate
PIP5K	Phosphatidylinositol-4-phosphate 5-kinase
PKC	Protein kinase C
PLC	Phospholipase C
PM	Plasma membrane
pMHC II	peptide-MHC II
pNPP	Para-Nitrophenylphosphate
PRR	Pattern recognition receptor
QP	Quenching Probe
Rab	Ras-related in brain
RE	Recycling endosome
REP	Rab escort protein
SCS	Subcapsular sinus
SDCM	Spinning disk confocal microscopy
SE	Sorting endosome
SHIP	Specific hybridization internalization probe
SHM	Somatic hypermutation
SIM	Structure illumination microscopy
SLE	Systemic lupus erythematosus
SLO	Secondary lymphoid organ
SMAC	Supramolecular Activation Cluster
SRRF	Super-resolution radial fluctuations
SSM	Subcapsular sinus macrophage
STED	Stimulated emission depletion
TCR	T cell receptor
TD	T cell-dependent
Th	T helper
TI	T cell-independent
TLR	Toll-like receptor
TM	Transmembrane
WASP	Wiskott-Aldrich syndrome protein
WB	Western blot
WT	Wild type

List of Original Publications

This dissertation is based on the following original publications, which are referred to in the text by their Roman numerals:

I **Hernández-Pérez S***, Vainio M*, Kuokkanen E, Šuštar V, Petrov P, Forstén S, Paavola V, Rajala J, Awoniyi LO, Sarapulov AV, Vihinen H, Jokitalo E, Bruckbauer A, and Mattila PK. B cells rapidly target antigen and surface-derived MHC II into peripheral degradative compartments. *J Cell Sci*., 2019; 133(5):jcs235192 (*equal contribution).

II **Hernández-Pérez S**[#] and Mattila PK[#]. A Specific Hybridization Internalization Probe (SHIP) compatible with super-resolution imaging to study antigen traffic in B lymphocytes. *Sci Rep*, 2022; 12, 620 ([#]corresponding authors).

III **Hernández-Pérez S**, Sarapulov AV, Balci MÖ, Harada A, and Mattila PK. Loss of Rab8a in B cells leads to hyperactive immune responses. *Manuscript.*

1 Introduction

The cells of the adaptive immune system -T and B lymphocytes- carry an overwhelmingly diverse repertoire of receptors. Due to this huge diversity, adaptive immunity is very specific and also known as antigen-dependent immunity (Jackson et al., 2013). B cell activation is triggered by specific antigen binding to the B cell receptors (BCRs) on the cell surface. As one of their main functions, B cells can recognise antigens and produce antibodies that help clear infections (Cooper, 2015). Although B cells can recognise different types of antigens, such as proteins, lipids or polysaccharides, the antibody responses against proteinaceous antigens are the best characterised. Protein antigens are also known as T-dependent antigens, as they trigger a robust T cell response (Allen et al., 2007; Miller and Mitchell, 1968; Mitchell and Miller, 1968).

In T-dependent antibody responses, B cells need to uptake protein antigens and process them into peptides in specialised endosomal compartments. Importantly, BCRs are not only responsible for the signalling but also they need to be internalised together with the antigen to deliver it to the right intracellular compartments for processing (Depoil et al., 2009; Song et al., 1995). The exact nature and origin of antigen-loading compartments are a long-standing debate. Because these compartments are dynamic, their study and classification has been technically challenging. In order to degrade the antigen and load the peptides, these compartments require low pH, loading chaperones (such as H2-M) and proteolytic enzymes (such as cathepsin S) together with the internalised antigen-BCR complexes and MHC II (Adler et al., 2017a; Vascotto et al., 2007a). The resulting peptides will be loaded onto MHC II molecules and presented to the T lymphocytes. Antigen presentation to T lymphocytes is critical for B cell activation, as T cells will provide the stimulus needed for the germinal centre reaction. In the germinal centres, activated B cells undergo several rounds of class switch recombination (CSR) and somatic hypermutation (SHM), leading to the generation of high-affinity class-switched IgG antibodies (De Silva and Klein, 2015; Stavnezer et al., 2008). All these processes rely on the precise and timely coordination of vesicular trafficking, and its dysregulation could lead to exacerbated or insufficient antibody responses.

Since their discovery, small Rab GTPases have been considered one of the main regulators of membrane trafficking, and they define the structural and functional identity of intracellular organelles (Wandinger-Ness and Zerial, 2014; Zerial and McBride, 2001). Rab proteins are regulators of the secretory and endocytic pathways, and they have been widely used as a tool to identify and study different vesicle populations. However, the role of Rab proteins in antigen processing and presentation, as well as antibody production, has not been extensively investigated. Particularly, there are few studies to date describing the role of Rab8 in immune cells, and studies are exceedingly scarce in B lymphocytes. Rab8 is a ubiquitous Rab protein that regulates a plethora of cellular functions in coordination with different effectors. Rab8 has been reported to localise to the endosomal recycling compartment together with Rab11 and Arf6 and to promote the polarized transport of newly synthesised proteins (Hattula et al., 2006). In T lymphocytes, Rab8 is implicated in TCR recycling and final docking to the immune synapse via its interaction with VAMP3 (Finetti et al., 2015b) and participates in the surface expression of CTLA-4 through LAX-TRIM binding (Banton et al., 2014). In macrophages, Rab8a interacts with PI3Kγ in membrane ruffles and early macropinosome membranes and regulates TLR signalling, inflammation and polarisation using the AKT/mTOR pathway (Luo et al., 2014; Luo et al., 2018; Tong et al., 2021; Wall et al., 2017; Wall et al., 2019).

This thesis focused on the characterisation of the antigen processing routes in B lymphocytes and the role of the small GTPase Rab8a in the B cell immune response. First, we tracked the internalisation of the antigen in mouse B cells and analysed its colocalisation with different endosomal markers using high-end microscopy. Second, we developed a specific hybridisation internalisation probe assay that allowed for the precise imaging of internalised antigen in B lymphocytes. Third, we investigated the role of Rab8a in B cell biology for the first time using conditional Rab8a KO mice.

Altogether, the results of this thesis provide new information to the different antigen processing routes in B lymphocytes and demonstrate, for the first time, the regulatory role of Rab8a in antibody production. In addition, this thesis presents a novel use of a specific hybridisation internalisation probe together with live-imaging and super-resolution microscopy to track internalised cargo in cells.

2 Review of the Literature

2.1 Membrane trafficking: a journey through the cell

Cells need a constant income of nutrients and continuous removal of unwanted molecules. All eukaryotic cells are delimited by a plasma membrane (PM) and contain multiple specialised membranous compartments that require constant regulation to maintain cell homeostasis (Redpath et al., 2020). Because of that, *membrane trafficking* (vesicular trafficking; vesicular transport) is one of the most critical processes of the cell. Membrane trafficking controls vital cell functions such as the organisation of cellular reactions and intra- and intercellular communication. Vesicular transport also enables the movement of lipids and proteins between cellular compartments (Stefan et al., 2017). Membrane trafficking, like a highway, can be simplistically illustrated as two major but interconnected roads that shuffle material in opposite directions: one inwards (endocytic pathway) and one outwards (biosynthetic-secretory pathway).

Endocytosis is a highly conserved and active process that regulates nutrient internalisation and maintains or modifies the plasma membrane composition in eukaryotic cells (Scita and Di Fiore, 2010). The endocytosis process consists of the invagination of the plasma membrane and the formation of vesicles through a process of membrane budding and fission. During this process, cells can internalise fluids, molecules, parts of its plasma membrane, particles, and other extracellular components, such as pathogens. Notably, endocytosis is also important in signal transduction, as endocytic pathways integrate diverse stimuli and orchestrate cell signalling (Sorkin and Von Zastrow, 2009). Although novel pathways are emerging, endocytosis has been classically divided into clathrin-dependent endocytosis (CDE), caveolae-dependent or clathrin-independent endocytosis (CIE), macropinocytosis, and phagocytosis, depending on the mechanism of internalisation (Boucrot et al., 2015; Kumari et al., 2010; McMahon and Boucrot, 2011; Watanabe and Boucrot, 2017). The fate of the internalised cargo depends greatly on its nature, the internalisation pathway, as well as the cell type. Most of our knowledge about endocytic pathways came from the study of CDE, the best-characterised pathway (Mettlen et al., 2018). In this pathway, cargo is internalised from the PM into early

endosomes (EEs), a tubulovesicular network also referred to as sorting endosomes (SEs). EE/SEs will sort the cargo back to the PM via recycling endosomes (REs) or mature into late endosomes (LEs) (Sönnichsen et al., 2000). After that, cargo will be transported to the lysosomes or lysosome-related organelles, the primary degradation site in the cell (Delevoye et al., 2019; Gruenberg, 2001; Raposo et al., 2007).

Exocytosis refers to the transport of intracellular proteins to the PM or extracellular environment. Exocytosis is involved, for instance, in membrane growth and repair, the removal of waste products and intracellular communication. Classically, newly synthesised proteins are transported from the ER to the Golgi and to the PM into secretory vesicles (Wu et al., 2014). These vesicles fuse with the PM to deliver proteins such as receptors or to secrete proteins such as cytokines to the extracellular medium (Li et al., 2018; Revelo et al., 2019). The exocytic vesicles deliver not only proteins but also the lipids needed for membrane growth (Holthusen et al., 2015).

In addition to endocytosis and exocytosis, additional pathways, such as polarised transport or autophagy, exist. Importantly, constant cross-talk is needed between these pathways to maintain a tight regulation between the different organelles and intracellular compartments in eukaryotic cells (Derby and Gleeson, 2007). *Autophagy* is a conserved degradative process that targets cytoplasmic material to the lysosomes, helping to maintain cellular homeostasis. This process, consisting on different pathways, can be triggered by many signals, such as organelle damage, nutrient deprivation conditions, or cellular stress (Eskelinen and Saftig, 2009; Mizushima and Komatsu, 2011; Yim and Mizushima, 2020). Importantly, all these pathways play important roles in our immune system, but we are only starting to understand their intricated regulation (Benado et al., 2009; Robbins and Morelli, 2014) (*see also* 2.4 Rab proteins in health and disease).

2.1.1 The Rab protein family

The small GTPase family, also known as the *Ras superfamily*, is a large family of proteins that can bind and hydrolyse guanosine triphosphate (GTP) (Salminen and Novick, 1987; Schmitt et al., 1986; Segev et al., 1988). This family of proteins is structurally and functionally similar to the α-subunit of heterotrimeric G-proteins (Gerwert et al., 2017). The Ras superfamily comprises hundreds of proteins divided into five main families - Ras, Ran, Rho, Rab, and Arf GTPases - based on the protein structure, sequence, and function (Wennerberg et al., 2005). Of these, the Rab (Ras-related in brain) protein family is the largest subfamily. Despite their classical role as membrane regulators, new roles emerge every year; thus, Rab proteins are now considered master regulators of cellular homeostasis (Borchers et al., 2021). Rab GTPases are conserved from yeast to humans and have been found in all eukaryotes, pointing to an important and conserved role in the cell (Zerial and McBride, 2001).

Approximately 70 Rab GTPases have been found in mammals, of which more than 60 are present in humans. Rab GTPases have been recently divided into small (Rab1 to Rab43) and large (Rab44, 45, and 46) Rab GTPases. The large Rab GTPases have been recently discovered, and their functions are currently being investigated (Srikanth et al., 2017; Tsukuba et al., 2021; Wang et al., 2019; Yamaguchi et al., 2018). Hence, I will focus here only on the small Rab proteins.

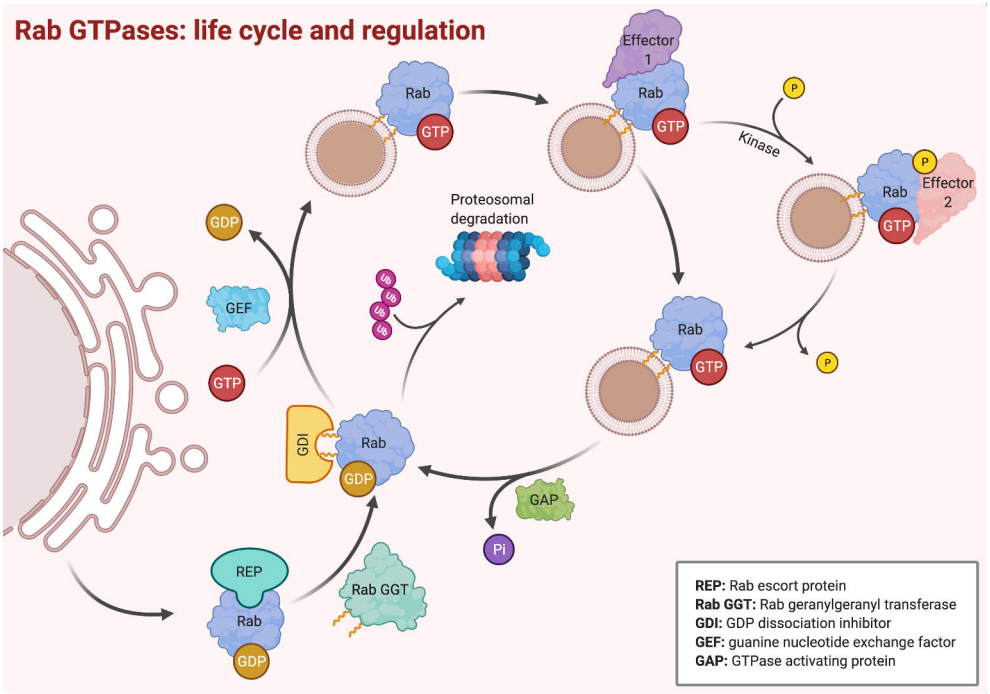

Figure 1. Rab GTPases: life cycle and regulation. Schematics of the Rab GTPase regulation process.

Since their discovery, *small Rab proteins* (20-25 kDa) have been considered one of the main hubs for membrane trafficking (Li and Marlin, 2015; Stenmark, 2009). Among all the different Rabs, the best-characterised proteins are the ubiquitous Rab4, Rab5, Rab6, Rab7 and Rab11. Rabs are regulators of the secretory and endocytic pathways, and they define the structural and functional identity of intracellular organelles by targeting different membrane compartments (Barr, 2013). Because of that, Rab proteins have been widely used as a tool to identify, follow, and modify intracellular compartments using fluorescently labelled wild-type or mutant Rab proteins. In addition, every Rab protein can interact with different effectors, controlling factors such as signal transduction, protein and lipid composition of the membrane, vesicle motility, budding, tethering and fusion

between distinct compartments (Stenmark, 2009; Stenmark and Olkkonen, 2001; Zerial and McBride, 2001). In some cases, effectors can be shared between various members of the Rab family, adding additional complexity to the signalling hubs (Grosshans et al., 2006).

Due to their essential role in vesicle trafficking, Rab proteins have different regulatory steps to achieve functional fine-tuning (**Figure 1**). Like other GTPases, Rab proteins alternate between an "on" GTP-bound and an "off" GDP-bound state. This reversible mechanism, tightly coordinated, allows them to function as molecular switches. The function of the Rab proteins is additionally regulated by their location dependent on prenylation (Chavrier et al., 1991; Leung et al., 2006; Shen and Seabra, 1996; Ullrich et al., 1993), phosphorylation (Lai et al., 2015; Steger et al., 2016; Steger et al., 2017; Xu et al., 2021), other post-translational modifications such as ubiquitination (Shinde and Maddika, 2018) and even by mRNA compartmentalisation (Mili et al., 2008).

Newly synthesised Rabs are first associated with a Rab escort protein (REP). The Rab-REP complexes are recognised by a Rab geranylgeranyl transferase (Rab GGT or RabGGTase) that prenylates one or two cysteines in the Rab C-terminal motif (-CAAX, -XXCC, -XCXC and -CCX) (Baron and Seabra, 2008). After prenylation, REP is recycled, and the inactive (GDP-bound) prenylated Rabs are associated with a guanine dissociation inhibitor (GDI) in the cytosol. In order to get activated, GDP has to be exchanged with GTP. First, GDI is released with the help of a GDI-displacement factor (GDF). Then, the exchange can be facilitated by one or more guanine nucleotide exchange factors (GEFs) (Barr and Lambright, 2010). The high cytosolic concentration of GTP ensures that GTP binds to Rab as soon as GDP has been released. Once in their active GTP-bound form, Rab proteins can target their specific organelle membrane and recruit a vast number of signalling partners and downstream effectors (Mizuno-Yamasaki et al., 2012). To terminate their activity, conversion from the GTP- to the GDP-bound form through GTP hydrolysis is needed. GTP conversion to GDP is not only driven by the GTPase activity of the Rab protein itself but with the help of GTPase-activating proteins (GAPs) (Nottingham and Pfeffer, 2009). Once in the GDP-bound form, the protein is ready to start a new cycle (Voss et al., 2019).

2.2 The immune system

Despite extensive research over the years, we are still far from fully understanding the whole complexity of our immune system. The *immune system* refers to a group of very different cells with various functions (**Figure 2**) and chemical and physical barriers that protect our body from the inside and the outside (Nicholson, 2016). The study of the immune system started over a hundred years ago, and the vertebrate immune system has traditionally been divided into two subsystems: innate immunity

and adaptive immunity (Flajnik and Kasahara, 2010). However, these two systems should be regarded as a duality rather than a dichotomy, as "the roots of adaptive immunity are buried deep in the soil of the innate immune system that preceded it" (Beutler, 2004), and both systems work intimately to clear the threats (Hillion et al., 2020; Iwasaki and Medzhitov, 2015; Stögerer and Stäger, 2020).

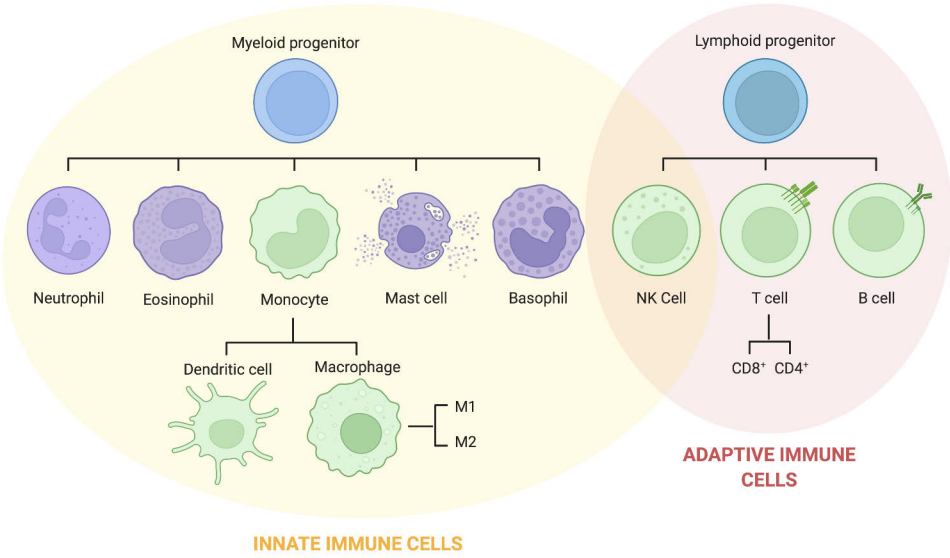

Figure 2. Cells of the immune system. White blood cells, or leukocytes, can be divided into granulocytes (in purple) and agranulocytes (monocytes and lymphocytes, in green). Common progenitors are shown in blue.

2.2.1 Innate immune system

The *innate immune system* is the first and evolutionarily older line of defence that our body has against a wide variety of pathogens (Gourbal et al., 2018). This form of immunity, often referred to as antigen-independent or non-specific, is in-born and protects the host from the invading pathogens from the first encounter. Compared to adaptive immunity, the innate responses are faster, but in order to gain speed, specificity needs to be sacrificed. Although the innate immune responses do not generate immunological memory to the same extent as the adaptive responses, the system does possess a certain degree of adaptability or "memory", termed trained immunity (Netea et al., 2011).

The arsenal of innate immunity counts with four different "weapons" or lines of defence: an anatomical barrier (skin and mucous), a physiological barrier (such as low pH and lysozymes), a cytokine barrier or inflammatory response, and the cellular barrier (Gallo and Nizet, 2008; Paludan et al., 2020). The inflammatory response is

a defence mechanism rapidly initiated after a breach of the anatomic and physiological barriers. The release of inflammatory chemicals helps recruit the innate immune cells: macrophages, neutrophils, eosinophils, basophils, mast cells, monocytes and natural killer (NK) cells (Duque and Descoteaux, 2014; Gasteiger et al., 2017; Moretta et al., 2007). These cells rely on germline-encoded pattern recognition receptors (PRRs) that recognise pathogen-associated molecular patterns (PAMPs) and damage-associated molecular patterns (DAMPs) to detect pathogens and tissue damage (Bianchi, 2007; Janeway, 1989). Stimulation of these receptors by microbial products leads to the expression of inflammatory cytokines. Hence, the innate immune system has emerged as a key regulator of inflammation. Proper inflammatory responses protect the body against infections, but chronic dysregulation is related to a wealth of diseases (Dinarello et al., 2012).

2.2.2 Adaptive immune system

The *adaptive immune* system has developed relatively recently - 500 million years ago - and it is only found in higher vertebrates and jawed fish (Flajnik and Kasahara, 2010). In contrast to the limited number of PRRs, the cells of the adaptive immune system, lymphocytes carry an overwhelmingly diverse repertoire of receptors (Goldrath and Bevan, 1999; Jackson et al., 2013; Trück and van der Burg, 2020). Hence, this second line of defence is, compared to innate immunity, much slower but also more specific. Because of that, it is also known as antigen-dependent immunity. Adaptive immunity is of vital importance when the innate system fails to eliminate the potential threat. In addition to that, it is also responsible for distinguishing self and non-self-antigens, as well as for the generation of immunological memory (Ratajczak et al., 2018).

There are two types of adaptive immune responses: humoral or antibody responses and cell-mediated responses. *Humoral immune responses* are carried out by B cells that secrete five major types of antibodies, each with a different biological function: IgM, IgD, IgG, IgA and IgE (Cancro and Tomayko, 2021). On the other hand, T lymphocytes are in charge of the *cell-mediated responses*.

2.2.2.1 Antigen-presenting cells

Antigen-presenting cells (APCs), defined as cells that present peptide antigens in the context of the Major Histocompatibility Complex (MHC), can be classified into two different categories: non-professional and professional APCs (Sprent, 1995). All nucleated cells in our body express MHC class I (MHCI) on the cell surface and are considered *non-professional APCs* (Nakayama, 2015). These cells can present peptide fragments derived from intracellular proteins, such as cytosolic antigens degraded by

the proteasome. Cytosolic antigens have two main origins: self-antigens (i.e., tumour antigens) or intracellular pathogen antigens (i.e., viral antigens). These peptides presented in the context of MHCI are recognised by $CD8^+$ T cells, or cytotoxic T cells, that will proceed to the elimination of the presenting cell (Hewitt, 2003). *Professional APCs*, or MHC class II (MHC II)-restricted APCs, include B cells, dendritic cells (DCs) and macrophages (Roche and Furuta, 2015; Vyas et al., 2008). These cells are highly specialised in presenting internalised antigens, taken up through phagocytosis, fluid-phase pinocytosis or receptor-mediated endocytosis, to $CD4^+$ or helper T cells (Th). These antigens are degraded by lysosomal proteolysis, and the digested peptides are presented on their surface bound to MHC II, together with co-stimulatory molecules. MHC II expression is highly regulated, transcriptionally and post-transcriptionally, in APCs (Chen and Jensen, 2008; Sprent, 1995).

In addition, a third group of commonly termed antigen-presenting cells differs from the previous two. These cells, such as follicular dendritic cells (FDCs), do not present antigen peptides but retain and display intact antigen on their cell surface independent of MHC, often as antigen-antibody complexes or opsonised antigens (Heesters et al., 2014). This type of presentation will be referred to as *antigen-retaining cells* (ARCs) throughout the text to avoid confusion.

2.3 B lymphocytes

B lymphocytes, or B cells, are a subtype of white blood cells or leukocytes (*see* **Figure 2**). Despite their small size (5-7 μm), they are mighty cells that occupy a unique niche in the adaptive immune system, as they play a central role in humoral immunity. Although B cells are often studied with a focus on antibody production against specific antigens, they can also perform a number of antibody-independent functions (reviewed in Upasani et al., 2021). Their name originated from the fact that they were first discovered in birds, inside a hindgut lymphoid organ called the bursa of Fabricius ("B" from bursa), where their maturation takes place (Glick, 1955; Glick, 1956; Glick et al., 1956). In mammals, however, they develop from stem cells to immature B cells in the bone marrow (BM), where they undergo two different types of selection: positive and negative selection (Pieper et al., 2013).

At any given time, most of the B cells in our body are found in the stroma of the secondary lymphoid organs (SLOs), where they spend most of their life. Naïve mature B cells constantly circulate through the secondary lymphoid organs (SLOs), scanning for possible threats (*see* 2.3.3 Antigen recognition). In order to recognise antigens and produce antibodies, B cells express specific antigen receptors, termed B cell receptors (BCRs), only present in these cells. The BCR is a clonal and highly specialised immune receptor that possesses an immense somatic diversity, hypothetically recognising every possible antigen, either in soluble form or presented

on the surface of other cells. Via antigen recognition, B cells can orchestrate other branches of the immune response and produce antibodies against that specific antigen. In numbers, the BCR is the most abundant receptor on the B cell surface, having 100.000-300.000 copies per cell (Mattila et al., 2013; Yang and Reth, 2010) and the total theoretical diversity of its repertoire is estimated to be 10^{11}-10^{13} (Calis and Rosenberg, 2014; Trepel, 1974). Once activated in the SLOs, B cells will differentiate into long-lived memory B cells or antibody-secreting plasma cells.

2.3.1 T-dependent and T-independent antibody responses

One of the key features of the adaptive immune system is the capacity to produce a robust humoral response in the form of secreted antibodies, providing life-long protection to the host (Cancro and Tomayko, 2021). Historically, antibody responses have been studied and categorised with a focus on the *type of antigen*, mainly employing murine models. Animals are often immunised with a small molecule or hapten, such as DNP, TNP, NP, NIP or phosphorylcholine able to elicit the production of antibodies when coupled to a carrier (**Table 1**). Antibody responses against such haptens have been well-characterised in the past (Jacob et al., 1991; McHeyzer-Williams et al., 1993; Takahashi et al., 1998). In the late 60s, a series of experiments conducted with neonatally thymectomised mice showed that some antigens could produce an antibody response even in the absence of the thymus and, therefore, in the absence of T cells (Miller and Mitchell, 1968; Mitchell and Miller, 1968). Based on these early experiments, the antibody responses were classified as *T-dependent* (TD) or *T-independent* (TI).

Proteinaceous or TD antigens can trigger a robust T cell response, particularly relevant for the germinal centre response (*see* 2.3.2 The germinal centre reaction), leading to the generation of high-affinity class-switched IgG antibodies (Allen et al., 2007). On the other hand, responses to non-proteinaceous or TI antigens tend to produce a milder response secreting low-affinity IgM antibodies. Most TI antigens are large, multivalent molecules that are able to highly crosslink membrane immunoglobulins (TI-2) or polyclonal activators (TI-1), causing high levels of B cell activation (Mond et al., 1995a; Mond et al., 1995b). TD activation is, compared to TI activation, often considered more desirable, especially for vaccine design, due to the increased affinity of the antibodies produced during TD responses, as well as the induction of T cell-dependent responses (Gilbert, 2012; Pollard and Bijker, 2020). Nonetheless, all bacterial, viral and fungal pathogens carry TI antigens on their surface to some extent, so the importance of TI responses should not be neglected. Indeed, TI responses are considered by some authors as a bridge between the innate response and the adaptive immune response (Cerutti et al., 2013). The information given in the following chapters is discussed in the context of TD responses unless specified otherwise.

Table 1. Summary of the T-dependent (TD) and T-independent type 1 and 2 (TI-1 and 2) antibody responses: most common antigens used for immunisation, main subset of B cells responding to the antigens, main antibody isotypes and affinity and typical response time after immunisation. KLH: Keyhole limpet hemocyanin. CGG: chicken gamma globulin. LPS: lipopolysaccharide. FO: follicular. MZ: marginal zone. SMH: somatic hypermutation. CSR: class-switch recombination.

Response	Carriers	Features	Subsets responding	Antibody affinity	Time
TD	Protein (KLH, CGG)	BCR-specific antigen	FO B cells	High-affinity SHM and CSR	Days to weeks
TI-1	LPS	Polyclonal activation	B-1 and MZ B cells	Low-affinity IgM or IgG3	Hours to days
TI-2	FICOLL	BCR crosslinking	B-1 and MZ B cells	Low-affinity IgM or IgG3	Hours to days

2.3.2 The germinal centre reaction

In order to produce antibodies, antigen-activated B cell need to differentiate into antibody-secreting cells (ASCs) (Tellier and Nutt, 2019). From the anatomical perspective, antibody responses and B cell differentiation can follow two distinct pathways: germinal centre (GC) or extrafollicular (EF) responses. GCs are highly organised and transient cellular microenvironments formed predominantly in TD responses in peripheral secondary lymphoid organs (Arulraj et al., 2021; Berek et al., 1991; Young and Brink, 2021). Germinal centres form within the follicles in the SLOs and are mostly comprised of naïve B cells (IgM^+, IgD^+) (**Figure 3**). A high concentration of TI antigens can also lead to the formation of GCs, but unlike TD antigens, the GC formation peaks in the first few days, followed by a sharp decrease due to the absence of T cell help (García De Vinuesa et al., 2000; Lentz and Manser, 2001). In the germinal centres, activated B cells undergo several rounds of class switch recombination (CSR) and somatic hypermutation (SHM) to produce high-affinity antibodies (De Silva and Klein, 2015). Because of that, germinal centres have received a great deal of attention, leaving other responses such as the EF responses not as well characterised. The contribution of EF responses to the immune system should not be disregarded, as dysregulated survival of EF B cells can lead to autoimmune diseases due to increased levels of autoantibodies (Ehlers et al., 2006; Enzler et al., 2006; Guinamard et al., 2000; Herlands et al., 2007; Zhou et al., 2011). The majority of the EF responses in the spleen are produced by marginal zone (MZ) B cells in response to TI antigens and can generate memory to provide a long-lasting response against bacterial and viral infections (Hsu et al., 2006; Obukhanych and Nussenzweig, 2006).

Following the initial antigen encounter, the formation of a mature GC starts. There, B cells undergo SHM, a random process of mutation of the genes encoding

their antigen-specific BCR in order to increase their affinity. Regulation of the GC reaction and SHM is thus critical and mutated B cells need to be selected to avoid the emergence of autoreactive B cell clones, while maintaining those clones that possess the highest affinity for the foreign antigen (Arulraj et al., 2021; De Silva and Klein, 2015). This is achieved by several rounds of competition between the different B cell clones inside the GC (Liu et al., 1989). In addition to SHM, B cells in the GC also undergo CSR. CSR, or isotype class-switching, is an intrachromosomal DNA recombination process that changes (switches) the antibody isotype (Chen and Wang, 2021; Stavnezer et al., 2008). During this process, the antigen specificity does not change, as only the IgM/IgD constant region (Ig heavy-chain locus) is replaced by the IgG, IgA or IgE constant region, awarding new effector functions. Although CSR has been considered a hallmark of GCs together with SHM, CSR can be detected in some models even two days after immunisation, suggesting that this process could be independent of GC formation (Jacob et al., 1991; Pape et al., 2003; Roco et al., 2019; Toellner et al., 1996).

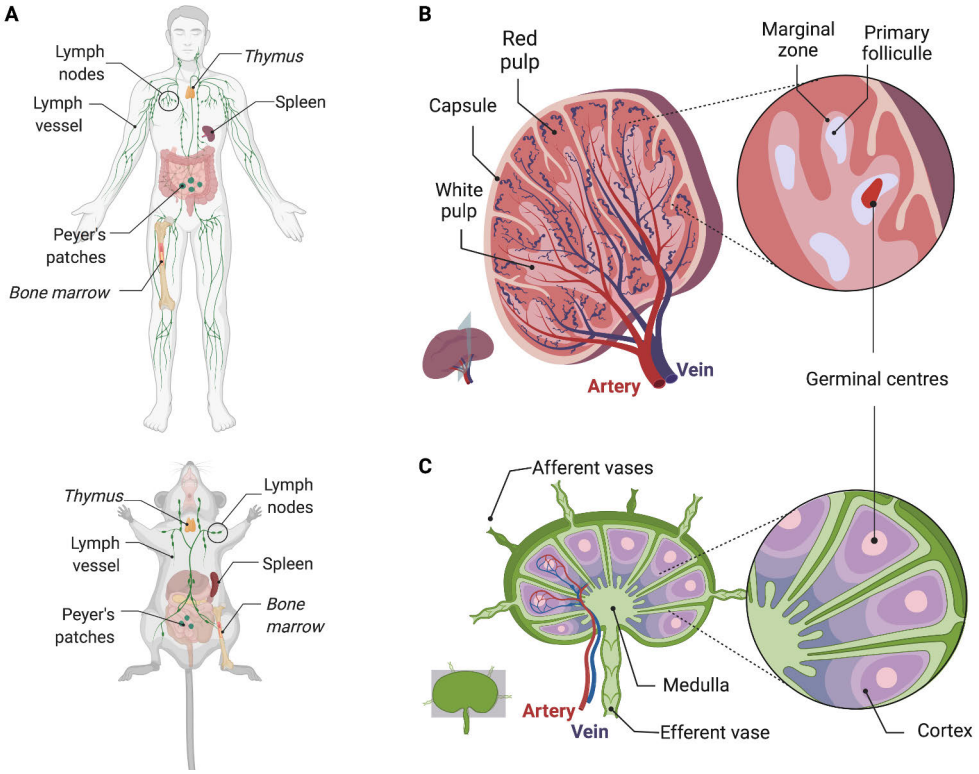

Figure 3. Primary and secondary lymphoid organs in human and mouse. (**A**) Lymphoid organs. Primary lymphoid organs in italics, secondary organs regular font. (**B, C**) Sections of the (B) spleen and (C) lymph nodes.

Ultimately, B cell activation in the GCs leads to the induction of ASCs and memory B cells (Takemori et al., 2015). ASCs are specialised B cells that differentiate from activated B cells and represent the end-stage of B lymphocytes. As antibodies in the serum possess a short half-life, ASCs need to actively secrete antibodies in order to maintain measurable levels in the blood (Vieira and Rajewsky, 1988). These cells are rare and comprise different populations: plasmablasts and plasma cells (PC; short-lived and long-lived). Plasmablasts are short-lived cells that appear early in the immune response in high numbers, and hence produce antibodies of low affinity against TD or TI antigens. On the other hand, PCs are a rarer subset of ASCs with exceptionally long life (Nutt et al., 2015; Tellier and Nutt, 2019). Long-lived PCs, together with memory B cells, contribute to the maintenance of immunity. Memory B cells are the cornerstone of the secondary immune responses. After reinfection with a known pathogen, memory B cells will rapidly elicit an antibody response to help clearing the pathogen in a faster and more efficient way (Good et al., 2009; Tarlinton and Good-Jacobson, 2013). Importantly, immune memory is also key for successful vaccination strategies.

2.3.3 Antigen recognition

B cell activation, understood here as activation via the BCR, is triggered by specific antigen binding to the BCRs on the cell surface (*see* 2.3.5 BCR signalling pathways). Antigen recognition occurs in the follicles of the SLOs (**Figure 3**). BCRs can bind soluble or membrane-bound antigens, but it has been shown that membrane-bound antigen recognition is more efficient *in vivo* (Carrasco and Batista, 2006a; Carrasco and Batista, 2006b). Small, soluble antigens (< 70 kDa) can passively penetrate the SLOs from the peripheral tissues via the afferent vessels of the lymph nodes or the trabecular artery in the spleen and reach the follicular B cells within 2 hours (Gretz et al., 2000; Pape et al., 2007; Roozendaal et al., 2009). On the other hand, larger antigens that cannot passively diffuse, such as opsonised antigens or immune complexes, are captured by ARCs in the SLOs. The ARCs, such as FDCs, subcapsular sinus macrophages ($CD169^{+}$), medullary macrophages or DCs, will retain and display these antigens to the B cells via their complement (CR1/CD35, CR2/CD21) or Fc (CD16/32) receptors (Carrasco and Batista, 2007; Phan et al., 2007; Suzuki et al., 2009). Recognition of the surface-bound antigen triggers the formation of an immune synapse between the B cell and the ARC (*see* 2.3.4 The immune synapse). Hence, antigen capture by these cells plays a crucial role in the GC reaction, SHM and affinity maturation, greatly contributing to the B cell-mediated immune responses, especially when the amount of antigen is limited. The role of FDCs and SCS macrophages in this process has long been known (Heesters et al., 2015; Klaus et al., 1980; Tew et al., 1980), but recently other types of cells, such as conventional DCs, have also been implicated in the presentation of native

antigen to B cells (Bergtold et al., 2005; Heath et al., 2019; Wykes et al., 1998). Interestingly, B cells themselves can also contribute to this process, as non-cognate B cells can enhance antigen capture by opsonisation and transfer these complexes to FDCs in the spleen and the lymph nodes (Cinamon et al., 2008; Ferguson et al., 2004; Roozendaal et al., 2009; Youd et al., 2002).

2.3.4 The immune synapse

The immune synapse or immunological synapse (IS) is a specialised cell-cell interaction platform that was first reported in T cells interacting via their TCRs with the pMHC II displayed by APCs (Dustin and Shaw, 1999; Grakoui et al., 1999; Monks et al., 1998; Shaw and Dustin, 1997). Shortly after that, the formation of this structure was also observed in NK cells (Davis et al., 1999). It was shown already in the early 90s that B cells can recognise both soluble antigens and antigens attached to the surface of neighbouring ARCs in the SLOs (Hartley et al., 1991; Koopman et al., 1991) and the BM (Russell et al., 1991). However, it was not until ten years later that Batista and colleagues demonstrated that B cells could also form an IS (Batista et al., 2001). It is important to note that B cells recognise the native antigen displayed on the surface of ARCs via their BCRs instead of recognising processed peptides as T cells do.

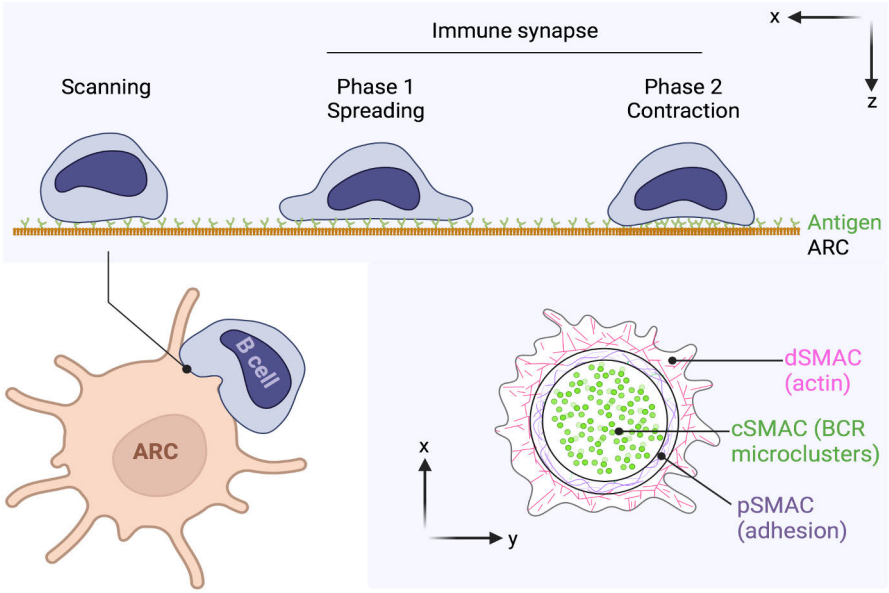

Figure 4. Formation of the immunological synapse: phases and subcellular organization. B cells encounter the antigen on the surface of antigen-retaining cells (ARCs) in the secondary lymphoid organs. Upon antigen recognition via the BCR, the formation of the IS begins. The schematic image represents the two phases of the IS formation (spreading and contraction; lateral view) and the organization of the mature IS (bottom view).

Since then, numerous studies have addressed both the structure and the function of the IS in B cells from different perspectives and employing a breadth of techniques. The formation of the IS is a mechanical process and a critical step for B cell activation, as it has been described that membrane-bound antigens are more efficiently recognised *in vivo*, allowing affinity discrimination and potentially lowering the threshold for B cell activation (Carrasco, 2010; Carrasco and Batista, 2006a; Carrasco and Batista, 2006b; Depoil et al., 2008; Depoil et al., 2009; Fleire et al., 2006; Natkanski et al., 2013). Moreover, the IS has been described as a platform not only for signalling and activation but also for antigen acquisition and degradation, highlighting its importance in the B cell immune response. From the structural point of view, the IS is well characterised (**Figure 4**). A mature IS can be divided into different Supramolecular Activation Clusters (SMAC): the central SMAC (cSMAC), the peripheral SMAC (pSMAC) and the distal SMAC (dSMAC) (Calvo and Izquierdo, 2021; Le Floc'H and Huse, 2015). Following antigen stimulation, the focal signalling sites or signalosomes start to form at the plasma membrane. These signalosomes are assemblies of microclusters of 50-500 BCR complexes together with the proximal tyrosine kinases that will initiate the BCR signalling cascades (*see* 2.3.5 BCR signalling pathways) (Avalos and Ploegh, 2014; Depoil et al., 2008; Depoil et al., 2009; Fleire et al., 2006).

In order to achieve full activation, the signalling and the actin cytoskeleton need to be tightly regulated, and a very intricate relationship exists between the two: cytoskeleton organisation can regulate signalling triggering, and signalling regulates the reorganisation of the cytoskeleton (Arana et al., 2008; Burbage et al., 2015; Li et al., 2019; Mattila et al., 2013). After antigen binding and recognition, B lymphocytes exhibit a two-phase response: first, B cells start spreading and scanning the antigen found on the surface of the ARC, followed by a contraction phase that will gather the antigen in the centre of the synapse. In order to spread efficiently, a first wave of actin depolymerisation is needed (Freeman et al., 2011). During the spreading phase, as many BCRs as possible are engaged by antigen. This phase lasts for 2-10 minutes, followed by a contraction phase (Fleire et al., 2006). During the contraction phase, the incipient synapse is reorganised, leading to the formation of a mature immune synapse. In the mature synapse, the BCR microclusters converge toward the centre of the synapse, forming the cSMAC, while the integrins form an adhesion ring called pSMAC and the actin concentrated in the dSMAC. The contraction phase is both actin and microtubule-dependent, and it is associated with the polarisation of the MTOC and other organelles, such as the Golgi apparatus, mitochondria, lysosomes (Yuseff et al., 2011), and the nucleus (Ulloa et al., 2022).

Once the IS has been formed, the antigen has to be extracted from the ARC, but the exact mechanisms remain unclear. The IS is a dynamic signalling platform, and both endocytosis and exocytosis can occur. Most studies about antigen

internalisation and processing over the years have been done using soluble antigens. Concerning soluble antigen, the majority of the antigen-BCR complexes are endocytosed via CDE (*see* 2.3.6 B cells as APCs: Antigen processing and presentation). However, when the antigen is encountered on an ARC, B cells need to extract the antigen from their surface (Batista et al., 2001; Suzuki et al., 2009). Different non-exclusive mechanisms have been proposed, mainly by two different groups (del Valle Batalla et al., 2018). It is believed that local secretion of hydrolases, originating from the lysosomes, boosts the extraction of the antigen, and this can also initiate the degradation of the antigen in the extracellular space (Yuseff et al., 2011). It is tempting to speculate that the resulting peptides could bind to the MHC II molecules present on the surface of the B cell, bypassing the endocytic pathway, as B cells have functional H2-M molecules on the cell surface (Arndt et al., 2000). Nevertheless, most of the antigen is internalised at the IS and enter the endocytic route (*see* 2.3.6 B cells as APCs: Antigen processing and presentation). On the other hand, Tolar´s group proposed that the extraction is based on mechanical forces exerted by the cell skeleton, as the B cell can physically pull out the antigen and internalise it (Natkanski et al., 2013; Nowosad et al., 2016; Spillane and Tolar, 2017). These forces have important implications for affinity discrimination, as they promote the internalisation of high-affinity antigens (Batista et al., 2001; Natkanski et al., 2013).

Vesicle trafficking is also important to initiate and maintain the IS, although its implications have been studied almost exclusively in T lymphocytes (Onnis et al., 2016). In T cells, there is active trafficking and recycling of the TCR from the intracellular compartments to the IS. The TCR has been found in early endosomes ($Rab5^+$), fast recycling endosomes ($Rab4^+$), and slow recycling endosomes ($Rab11^+$). Other studies also point to some roles of other less studied Rab proteins, such as Rab3, Rab6, Rab8, Rab35, Rab29, in the TCR recycling (Carpier et al., 2018; Finetti et al., 2015b; Liu et al., 2000; Onnis et al., 2015; Patino-Lopez et al., 2008; Soares et al., 2013).

2.3.5 BCR signalling pathways

BCR signalling needs to be tightly regulated, as excessive signal responses can lead to autoreactive B cells or malignant proliferation. B cell activation, understood here as activation via the BCR, is triggered by specific antigen binding to the BCRs on the cell surface (**Figure 5**). Nevertheless, other receptors, such as TLRs (Toll-like receptors), CD40 or BAFFR, also participate in B cell activation to achieve fine-tuned responses. BCR activation triggers not only proximal kinase signalling but also many other pathways, leading to BCR-antigen internalisation, antigen processing, integrin adhesion and reorganisation of the cytoskeleton. Although BCR signalling has been

extensively studied (Kurosaki, 2002; Kurosaki, 2011; Kurosaki and Hikida, 2009; Packard and Cambier, 2013; Tanaka and Baba, 2020), we are barely starting to understand the links between all these interrelated pathways and their regulation. Notably, BCR signalling has been studied with a focus on the protein interactions, but other components, such as membrane microdomains (lipid rafts) (Cheng et al., 1999b; Dykstra et al., 2003; Stoddart et al., 2002) and microRNAs (Borbet et al., 2021), also play a role. It is also worth mentioning that the vast majority of the studies have been performed *in vitro* and that the form of antigen encounter can modify the signalling. For instance, CD19 signalling is required for B cell activation by membrane-bound antigens but not by soluble ones (Depoil et al., 2008). Here, I describe the more prominent signalling pathways regardless of the type of stimulation.

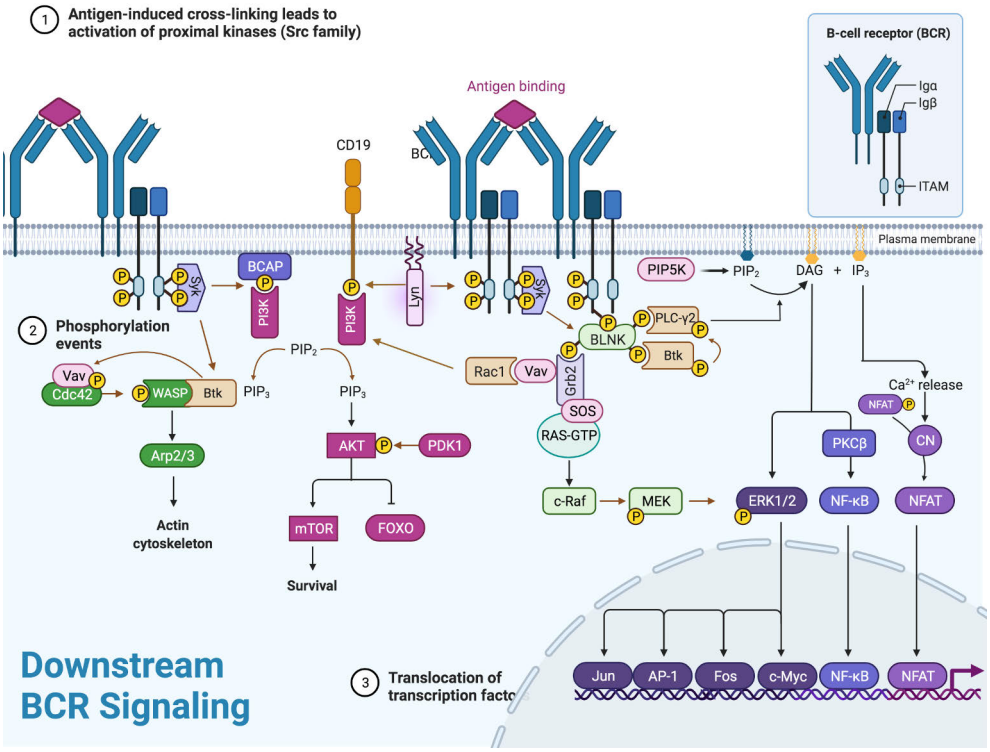

Figure 5. Downstream BCR signalling. Brown arrows indicate phosphorylation events.

The BCR is composed of a membrane-bound immunoglobulin (mIg) that mediates the antigen recognition and a transmembrane (TM) heterodimer, the Igα/β (CD79a/CD79b) sheath forming a complex with 1:1 stoichiometry (Reth, 1989; Reth and Wienands, 1997; Schamel and Reth, 2000). Igα and β are covalently bound together through disulfide bonds and are required for intracellular signalling

(Hombach et al., 1990; Siegers et al., 2006). The mIg has a tiny intracellular tail (3-28 amino acids depending on the Ig isotype) unable to directly transduce the cues from the extracellular environment (Venkitaraman et al., 1991). Therefore, this Ig relies on its association with the Igα/Igβ complex (about 26 amino acids tail), which contains several Immunoreceptor Tyrosine-based Activation Motifs (ITAMs; consensus sequence [YxxL/I $(x)_{6-8}$ YxxL/I]) (Flaswinkel and Reth, 1994; Sanchez et al., 1993). The Igα/Igβ complex is important not only in signal transduction but it is also required for the correct traffic and internalisation of BCR to and from the PM (Gazumyan et al., 2006; Hou et al., 2006). Upon binding of the antigen to the BCR, the ITAM domains are exposed. To date, multiple models exists on how the antigen binding to the BCR triggers the assembly of the signalling complexes in the intracellular space. Multiple models of BCR activation have been proposed, and they have been reviewed elsewhere (Gold and Reth, 2019; Harwood and Batista, 2010; Treanor, 2012). Following the exposure, the two tyrosines of the ITAM motifs are phosphorylated within seconds by Lyn, a Src-family kinase, followed by the recruitment and activation of Syk via its SH2 domain. Syk is then activated by autophosphorylation forming a BCR/Syk signalling nanocluster. The adaptor BLNK (also known as SLP-65) is recruited to the phosphorylated Igα (non-ITAM pY204) via its SH2 domain (Engels et al., 2001; Kabak et al., 2002) and phosphorylated by Syk. Other proximal kinases such as Fyn and Blk also contribute to the activation process. The new phosphorylation sites will serve as docking sites for PLC-γ2, Vav, Grb2 and Btk, serving as the seeding point for several signalling pathways. It is noteworthy that different pathways are interconnected, and several feedback loops exist at multiple points, helping sustain BCR signalling.

The PLC-γ2 pathway: The recruitment of Btk (Burton´s tyrosine kinase) to PIP_3 (phosphatidylinositol 3,4,5 trisphosphate) sites (*see* PI3K pathway) leads to the recruitment of PIP5K (phosphatidylinositol-4-phosphate 5-kinase) from the cytosol to the plasma membrane resulting in an increase in the local PIP_2 (phosphatidylinositol 4,5-bisphosphate) concentration (Saito et al., 2003). PLC-γ2 is then recruited to the plasma membrane to catalyse PIP_2 conversion to the second messengers DAG (diacylglycerol) and IP_3 (inositol 1,4,5-trisphosphate). IP_3 causes first calcium release from the ER, leading to the opening of the plasma membrane CRACs (Calcium Release-Activated Calcium Channels) to further sustain the intracellular Ca^{2+} increase (Baba and Kurosaki, 2015; Hogan et al., 2010). This increase is recognised by the Ca^{2+} dependent phosphatase calcineurin that will dephosphorylate the NFAT transcription factor and promote its translocation to the nucleus. DAG, on the other hand, can activate two different pathways: NFkB and MAPK. DAG binds to RasGRP (Ras guanyl nucleotide-releasing protein) and mediates the activation of PKCβ (protein kinase Cβ) that will phosphorylate CARMA1, leading to IKK phosphorylation and NFkB activation as well as

promoting the activation of the MAPK pathway. Activation of these pathways results in cell survival and proliferation (Blonska and Lin, 2010).

The PI3K pathway: Antigen binding to the BCR results in the phosphorylation of the cytoplasmic tails of the Igα/Igβ sheath, the BCR co-receptor CD19 and the adaptor protein BCAP (Okada et al., 2000) by Lyn. Phosphorylated CD19 and BCAP provide a docking site for PI3K (p85a). The activated PI3K mediates the phosphorylation of PIP_2 to the lipid second messenger PIP_3. PIP_3 can then activate AKT, inducing cell survival. PIP_3 also serves as a docking point for Btk, that binds to PIP_3 via the Btk pleckstrin-homology (PH) domain. Btk can activate WASP by phosphorylating Vav and Cdc42, leading to the organisation of the actin cytoskeleton (Sharma et al., 2009).

The Ras/MAPK pathway: the activation of Ras is triggered by the recruitment of its GEF, Sos, mediated by the activation of the adaptor protein Grb2. Active GTP-bound Ras recruits the protein kinase c-Raf, which activates MEK1/2, which in turn activates ERK1/2. This results in the activation of a number of transcription factors, such as Fos and Jun, that regulate cell proliferation and survival (Greaves et al., 2018; Rowland et al., 2010).

2.3.6 B cells as APCs: Antigen processing and presentation

After antigen binding to the BCR and activation, either in soluble form or bound to an ARC, the BCRs on the surface play a dual role. Not only BCRs are responsible for the triggering and maintenance of the signalling but they also need to be internalised to deliver the antigen to the right intracellular compartments for further processing and presentation to the T cells (**Figure 6**). This process is fundamental as B cells need T cell help to achieve full activation and effectively undergo processes such as CSR and SMH (Lanzavecchia, 1990). Studies on antigen presentation have primarily focused on DCs and macrophages - professional APCs with phagocytic functions – leaving the more specific type of antigen processing and presentation in B cells less understood (Ghosh et al., 2021).

B cells, like other immune cells, can take up antigen by fluid-phase pinocytosis. However, B lymphocytes are unique APCs, as they are the only cells that can present and recognise clonotypically restricted antigens via their BCR. In such a manner, B cells can detect and present as little as 10^4-fold lower antigen concentrations when recognised by the BCR in comparison to unspecific pinocytosis (Grey and Chesnut, 1985; Lanzavecchia, 1985; Lanzavecchia, 1990; Vidard et al., 1996). Therefore, the presentation of specific antigens recognised by the BCR quickly emerged as the primary and superior way of processing antigens in B cells. This mechanism might be necessary in physiological conditions where the amount of antigen is limited or to outcompete other B cell clones during affinity maturation in the germinal centres (Adler et al., 2017a; Batista and Neuberger, 1998).

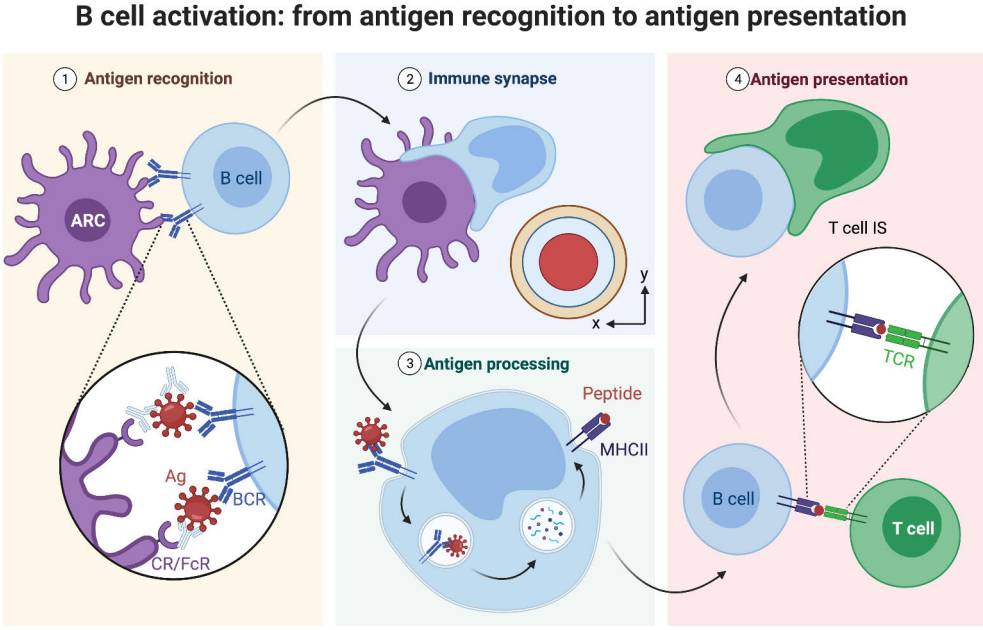

Figure 6. B cell activation: from antigen recognition to antigen presentation. (1) B cells first encounter the antigen on the surface of ARCs, such as FDCs. (2) After antigen recognition, BCR signalling is triggered, and B cells form an immune synapse with the ARC. (3) BCR-antigen complexes are internalised and trafficked to antigen-processing compartments. The resulting peptides are loaded on MHC II. (4) The peptide-MHC II on the surface of the B cells is recognised by specific T cells via their TCR, leading to subsequent activation.

B cells internalise antigens mainly through clathrin-dependent endocytosis (Natkanski et al., 2013; Salisbury et al., 1980) in an actin-dependent manner (Brown and Song, 2001; Sharma et al., 2009; Stoddart et al., 2002). The clathrin adaptor AP-2 binds to the phosphorylated ITAM domains of Iga/Igb, leading to the recruitment of clathrin and triggering BCR internalisation at the signalling sites (Busman-Sahay et al., 2013). Furthermore, BCR internalisation and signalling are interdependent events, as Src-family kinase activity is required for clathrin heavy chain phosphorylation and subsequent BCR internalisation (Ma et al., 2001; Stoddart et al., 2002). Nevertheless, clathrin-independent endocytosis of the BCR has also been described, indicating some level of redundancy in this process (Malinova et al., 2021; Stoddart et al., 2005). Interestingly, a recent study suggests that the amount of antigen encountered by the cell could determine the nature of the endocytic structures (Roberts et al., 2020). Hence, the relationship between signalling and internalisation remains controversial. Some reports suggest that BCR signalling and internalisation are mutually exclusive events: a single BCR can signal if certain tyrosine motifs are phosphorylated or be internalised if not (Hou et al., 2006).

However, other studies suggest that some BCRs can signal once internalised (Chaturvedi et al., 2011). In addition to endocytosis, some studies have reported that B cell can present endogenous or viral antigens on MHC II molecules via autophagy (Arbogast et al., 2019; Arnold et al., 2016; Paludan et al., 2005; Zhou et al., 2005).

After internalisation, the antigen needs to be processed into peptides and loaded on MHC II molecules for presentation (Davidson and Watts, 1989; Simitsek et al., 1995; Watts et al., 1989; West et al., 1994). MHC II molecules are composed of two different chains (α/β dimer) that assemble in the endoplasmic reticulum (ER) and associate with a specific chaperone termed invariant chain (Ii, CD74) (Brown et al., 1993; Viville et al., 1993). The invariant chain is critical throughout this process, as it not only helps proper MHC II folding but also protects the MHC II peptide-binding groove against unspecific binding and directs the MHC II towards the right endosomal compartment (Bakke and Dobberstein, 1990; Margiotta et al., 2021). BCR binding to the antigen triggers the recruitment of MHC II and the internalised antigen towards a special lysosome-like compartment, usually referred to in the literature as antigen-processing compartment or MHC II compartment (MIIC) (Neefjes et al., 1990; Peters et al., 1991), for efficient loading.

The exact nature and origin of MIIC have been for long a matter of debate. The main hallmarks of the MIIC are the low pH, loading chaperones (such as H2-M) and proteolytic enzymes (such as cathepsin S; CatS) together with antigen-BCR complexes and MHC II (Guagliardi et al., 1990). In addition to MIIC, other terms have arisen to describe similar structures, such as class II vesicles (CIIV) (Amigorena et al., 1994a), an early endocytic compartment. These compartments are not static, and they can change upon BCR stimulation, making their study and classification technically challenging and possibly explaining the discrepancies between different reports.

BCR signalling is needed not only to promote maturation of the MIIC, changing its biochemical and physical properties, but also to correctly and rapidly deliver the internalised antigen to such compartments (Aluvihare et al., 1997; Anderson et al., 1999; Cheng et al., 1999a; Lankar et al., 2002; Xu et al., 1996). Shortly after antigen binding to the BCR, newly synthesized MHC II molecules accumulate in the MIIC, and, at the same time, the pH of the compartment decreases to facilitate antigen degradation (Siemasko et al., 1998). Once the MHC II molecule has reached the acidic compartments, Ii is degraded by proteolytic enzymes, such as cathepsin S and cathepsin L (Neefjes and Ploegh, 1992; Riese and Chapman, 2000). From the original invariant chain, only a small peptide called CLIP (20 residues) remains, protecting the peptide-binding groove (Roche and Cresswell, 1990). This peptide has to be eliminated at a precise time and location so that the antigenic peptide can bind. It has been known for a long time that CLIP removal is catalysed by HLA-DM (Denzin et al., 1996; Martin et al., 1996; Mosyak et al., 1998; Sloan et al., 1995).

More recently, it has been shown that a second molecule, HLA-DO, regulates HLA-DM (Denzin et al., 2005), although the mechanism remains unclear. In the germinal centres, cells express less HLA-DO and have enhanced antigen presentation (Glazier et al., 2002), suggesting that the HLA-DM/DO ratio could modulate antigen presentation at different stages (Jiang et al., 2015). Once CLIP has been removed, the antigenic peptides can be loaded into the MCHII (pMHC II). The exact mechanism of peptide loading is not known, but a recent report using FRET showed that antigen-BCR complexes associate with MHC II molecules to mediate the exchange (Barroso et al., 2015). Once delivered back to the cell surface, the recognition of the pMHC II complex by the cognate T cells will lead to the formation of a new immunological synapse. Antigen presentation to T cells is critical for B cells, as, in the context of TD responses, T cells will provide the stimulus needed for activation and antibody production.

While most studies claim that peptide loading occurs in this specialised MIIC (Amigorena et al., 1994a; Qiu et al., 1994; Tulp et al., 1994), other studies indicate that loading can occur at any point of the endocytic pathway, including early endosomes and the PM (Arndt et al., 2000; Castellino and Germain, 1995; Pinet and Long, 1998; Pinet et al., 1995). Notably, the peptide repertoire seems to differ depending on the compartment (Griffin et al., 1997; Lindner and Unanue, 1996). Supporting this, a significant amount of MHC II molecules are present on the PM or in peripheral vesicles in resting B cells, instead of being in late endosomal compartments such as in DCs and macrophages (Lankar et al., 2002). The amount of time needed for antigen presentation is also a matter of debate. Early studies showed that degradation of the antigen could be detected as early as 10-20 min after shifting the cells to 37 °C (Davidson and Watts, 1989). In line with these studies, antigen could be detected in the late endosomes after 10 minutes, and presentation after 20 minutes (Aluvihare et al., 1997). Although MHC II can be internalised and recycled from the PM (Reid and Watts, 1992; Roche et al., 1993), these early studies showed that the majority of the processed antigen binds to newly synthesised MHC II molecules (Aluvihare et al., 1997; Davidson et al., 1991).

Many BCR signalling molecules have been described to regulate antigen processing, including BLNK (Siemasko et al., 1999; Siemasko et al., 2002), Vav (Malhotra et al., 2009) and Igα/β. Other factors such as the extent of receptor crosslinking (Song et al., 1995), BCR signalling-dependent ubiquitination (Drake et al., 2006; Katkere et al., 2012; Zhang et al., 2007), the lipid microenvironment (Busman-Sahay et al., 2011; Katkere et al., 2010) or the cytoskeleton (Thaunat et al., 2012; Vascotto et al., 2007b; Yuseff et al., 2013) can control antigen internalisation and processing. Although the colocalisation of antigen in different compartments has been studied (Lankar et al., 2002), not much is known about the functional roles of the different Rab proteins in antigen processing and presentation. In this context,

Rab7 is one of the best-known Rab GTPases. Some reports show that Rab7 is upregulated in B cells activated with LPS or CD40L, increasing the rate of antigen presentation (Bertram et al., 2002), and it plays a role in antibody responses (Lam et al., 2016; Pone et al., 2015).

2.4 Rab proteins in health and disease

Due to the prominent role of Rab proteins in the intracellular trafficking, mutations or alterations in their expression or activity give rise to pathological scenarios (Mitra et al., 2011). To date, mutations in five of the 66 human Rab genes have been found to cause genetic disorders (**Table 2**). In addition, although no Rab mutations have been related to tumorigenesis, altered activity or expression profiles have been linked to cancer progression and metastasis (Jin et al., 2021; Recchi and Seabra, 2012). Alterations of Rab GTPases or their effectors are also associated with neurological, metabolic and inflammatory disorders, such as Alzheimer´s disease, diabetes, and Crohn´s disease, respectively (Ginsberg et al., 2010; Kiral et al., 2018; Ohira et al., 2009).

Although all cells need a tight regulation of the endosomal traffic, this is imperative in immune cells. To no surprise, given their importance in regulating vesicular trafficking, Rab GTPases and their effectors play a role in regulating immune responses (Krzewski and Cullinane, 2013; Pei et al., 2012; Prashar et al., 2017) and in pathogen invasion. Cells of the innate and adaptive immune system (*see* 2.2 The immune system) rely on the endosomal traffic to regulate, for instance, signal transduction, phagocytosis, cytotoxic degranulation, cytokine secretion or antigen presentation. At least 20 different Rab proteins are involved in phagosome activity, being Rab5, Rab7, Rab10, Rab11, Rab14 and Rab34 the best-characterised proteins in this process (Gutierrez, 2013).

The best characterised Rab in relation to the immune response in humans is Rab27, a small Rab GTPase that regulates exocytosis in immune cells and melanocytes (Ostrowski et al., 2010). Genetic mutations in Rab27 lead to Griscelli syndrome (GS) type 2 (GS2), a rare autosomal recessive disorder characterised by variable immunodeficiency due to impaired cytotoxic T lymphocyte activity. GS is also associated with mutations in myo5a and melanophilin, causing neurological dysfunction (GS1) or hypopigmentation defects (GS3), respectively (Barral et al., 2002; Ménasché et al., 2000). In addition to GS, other mutations in vesicular proteins can lead to faulty immune responses. Mutations in the gene encoding Munc13-4, a Rab27 effector, cause Familial Hemophagocytic Lymphohistiocytosis (FHL) Type 3. Since the Rab27a-Munc13-4 complex is necessary for effective degranulation of NK and T cells, both FHL and GS2 patients present increased susceptibility to infections (Elstak et al., 2011; Feldmann et al., 2003). The Hermansky-Pudlak

syndrome (HPS), an inherited disorder, is characterised by hypopigmentation and patients can also present immunodeficiency (Di Pietro and Dell'Angelica, 2005; Huizing and Gahl, 2005). In the murine *gunmetal* and *chocolate* models, Rab38 and RabGGT mutations cause a phenotype similar to the human HPS. However, no mutations of RabGGT or Rab38 have been found in HPS patients to date (Wei and Li, 2013). Similarly, Rab14 has been associated to Chediak-Higashi syndrome, a rare lysosomal disorder that presents with immune deficiency due to impaired cytotoxic T lymphocyte activity, but the mutation has not been confirmed in humans (Kypri et al., 2013). Other Rab proteins, such as Rab13 or Rab39, have been associated with immune-related phenotypes in murine models, but their association to human diseases has not been confirmed (Cruz et al., 2020; Nishikimi et al., 2014).

Table 2. Rab GTPases and genetic disorders in humans.

Protein	Disease	Mutation	References
Rab7a	Charcot-Marie-Tooth Type 2B Disease	4 missense mutations (enhanced activity)	(Spinosa et al., 2008; Verhoeven et al., 2003)
Rab18	Warburg Micro syndrome	Loss-of-function	(Bem et al., 2011)
Rab23	Carpenter Syndrome	4 nonsense mutations (truncated protein) 1 missense mutation (disruption of protein folding)	(Jenkins et al., 2007)
Rab27	Griscelli Syndrome (type II)	3 missense mutations 1 nonsense mutation 6 frameshift mutations All produce inactive proteins	(Barral et al., 2002; Ménasché et al., 2000; Stinchcombe et al., 2001)
Rab39b	X-linked intellectual disability	1 nonsense and 1 point-mutation (loss-of-function)	(Giannandrea et al., 2010)

In addition to immunodeficiency, faulty immune responses can cause autoimmunity. Autoimmune diseases are syndromes that result from dysfunctional immune responses leading to the host´s immune system to mistakenly attack itself. There are over 100 different types of autoimmune diseases; the cause of many of them is believed to be multifactorial, though linked to genetics, and they can affect one specific organ or multiple organs in the body. Notably, up to 75% of newly generated immature B cells are autoreactive, carrying to some level the potential to unleash autoimmunity (Plotz, 2003; Wardemann et al., 2003); hence, an exquisite regulation is needed to maintain healthy responses. Several studies acknowledged the role of extracellular vesicles in the development of autoimmune or autoinflammatory

diseases such as systemic lupus erythematosus (SLE), rheumatoid arthritis, and multiple sclerosis (Buzas et al., 2014; Nielsen et al., 2012; Sáenz-Cuesta et al., 2014; Sellam et al., 2009; Ullal et al., 2011). Although no mutations have been found to date in autoimmune diseases in humans, several studies in murine models suggest a link between Rab proteins and dysregulated immunity. For instance, two reports showed that Rab7 plays a role in CSR and production of autoantibodies (Lam et al., 2016; Pone et al., 2015). Rab44 deficiency might also be associated to autoimmune disease, but further studies are needed to support this conclusion (Comrie et al., 2018; Tsukuba et al., 2021).

Pathogens are known to exploit the machinery of the host cell to their own advantage at many different levels (Colonne et al., 2016; Derré, 2017; Gioseffi et al., 2021; Mañes et al., 2003; Silmon De Monerri and Kim, 2014). Not surprisingly, Rab proteins are also involved in the progression of infectious diseases, as many pathogens utilise the endocytic pathways to enter and infect the host cell (Spanò and Galán, 2018). Most of these strategies target the lysosomes or phagosomes, interfering with their normal maturation to impede the degradation of the pathogens. In addition, viruses can target different Rab proteins to promote the transport of viral proteins, accelerating virus budding. Understanding how pathogens interfere with the vesicular machinery can shed some light on new trafficking routes and help to understand the biological importance of these pathways.

2.5 The roles of Rab8

Rab8 is a ubiquitous Rab protein with two isoforms, Rab8a and Rab8b. It was first identified as a transforming gene using a melanoma cell line (Nimmo et al., 1991). Since then, Rab8 has been described to regulate a plethora of functions in multiple pathways in coordination with different effectors (Peränen, 2011). Rab8 has been reported to localise to the Golgi region and the endosomal recycling compartment and to play a role on the recycling pathway together with Rab11 and Arf6 to promote the polarized transport of newly synthesised proteins and mediate protrusion formation and cell shape remodelling (Hattula et al., 2006; Huber et al., 1993; Peränen et al., 1996; Vidal-Quadras et al., 2017). Interestingly, Rab8 has an additional regulation step, as it can be phosphorylated in the tyrosine 72 (T72) by LRRK2. LRRK2 is a tyrosine kinase highly expressed in immune cells, such as macrophages, neutrophils and DCs (Wallings and Tansey, 2019), and associated to Parkinson´s disease (Steger et al., 2016) and some autoimmune disorders, such as Crohn´s disease (Barrett et al., 2008; Witoelar et al., 2017). LRRK2 is required for the recruitment of Rab8a and Rab10 to the phagosomes in phagocytic cells (Lee et al., 2020), and it is upregulated following recognition of microbial structures (Gardet et al., 2010; Hakimi et al., 2011; Kim et al., 2012; Moehle et al., 2012).

Polarised transport of proteins is especially important for certain functions in specialised cell types, such as nutrient absorption in intestinal epithelial cells. Aberrant apical transport can impair the microvillus function and nutrient uptake causing neonatal enteropathies. Rab8a is responsible for cell polarity of intestinal epithelial cells *in vivo*, regulating the localization of apical proteins. Thus, mice with Rab8 deficiency show a phenotype similar to that of the human disease microvillus atrophy, although no Rab8 mutations have been found in these patients. Rab8a$^{-/-}$ (knock-out; KO) mice present diarrhoea and progressive wasting soon after birth and die at 3-4 weeks after birth (Sato et al., 2007), while the double KO mice (Rab8a$^{-/-}$/b$^{-/-}$) die at week 2-3 (Sato et al., 2014). This phenotype is due to the mislocalisation of several apical markers in the intestinal epithelial cells, leading to a shortening of apical microvilli (Sato et al., 2007; Sato et al., 2014). Rab8 is also found in the ciliary membrane and it plays a role in ciliogenesis together with Rab11, and it is involved in the pathogenesis of ciliopathies such as Barder-Biedl syndrome (Knödler et al., 2010; Lu and Westlake, 2021; Westlake et al., 2011). In addition, Rab8 promotes the turnover of focal adhesions and induce Rac1- and Tiam1-dependent actin polymerisation, therefore controlling the directionality of cell migration (Bravo-Cordero et al., 2016). In cancer cells, Rab8 regulates invasion by controlling the traffic and activity of MT1-MMP (membrane type 1-matrix metalloproteinase) in the invasive structures (Bravo-Cordero et al., 2007).

However, there are only a handful of studies describing the role of Rab8 in immune cells. Some authors defend that the T cell immune synapse resembles the primary cilium, as they both share vesicular proteins that were classically involved in the intraflagellar transport (IFT) system (Blacque et al., 2018; Finetti et al., 2015a). Hence, since Rab8 participates in ciliogenesis (Knödler et al., 2010), Finetti et al. investigated its participation in the T cell immune synapse. In T lymphocytes, Rab8 colocalises with IFT20 and Rab11, and it is implicated in TCR recycling and final docking to the immune synapse via its interaction with VAMP3 (Finetti et al., 2015b). It has also been shown that Rab8 participates in the surface expression of CTLA-4 through LAX-TRIM binding (Banton et al., 2014). Rab8 can also localise to macropinosomes (Hattula et al., 2006). In macrophages, PI3Kγ (p110 catalytic subunit) has been identified as a Rab8a effector. Rab8a interacts with PI3K in membrane ruffles and early macropinosome membranes and regulates TLR signalling, inflammation and polarisation using the AKT/mTOR pathway (Luo et al., 2014; Luo et al., 2018; Tong et al., 2021; Wall et al., 2017; Wall et al., 2019). Rab8a can also promote IL-1β secretion in an autophagy-dependent manner (Dupont et al., 2011).

The studies on Rab8 are exceedingly scarce in B lymphocytes. Porter et al. showed that Rab8a mRNA turnover is regulated in B cells, as its stability increases upon CpG stimulation via PTB (polypyrimidine tract-binding protein) (Porter et al.,

2008). Hence, the authors hypothesized that Rab8a might be required during activation-induced proliferation and antigen processing. Recent studies also suggest a role for Rab8 during infectious processes. A comparative microarray study using whole lung gene expression signatures showed that Rab8a, together with other Rab GTPases such as Rab10, Rab20, Rab 24 and Rab32, are upregulated during *Mycobacterium tuberculosis* infection in mice (Gonzalez-Juarrero et al., 2009). In addition, two independent reports showed that SopD, a *Salmonella* effector protein, interacts with Rab8. Savitskiy and Itzen reported that SopD could act as a GAP and specifically bind and inactivate Rab8a, while Lian and colleagues showed that SopD could regulate the inflammatory responses by positively and negatively modulating Rab8 (Lian et al., 2021; Savitskiy and Itzen, 2021). Through its Rab8 GAP activity, expression of SopD in macrophages resulted in the inhibition of LPS-mediated AKT activation leading to a shift toward pro-inflammatory cytokine profiles and enhancing the inflammatory response. On the other hand, the association of Rab8 and SopD could displace Rab8 from its GDI, leading to enhanced signalling and suppression of the inflammatory response. How these two opposite activities are coordinated in time during *Salmonella* invasion remains unknown, but Lian et al. postulated that the pro-inflammatory function would precede the anti-inflammatory response.

3 Aims

The main objective of this study was to reveal the function of the vesicular machinery, with a focus on Rab GTPases, in antigen processing and presentation and its interplay with the development of fully mounted antibody responses.

The specific Aims of this thesis were:

I To characterise the antigen processing and loading compartments in B cells using microscopy.

II To develop a new internalisation assay compatible with live and super-resolution microscopy techniques and test its applicability to the study of antigen vesicles in B cells.

III To unveil the role of Rab8a in B cells *in vivo* and *in vitro.*

4 Materials and Methods

This dissertation is based on three original publications, which are referred to in the text by their Roman numerals (I, I, II) (*see* List of Original Publications).

4.1 Antibodies, reagents and buffers (I, II, III)

The complete list of antibodies, reagents and buffers used during the thesis are shown in **Table 3**, **Table 4**, and **Table 5**, respectively.

Table 3. Antibodies. JIR: Jackson Immunoresearch. CST: Cell Signalling Technologies. SB: Southern Biotech. SA: Sigma-Aldrich. SCB: Santa Cruz Biotechnology. Thermo: Thermo Fischer. BL: Biolegend. BD: BD Biosciences. AF: Alexa Fluor®. RRx: Rhodamine Red X

Name	Company	Catalogue number	Publication (s)
6 nm Gold rat anti-mouse IgM	JIR	115-195-075	I
AF 488 AffiniPure Donkey anti-mouse $F(ab')_2$ IgM	JIR	715-546-020	I
AF 488 anti-mouse IgD [11-26c.2a]	BL	405718	III
AF 488 anti-phospho-Btk	BD	558507	III
AF 488 anti-phospho-PLC-γ2	BD	564847	III
AF 488 donkey anti-mouse $F(ab)_2$ IgM	JIR	715–546-020	II
AF 488/555 Donkey anti-goat IgG (H+L)	Thermo	A11055, A21432	I
AF 488/555/647 Donkey-anti-rabbit IgG (H+L)	Thermo	A21206, A31572, A31573	I
AF 488/RRx/647 Goat-anti-mouse IgG Fcy subclass 1	JIR	115-545-205 115-295-205 115-605-205	I
AF 488/RRx/647 Mouse anti-rat IgG Fcy Fragment Specific	JIR	212-545-104 212-295-104 212-605-104	I
AF 633 goat anti-mouse IgG2b	Thermo	A21146	I
AF 647 AffiniPure Donkey anti-mouse IgM	JIR	715-605-140	I
AF 647 donkey anti-mouse $F(ab)_2$ IgM	JIR	715-606-020	II
AF 647-biotin Donkey anti-mouse IgM	In-house	715-605-140 + Thermo 21343	I
AF 700 anti-mouse CD19 [6D5]	BL	115528	III

Name	Company	Catalogue number	Publication (s)
Anti-Cathepsin S	LSbio	B2550	I
Anti-Cathepsin S	SCB	sc-271619	I
Anti-EEA1	SCB	Sc-6415	I
anti-Eα-MHC II antibody	Invitrogen	14-5741-85	III
Anti-IgM-biotin	SB	1021-08	I
Anti-LAMP1	DSHB	1D4B	I
Anti-MHC II	SCB	Sc-59322	I
Anti-MHC II-AF488	In-house	Sc-59322 + Thermo A20000	I
Anti-mouse IL-2	BL	503804	I
Anti-mouse IL-2, biotin	BL	503702	I
Anti-PCM1-AF 647	SCB	Sc-398365 AF647	I
Anti-Rab11	CST	5589	I
Anti-Rab5	CST	3547	I
Anti-Rab6	CST	9625S	I
Anti-Rab7	SCB	Sc-376362	I
Anti-Rab9	CST	5118	I
APC anti-CD19	BL	392503	III
APC anti-mouse CD19 [6D5]	BL	115512	III
APC/Cy7 anti-mouse/human CD45R/B220 [RA3-6B2]	BL	103224	III
BD HorizonTM V450 Rat Anti-Mouse IgM Clone R6-60.2	BD	560575	III
C57BL/6 Mouse Ig Panel	BD	553406	III
Donkey anti-mouse IgM	JIR	715-005-020	II
Fc-block	BL	422301	III
FITC anti-mouse IgM	JIR	715-095-140	I
FITC Goat anti-mouse IgG2c	JIR	115-095-208	III
FITC Rat anti-mouse IgG1	BD	553443	III
FITC Rat anti-mouse IgG2b	BD	553395	III
FITC Rat anti-mouse IgG3	BD	553403	III
Goat anti-mouse IgG, Fc fragment specific	JIR	115-005-071	III
Goat anti-mouse IgG1 biotin	SB	1071-08	III
Goat anti-mouse IgG2b biotin	SB	1091-08	III
Goat anti-mouse IgG2c biotin	SB	1078-08	III
Goat anti-mouse IgG3 biotin	SB	1003-08	III
Anti-IgA	BL	407002	III
Anti-IgE	BL	406902	III
PE anti-CD3	BL	100308	III
RRX AffiniPure Donkey anti-mouse IgM	JIR	715-295-140	I
RRx goat anti-mouse $F(ab)_2$ IgM	JIR	115-006-020	II

Table 4. **Reagents.** MCE: MedChemExpress. Bangs: Bangs Laboratories. Merk: Merk Millipore. SA: Sigma-Aldrich. SCB: Santa Cruz Biotechnology. Thermo: Thermo Fischer. BL: Biolegend. BD: BD Biosciences. AF: Alexa Fluor®. BST: BioSearch Technologies.

Name	Company	Catalogue number	Publication(s)
100 nm Streptavidin beads	Bangs	CP01000, Lot 14817	III
200 nm Dragon Green Streptavidin beads	Bangs	CFDG001, Lot 13743	III
50 K MWCO Amicon filter	Merk	UFC5050	II
7K Zeba spin desalting column	Thermo	89882	II
Abberior-FIP (5′ Abberior® STAR 635P-TCAGTTCAGGACCCTCGGCT-N3 3′)	BioSynthesis Inc.	-	II
Acti-stain 555	Cytoskeleton Inc	PHDN1-A	III
AF 633 Streptavidin	Life Technologies	S-21375	I, II, III
ATTO 647 NHS	SA	07376-1MG-F	II
ATTO 647N-FIP (5′ ATTO 647N-TCAGTTCAGGACCCTCGGCT-N3 3′)	BioSynthesis Inc.	-	II
C57BL/6 immunoglobulin panel	SB	5300-01B	III
Cell Trace Violet	Thermo	C34571	III
CellTak	Corning	354240	III
CFSE	SA	21888	
Click-iT™ SDP Ester sDIBO alkyne	Thermo	C20025	II
CpG ODN 1826	Invivogen	Tlrl-1826	III
CXCL12 / SDF-1α	Bio-Techne	460-SD-010	III
CXCL13	PeproTech	250-24	III
DAB substrate	SCB	Sc-24982	
DQ-OVA-biotin	In-house	Thermo D12053 + 21901BID	I
dsDNA from calf serum	SA	D4522	III
EasySep™ Mouse B Cell Isolation Kit	StemCell	19854	I, III
EasySep™ Mouse T Cell Isolation Kit	StemCell	19851	I, III
eBioscience™ Fixable Viability Dye eFluor™ 780	Thermo	65-0865-14	III
ELISA MAX Deluxe Mouse IL-6	BL	431304	III
ELISA plates, half-area	Greiner Bio-One	675061	III
ELISpot plates	Mabtech	3654-TP-10	III
ExtrAvidin-AP (alkaline phosphatase)	SA	E2636	I
FAST pNPP substrate tablet	SA	N2770-5SET	I
Fibronectin	Sigma	F4759-2MG	I
Fluo-4	Thermo	F14201	III
FluoroMount-G containing DAPI	Thermo	00495952	I, II, III
Fura Red	Thermo	F3021	III
Glutathione Sepharose 4B beads	SA	GE17-0756-01	III
HEL-biotin	In-house	SA L6876+ Thermo 21338	I

Name	Company	Catalogue number	Publication(s)
Hen Egg Lysozyme (HEL)	SA	#L6876	I
High-precision coverslips	Marienfeld	0117650	II
HRP Streptavidin	Thermo	21130	I
Imject Alum	Thermo	77161	III
Immobilon Western Chemiluminescent HRP Substrate	Millipore	WBKLS0500	III
LPS, Lipopolysaccharides from *E. coli*	SA	L2887-5MG	III
LysoTracker Deep Red	Thermo	L12492	I
LysoTracker Green DND-26	Thermo	L7526	II
MatTek dish	MatTek	P35G-1.5-10-C	I, II
Microscopy slides	Thermo	J1800AMNZ	II
NP-LPS	BST	N-5065-5	III
$NP_{(1-9)}$-BSA	BST	N-5050L	III
NP_{24}-BSA	BST s	N-5050H	III
NP_{31}-KLH	BST	N-5060	III
NP_{40}-FICOLL	BST	F-1420	III
OVA-biotin	Lab-made	SA A5503+ Thermo 21338	III
Ovalbumin (OVA)	SA	A5503	
Prolong Gold with DAPI	Thermo	P36941	III
ProLong™ Diamond Antifade Mountant	Thermo	P36970	II
PVDF membranes	Bio-Rad	1704157	II, III
Quenching probe (5′ AGCCGAGGGTCCTGAACTGA-BHQ3 3′)	BioSynthesis Inc.	-	II
Recombinant mouse CD40L	RD Systems	8230-CL-050	III
Recombinant mouse IL-2	Bio-Rad	PMP38	I, III
Recombinant mouse IL-4	RD Systems	404-ML-010	III
Resiquimod (R848)	MCE	HY-13740	III
SIGMAFAST p-nitrophenyl phosphate solution (pNPP)	Sigma	N2770	I, III
ssDNA from calf serum	SA	D8899	III
Streptavidin	Thermo	S4786	I
TMB	Mactech	3651-10	III
Transwell chambers (5-µm pore size)	SA	CLS3421-48EA	III
TRIsure™	Bioline	BIO-38032	III
Twelve-well PTFE diagnostic slides	Thermo	10028210	I, II, III

Table 5. Buffers and media.

Buffers and media	Composition	Publication(s)
Complete RPMI (cRPMI)	RPMI 1640 with 2.05 mM L-glutamine supplemented with 10% fetal calf serum (FCS), 50 µM β-mercaptoethanol, 4 mM L-glutamine, 10 mM HEPES and 100 U/ml penicillin/streptomycin	I, II, III
2S transfection buffer	5 mM KCl, 15 mM $MgCl_2$, 15 mM HEPES, 50 mM sodium succinate, 180 mM Na_2HPO_4/ NaH_2PO_4 pH 7.2	I, II, III
Imaging Buffer	10% FCS in PBS	I, II, III
Blocking/permeabilization buffer	5% donkey serum with 0.3% Triton X100 in PBS	I, II, III
Staining Buffer	1% BSA, 0.3% Triton X100 in PBS	I, II, III
DAB buffer	70 mM NaCl, 20 mM HEPES, 2 mM $CaCl_2$ and 50 mM ascorbic acid	I
Isolation Buffer	2% FCS, 1 mM EDTA in PBS	I, III
Blocking buffer	1% BSA in PBS	I, II, III
Acquisition buffer	2.5% FCS in PBS	III
TBST (TBS-Tween)	0.05% Tween-20 in TBS	I, III
4X Laemmli buffer	Biorad #1610747	II, III
Washing buffer	0.05% Tween-20 in PBS	I, III
Calcium buffer	20 mM HEPES, 5 mM glucose, 0.025% BSA, 1 mM $CaCl_2$, 0.25 mM sulfinpyrazone, and 2.5% FCS in PBS	III
Chemotaxis medium	0.5% BSA, 10 mM HEPES in RPMI	III

4.2 Cells and mice (I, II, III)

The A20 mouse lymphoma cells [H-2^d; IgG2a,k (Mandel, 1980)] stably expressing a hen egg lysozyme (HEL)-specific IgM BCR (D1.3) (Williams et al., 1994) and the 1E5.111 T cells stably expressing a transgenic TCR specific for $HEL^{108–116}$ in the context of I-Ad (Adorini et al., 1993) were kind gifts from Prof Facundo Batista (the Ragon Institute of MGH, MIT and Harvard, USA). Both A20 D1.3 mouse B cells (I, II, III) and 1E5T mouse T cells (I) were maintained in complete RPMI (cRPMI).

The MD4 colony (I, III) was acquired from The Jackson Laboratory (C57BL/6-Tg(IghelMD4)4Ccg/J). The CD19 Cre mouse colony (III) was backcrossed from a CD19 Cre $RhoQ^{flox/flox}$ strain (Burbage et al., 2017), and the $Rab8^{flox/flox}$ mouse colony (III) was shared by Akihiro Harada (Osaka University, Japan) and have been previously described elsewhere (Sato et al., 2007). OT-II mice (III), expressing a transgenic TCR (Vα2/Vß5) specific for a peptide 323-339 of chicken ovalbumin presented by I-Ab (Barnden et al., 1998), were a kind gift from Maija Hollmén (University of Turku, Finland). Wild-type C57BL/6NCrl mice (III) were purchased from the University of Turku Central Animal Laboratory (UTU-CAL, Turku, Finland).

All strains were on a C57BL/6 background and maintained under specific-pathogen-free conditions. All experiments were done with age- (8-12 weeks), and sex-matched animals and WT littermate controls ($CD19^{WT/WT}$, $Rab8a^{flox/flox}$) were used whenever possible. When indicated, CD19 Cre mice ($CD19^{WT/Cre}$, $Rab8a^{WT/WT}$) were also used as control. All animal experiments were approved by the Ethical Committee for Animal Experimentation in Finland and in adherence with the rules and regulations of the Finnish Act on Animal Experimentation (62/2006; animal license numbers: 7574/04.10.07/2014, KEK/2014-1407-Mattila, 10727/2018).

4.3 Transfection (I, II, III)

Rab5a–GFP and Rab7-RFP plasmids were a kind gift from Prof. Johanna Ivaska (Turku Bioscience, Turku, Finland). Rab8a-Citrine, a GFP derivative, plasmid was a gift from Daniel Abankwa (University of Luxembourg). A20 D1.3 cells were transfected as previously described (Šuštar et al., 2018). Briefly, $2\text{-}4\times10^6$ cells were resuspended in 180 µl of 2S transfection buffer containing 2-4 µg of plasmid and electroporated using an AMAXA electroporation machine (program X-005, Biosystem) in a 0.2 cm-gap electroporation cuvette. Cells were then quickly transferred to 2 ml of pre-warmed cRPMI with 1% DMSO and let to recover overnight.

4.4 B and T Cell Isolation (I, III)

Splenic B cells or T cells were isolated with EasySep™ Mouse B or EasySep™ Mouse T Cell Isolation Kit (StemCell) according to the manufacturer's instructions and let to recover in cRPMI in an incubator at 37 °C and 5% CO_2 for 1 h before every experiment. B cells were also isolated from lymph nodes using the same procedure as described above.

4.5 Preparation of the fluorescence internalisation probe (FIP; II)

The fluorescent FIP-azide probes and the quenching probe (QP) were purchased from BioSynthesis Inc. and dissolved in nuclease-free water. The donkey anti-mouse IgM antibodies were functionalized with a 10-fold molar excess of Click-iT™ SDP Ester sDIBO alkyne for 2 h at RT. Antibodies were then purified using a 7K Zeba spin desalting column. After desalting, the functionalised antibodies were incubated with a 2-fold molar excess of fluorescent-FIP-azide at 4 °C O/N and purified using a 50 K MWCO Amicon filter. As a control, the same donkey anti-mouse IgM antibody was labelled with a 2-fold molar excess of ATTO 647 NHS and dialysed

O/N at 4 °C. Effective labelling of the Abberior STAR 635P FIP-labelled anti-IgM (Abberior-FIP-IgM), the ATTO 647N FIP-labelled anti-IgM (ATTO-FIP-IgM) and the ATTO 647 anti-IgM antibodies was confirmed using a NanoDrop spectophotometer.

4.6 B cell activation and visualization of antigen vesicles by immunofluorescence microscopy (I, II, III)

Fixed samples (SDCM and Airyscan; I, II, III). Twelve-well PTFE diagnostic slides were coated with 4 µg/ml fibronectin in PBS. A20 D1.3 or primary B cells isolated from murine spleens were labelled on ice for 10 minutes with 10 µg/ml of Alexa Fluor® 647 $F(ab)_2$ donkey anti-mouse IgM, RRx $F(ab)_2$ goat anti-mouse IgM, Alexa Fluor® 488 $F(ab)_2$ donkey anti-mouse IgM, Abberior-FIP-IgM or ATTO-FIP-IgM (*see* 4.5). Cells were washed with PBS to remove unbound antigen and resuspended in Imaging Buffer. After washing, cells were seeded on the fibronectin-coated wells and incubated at 37 °C to trigger activation. For those samples activated with FIP-IgM (II), slides were incubated on ice with 10 µl of 1 µM Quenching Probe (QP) for 5 minutes prior to fixation. Fixation was done using 4% paraformaldehyde (PFA) for 10 min at RT and samples were blocked/permeabilized for 20 min at RT. After blocking, samples were stained with primary antibodies for 1 h at RT or 4 ºC O/N in staining buffer, followed by washes with PBS and incubation with the fluorescently labelled secondary antibodies for 30 min at RT in PBS. Samples were mounted using FluoroMount-G containing DAPI.

Fixed samples (STED; II). A20 D1.3 cells were labelled with fluorescent antigen as described above. After washing, cells (2×10^5/coverslip) were activated for different time points in an incubator (5% CO_2, 37 °C) on fibronectin-coated high-precision coverslips (13 mm). After activation, internalisation was stopped by placing the samples on ice. Samples were incubated on ice for 5–10 min in Quenching solution (100 µl of 1 µM QP in Imaging Buffer), followed by fixation with 4% PFA for 10 min at RT. Samples were washed once with PBS and mounted on a slide using ProLongTM Diamond Antifade Mountant. Samples were imaged after curing for at least 20 h at RT.

Live imaging (SDCM; I, II). For live imaging, unlabelled A20 D1.3 cells, cells labelled with 125 nM LysoTracker Deep Red (I; 1h at 37 °C) or 100 nM LysoTracker Green DND-26 (II; 10 min at 37 °C) or cells transfected with GFP-Rab5 and RFP-Rab7 were used. *In the original publication I,* cells were first labelled with 10 µg/ml of $F(ab')_2$ Alexa Fluor® 488 donkey anti-mouse IgM on ice for 10 min and washed with cold PBS. For surface MHC II internalisation experiments, cells were stained on ice with Alexa Fluor 488® anti-MHC II and 10 µl/ml donkey Rhodamine Red™-

X anti-mouse IgM for 5 min and washed with cold PBS. Cells were resuspended in cold Imaging Buffer and seeded on four-well MatTek dishes on ice. After seeding, cells were activated at 37 °C inside the environmental chamber of the microscope and image immediately. *In the original publication II*, cells (10^6/ml; 100 µl per well) were seeded on a fibronectin-coated (500 ng/well) MatTek dish for 30 min in an incubator (5% CO_2, 37 °C). Dishes were washed with PBS to remove unbound cells and transferred to ice. Cells were then stained with 10 µg/ml ATTO-FIP-IgM in Imaging Buffer for 5–10 min on ice. When indicated, cells were simultaneously labelled with Alexa Fluor® 488 donkey anti-mouse IgM F(ab)'$_2$. Samples were washed and transferred to the environmental chamber of the microscope (37 °C) and imaged. Quencher was added (10 µl of 10 µM QP in Imaging Buffer) at different time points.

4.7 Synapse formation (III)

Twelve-well PTFE diagnostic slides were coated with 5 µg/ml donkey anti-mouse IgM or CellTak in PBS at RT for at least 1 hour. Primary B cells isolated from WT and KO spleens were resuspended in RPMI (10^6 cells/ml) and labelled, or not, with 0.5 µM Cell Trace Violet (CTV). Labelled and unlabelled cells were mixed (1:1 ratio) and seeded at a density of 80.000 cells/well. Dye-switched experiments were performed systematically. Cells were activated for 15 min (37 °C, 5% CO_2), fixed in 4% PFA for 10 min at RT, and permeabilized/blocked (5% donkey serum with 0.3% Triton X100 in PBS) for 20 min at RT. Cells were stained with Alexa Fluor® 488 anti-phospho-PLC-γ2 or anti-phospho-Btk (1:100) and Alexa Fluor® 555 Phalloidin (1:150) for 1 hour in staining buffer. Samples were mounted in FluoroMount-G. Images were acquired on a 3i CSU-W1 Marianas spinning disk confocal microscope.

4.8 Antigen degradation (I)

DQ-OVA proteolysis reporter. DQ-Ovalbumin was biotinylated in- house with EZ-Link Maleimide–PEG2–biotin. HEL was biotinylated using EZ-LinkTM Sulfo-NHS-LC-LC-Biotin. A20 D1.3 cells were first incubated with 10 µg/ml biotin-HEL or biotinylated anti-IgM for 10 min on ice. After washing with PBS, cells were incubated for 5 min on ice with unlabelled streptavidin for immunofluorescence samples or Alexa Fluor 633-labelled streptavidin for flow cytometry samples, washed with PBS, and incubated 5 min on ice with biotinylated DQ-OVA. After three washes with PBS, cells were activated in an incubator (5% CO_2, 37 °C) to allow internalisation of the probe-linked antigen. After the activation, cells were placed on ice and analysed by flow cytometry immediately. For immunofluorescence samples, cells were activated on 12-well slides coated with fibronectin in the incubator, fixed

with 4% PFA after activation, and stained as previously described. DQ-OVA was excited with 488 nm laser and measured with filters identical to Alexa Fluor 488 or GFP.

Assessment of low pH for flow cytometry. A20 D1.3 cells were stained on ice for 10 min with anti-IgM conjugated to Alexa Fluor 647 (5 μg/ml) and FITC (5 μg/ml) and washed with PBS. Cells were then incubated at 37 °C and 5% CO_2 at different time points in a 96-well plate for flow cytometry analysis. After incubation, cells were kept on ice and analysed using a BD LSR Fortessa analyser equipped with four lasers (405, 488, 561 and 640 nm). As time 0, the samples were kept on ice all the time. Data was analysed using FlowJo v10 (Tree Star).

4.9 Image acquisition (I, II, III)

Spinning disk confocal microscopy. Images were acquired using a 3i (Intelligent Imaging Innovations) Marianas spinning disk confocal system built on an inverted Zeiss Cell Observed microscope equipped with a Yokogawa CSU-W1 confocal scanner unit. The microscope was controlled using the SlideBook software. For fixed samples, the following objective, camera, laser lines and filters were used: an oil-immersion 63×Zeiss Plan-Apochromat (1.4 NA, working distance 0.19 mm) objective, a Photometrics Prime BSI back-illuminated scientific CMOS camera (2048 × 2048 pixels, 1 × 1 binning, pixel size 6.5 × 6.5 μm), 405 (100 mW), 488 (150 mW), 561 (100 mW) and 640 (100 mW) nm laser lines and 445/45 nm (DAPI), 525/30 nm (Alexa Fluor® 488), 617/73 nm (Alexa Fluor® 555) and 692/40 nm (Alexa Fluor® 647) filters. For live imaging, the following objective, camera, laser lines and filters were used: an oil-immersion 63x Zeiss Plan-Apochromat (1.4 NA, working distance 0.17 mm), a Photometrics Evolve Delta EMCCD (512 × 512 pixels, 1 × 1 binning, pixel size 16 × 16 μm) camera, 488 (150 mW), 561 (150 mW) and 640 (100 mW) nm laser lines and 525/30 nm (Alexa Fluor® 488), 617/73 nm (Alexa Fluor® 555) and 692/40 nm (Alexa Fluor® 647) filters. The gain was set to 1, and laser power to 30%. The microscope was equipped with an Okolab temperature control and environment chamber for live imaging.

Airyscan confocal microscopy. Images were acquired using a laser scanning confocal microscope LSM880 (Zeiss) with an Airyscan detector equipped with 405 (Diode), 488 (Argon) and 633 (HeNe) laser lines and an oil-immersion 63×Zeiss Plan-Apochromat (1.4 NA, working distance 0.14 mm) objective. The following parameters were used: 1 × 1 binning, laser power 6%, gain 850, unidirectional line scanning, × 16 averaging, and 0.09×0.09×0.22 μm pixel size (XYZ). The microscope was controlled using the Zen Black (2.3) software, and images were acquired using the standard super-resolution mode (pinhole 2.77 AU). 3D Airyscan processing was done with Auto settings.

Stimulated emission depletion microscopy (STED). An Abberior STED/RESOLF system (Abberior Instruments GmbH, Germany) equipped with a 100 × oil-immersion Olympus UPLSAPO objective (NA 1.4, working distance 0.13 mm) was used. Abberior-FIP-IgM was excited with a pulsed 635 nm laser and depleted using a 775 nm pulsed depletion laser, and emission signal was detected in the Cy5 channel (685/35 nm). Confocal images of Alexa Fluor® 488 anti-IgM F(ab)'$_2$ were taken using the 488 nm laser, and the emission signal was detected in the GFP channel (525/25 nm). A 20 nm × 20 nm pixel size was used.

4.10 Image processing and image analysis (I, II, III)

Huygens deconvolution (I, II, III). Where indicated, SDCM images were deconvolved with Huygens Essential version 16.10 (Scientific Volume Imaging, The Netherlands, http://svi.nl), using the CMLE (I) or Quick MLE (II, III) algorithm.

Colocalisation (I, II, III). Colocalisation analysis in SDCM samples was done on Huygens Essential (I) or ImageJ using the Colocalisation Threshold plugin (I, II, III). As a control for random colocalization, the antigen channel was rotated 90° and colocalization was measured. Colocalisation on SRRF images was performed with ImageJ using the Colocalisation Threshold tool (I).

Immune synapse (III). Cells were imaged at the plane of contact, and 5–10 fields of view per sample were acquired. Images of F-actin, pBtk, and pSyk were processed with ImageJ using the CTV channel to discriminate between WT or Rab8a KO cells. Using an ImageJ macro, spreading area (determined on the phalloidin channel) and mean fluorescence intensity of pBtk or pSyk staining were analysed (> 100 cells per condition per experiment, at least n = 4 independent experiments).

Super-resolution radial fluctuations (SRRF; I, II). For SRRF processing 100 frames (135 × 135 pixels) were used for the reconstruction (Culley et al., 2018b; Gustafsson et al., 2016). For live imaging, 50×20 ms frames (85×85 pixels) were used. The parameters were as follows: 2.3 Ring Radius, 9 Radiality Magnification and 7 Axes in Ring. All other parameters were run in default mode. Parameters were defined using SQUIRREL analyses (resolution-scaled error (RSE) and resolution-scaled Pearson (RSP) values) (Culley et al., 2018a).

Content-aware image restoration (CARE) (II). For 4D (xyzt) imaging, movies were recorded using a SDCM and a Photometrics Evolve camera as described before. After imaging, samples were fixed with 4% PFA, and pairs of low signal-to-noise ratio (20 ms exposure time, as used for 4D live imaging) and high signal-to-noise ratio (500 ms) images were acquired. These images were used for training as input and target images, respectively. The CARE 2D model was trained from scratch for 100 epochs on 700 paired image patches (image dimensions: (100,100), patch size: (16,16)) with a batch size of 16 and a Laplace loss function, using the CARE 2D

ZeroCostDL4Mic notebook (v1.12) (von Chamier et al., 2021; Weigert et al., 2018). Key python packages used include TensorFlow (v1.15), Keras (v2.3.1), CSBDeep (v0.6.2), NumPy (v1.19.5), CUDA (v11). The training was accelerated using a Tesla T4 GPU. Default Advanced Parameters were enabled, and no augmentation was used for training. The model was validated using unseen images, obtaining a structural similarity index measure (mSSIM) of 0.723.

4.11 Antigen internalisation by flow cytometry (I, II, III)

A20 D1.3 cells (10^7/ml) were stained for 5 min on ice with biotinylated anti-IgM, Alexa Fluor® 647 anti-IgM, FITC anti-IgM, ATTO 647 anti-IgM, Abberior-FIP-IgM or ATTO-FIP-IgM. Cells (5 x 10^4/well, 96-wp) were then incubated at 37 °C and 5% CO_2 for 45, 30, 15 and 5 min. As a control (time 0), samples were kept on ice at all times. After incubation, cells activated with biotinylated anti-IgM were stained with Alexa Fluor® 633 Streptavidin and cells activated with FIP-IgM were quenched using 40 µl of 10 µM QP in PBS on ice for 20 min. Samples were then washed with cold PBS and analysed. A BD LSR Fortessa analyser equipped with four lasers (405, 488, 561, and 640nm) was used. Data were analysed using FlowJo v10 (Tree Star).

The internalisation rate for the FIP-IgM samples was calculated as:

$$\%\ antigen\ on\ the\ cell\ surface = 100 - \left(\frac{F_Q - F_{bg}}{F_{noQ} - F_{bg}}\right) x100$$

where F_Q represents the signal after quenching and F_{noQ} the signal before quenching for every given time point, and F_{bg} the background signal.

The internalisation rate for the biotinylated anti-IgM samples was calculated as:

$$\%\ antigen\ on\ the\ cell\ surface = \left(\frac{F_x - F_{bg}}{F_0 - F_{bg}}\right) x100$$

where F_x represents the signal at time x, F_0 the signal at time 0 (non-internalised control; 100%), and F_{bg} the background signal.

4.12 DAB endosome ablation (I)

The endosome ablation assay was adapted from Pond and Watts (Pond and Watts, 1999). A20 D1.3 cells (10^7/ml) were incubated in FCS-free RPMI for 45 min at 37 °C. Cells were surface-stained on ice with 10 µg/ml of anti-IgM conjugated to biotin for 10 min, followed by one PBS wash. Then, cells were incubated with streptavidin–HRP for 10 min on ice and washed twice with PBS. Internalisation of anti-IgM–HRP was initiated by incubation at 37 °C and 5% CO_2 for different times (10, 20 and 40 min). After that, vesicle trafficking was stopped by incubation on ice

and anti-IgM–HRP-containing endosomes were ablated by addition of 0.1 mg/ml DAB and 0.025% H_2O_2 in freshly prepared DAB buffer for 30 min on ice in the dark. Ascorbic acid is a membrane-impermeable molecule that acts as a radical scavenger inhibiting extracellular HRP activity to avoid DAB deposits on the plasma membrane. As a control, cells were incubated in DAB buffer with 0.1 mg/ml DAB, but without HRP or without H_2O_2. Cells were then washed three times with PBS containing 1% BSA and kept on ice. Viability after the endosome ablation, assessed by Trypan Blue staining, was 95–98%.

4.13 Immunophenotyping (III)

All cells were isolated in Isolation Buffer. Bone marrow cells were isolated by flushing the buffer through mouse femoral and tibial bones. Splenocytes and lymph node cells were isolated by mashing the spleen and lymph nodes in Isolation Buffer with a syringe plunger. Cell suspensions were filtered through 70-µm nylon cell strainers. All steps were carried out on ice in U-bottom 96-well plates at a cell density of 0.25–0.5 × 10^6/well. Fc-block was done with 0.5 µl of anti-mouse CD16/32 antibodies in 70 µl of blocking buffer for 10 min, and cells were stained for 30 min. Washings were done three times in 150 µl of blocking buffer. Before acquisition, cells were resuspended in 130 µl of acquisition buffer. Samples were acquired on BD LSR Fortessa, equipped with four laser lines (405, 488, 561, and 640 nm). The compensation matrix was calculated and applied to samples either in BD FACSDivaTM software (BD Biosciences) or in FlowJo (Tree Star, Inc) based on fluorescence of conjugated antibodies using compensation beads (01-1111-41, Thermo Fisher Scientific). FMO (fluorescence minus one) controls were used to assist gating. Data were analysed with FlowJo software.

4.14 Immunizations (III)

At the age of 8-10 weeks, groups of WT ($CD19^{WT/WT}$ $Rab8a^{flox/flox}$) and $Rab8a^{-/-}$ ($CD19^{WT/Cre}$ $Rab8a^{flox/flox}$) females were immunized with NP-LPS for T-independent (TI-1) immunisation, NP_{40}-FICOLL for T-independent (TI-2) immunization or NP_{31}-KLH for T-dependent (TD) immunization. Each mouse received 25 µg of NP-LPS/50 µg of NP_{40}-FICOLL in 150 µl of PBS or 50 µl of NP_{31}-KLH in 150 µl of Imject Alum-PBS by intraperitoneal injection. Blood (~100 µl) was sampled from lateral saphenous veins on day −1 (preimmunization) and every week after immunization on days +7, +14, +21, and +28 for both FICOLL and KLH cohorts. For the LPS cohort, blood was sampled on days -1, 3, 6, 9, and 12. Secondary immunization of NP-KLH cohort (50 µg in 150 µl of PBS) was performed on day +87 (0) and blood was sampled on days +85 (−2), +91 (+4), +95 (+8), and +102

(+15). Coagulated blood was spun at +4 °C/2.500 rpm for 10 min, and serum was collected and stored at −20 °C.

4.15 Resiquimod-induced lupus model (III)

Mice (8-9 weeks) were treated with resiquimod (R848) to induce lupus-like autoimmunity (Yokogawa et al., 2014). The mice were treated topically on the left ear with 100 µg of R848 in 20 µl of acetone three times per week for six weeks. Blood was sampled as described above (*see* 4.14 Immunizations (III) once per week and sera were stored at -20 °C. Animal welfare was continuously monitored, and urine was sampled once per week and analysed using a Combur-Test strip (Roche) to detect proteinuria. After euthanasia, blood, spleen and kidneys were collected. Haematology and clinical chemistry analyses were done on blood within two hours of collection. The critical care profile was done on a VetScan VS2 analyser using lithium-heparin whole blood. The haematology profile was done on a HM5c haematology analyser using EDTA-treated whole blood. Cells and tissues were analysed using flow cytometry (*see* 4.13 Immunophenotyping (III) and immunohistochemistry (*see* 4.16 Immunohistochemistry (III).

4.16 Immunohistochemistry (III)

Spleens from non-immunised (alum) or NP-KLH-immunised animals were collected 9 days after immunization. Spleens were embedded in O.C.T. compound and snap-frozen in chilled isopentane. 10 µm longitudinal sections were cut with a cryostat by the Histology core facility of the Institute of Biomedicine, University of Turku, Finland. Sections were dried and fixed in 4% PFA for 15 minutes, followed by blocking with Imaging Buffer for 1h at RT. Sections were stained using a three-colour protocol with 1:100 of each of the following antibodies in Imaging Buffer at 4 °C O/N: Alexa Fluor 488® anti-mouse GL-7 (GL-7; Biolegend, #144612), PE anti-mouse CD3 (145-2C11; Biolegend, #100308) and Alexa Fluor 647® anti-mouse B220 (RA3-6B2; Biolegend, #103229). After washing 3 times with PBS, samples were mounted using Prolong Gold with DAPI. Sections were imaged using a Pannoramic Midi fluorescence slide scanner (3DHistech) equipped with a 20X objective and 4 filter sets (DAPI, FITC, Rhodamine/TRITC, Cy5). Tiled sections were exported to TIFF format and analysed with ImageJ.

4.17 ELISpot (III)

NP-specific antibody-secreting cells (ASCs) were measured by ELISpot. ELISpot plates were pre-wet with 15 µl/well of freshly prepared 35% ethanol for < 1 min at

RT. Plates were washed twice with 150 µl/well of sterile water, and wells were coated O/N with 25 µg/ml NP_{24}-BSA in PBS at 4 °C. The next day, plates were washed with PBS and blocked with 200 µl/well of cRPMI for 2 h at RT. Splenocytes were isolated, resuspended in cRPMI and seeded in the wells performing serial dilutions (6, 3 and 1.5 x 10^5 cells/well). Cells were incubated at 37 °C, 5% CO_2 for 18 hours. Cells were washed 5 times with 150 µl/well washing buffer. Biotin-conjugated detection antibodies (2 µg/ml) in 100 µl of blocking buffer were added for 2h at RT followed by 100 µl streptavidin-HRP (1:000) in blocking buffer for 1 h at room temperature (RT). Filtered (0.45 µm pore) TMB was added to the plates for 5 minutes, and wells were extensively washed under running mQ water. Plates were imaged using an AxioZoom microscope (Zeiss) and dots were counted using ImageJ.

4.18 Eα peptide presentation (III)

Antigen presentation was measured using the Eα peptide system (Barlow et al., 1998). For coating, 200 nm Dragon Green Streptavidin beads were used. Beads were washed with 2% FCS in PBS, sonicated to disrupt bead:bead aggregates (Bioruptor®: HIGH, 5 cycles, 30" on/off) and coated with different ratios of biotinylated anti-IgM and biotinylated $E\alpha_{52\text{-}68}$ peptide (Biotin-GSGFAKFASFEAQGALANIAVDKA-COOH) for 1 h at 37 °C. Beads coated with biotinylated anti-IgM alone were used as a control. Cells and beads were incubated for 30 min at 37 °C to allow binding and internalisation, washed, and incubated again at 37 °C. After 4 hours, samples were transferred on ice, washed, blocked with Fc-block and stained with anti-Eα-MHC II antibody for 30 minutes. Then, samples were washed and stained with Alexa Fluor® 633 goat anti-mouse IgG2b (1:500) for another 30 minutes. Samples were washed one more time and acquired on BD LSR Fortessa.

4.19 OT-II proliferation (III)

Streptavidin beads (100 nm) were prepared as described above (*see* 4.18) and coated with different ratios of biotinylated anti-IgM and biotinylated ovalbumin (OVA) (conjugated in-house) for 1 h at 37 °C. Beads coated with biotinylated anti-IgM alone were used as a control. B cells purified from WT or KO spleens labelled with 1 µM carboxyfluorescein succinimidyl ester (CFSE) and T cells purified from OT-II spleens were labelled with 5 µM Cell Trace Violet (CTV) for 20 min at 37 °C in RPMI. Labelled B cells were incubated with the beads for 30 min at 37 °C, washed and incubated together with the labelled T cells (1:1) in a 96-well U-bottom plate for 72 hours. After 3 days, supernatants were transferred to a new plate for cytokine quantification in ELISA and cells were washed, blocked with Fc-block and stained with Fixable Viability Dye eFluor™ 780 (1:1000), APC anti-CD19 (1:200) and PE

anti-CD3 (1:200). Samples were washed one more time and acquired on BD LSR Fortessa. B and T proliferation was analysed using the Proliferation Module in FlowJo.

4.20 ELISA (I, III)

IL-6 secretion was quantified using an ELISA MAX Deluxe Set Mouse IL-6 according to the manufacturer's instructions. Total and NP-specific antibody levels and IL-2 secretion were measured by ELISA on half-area 96-well plates as previously described (Hernández-Pérez et al., 2020; Sarapulov et al., 2020). Autoantibody levels were measured by ELISA using DNA coated plates. Wells were coated overnight at 4 °C with capture antibodies (2 µg/ml), ssDNA (20 µg/ml), dsDNA (20 µl/ml) or NP-conjugated carrier proteins (50 µg/ml; $NP_{(1–9)}$-BSA for high affinity or $NP_{(>20)}$-BSA for all affinities) in 25 µl PBS. Non-specific binding sites were blocked for 1-2 h in 150 µl of blocking buffer and 50 µl of serum samples (for antibody measurements) or supernatant samples (for cytokine measurements) were diluted in blocking buffer and added to the plates (O/N, 4 °C). Results reported correspond to the following serum dilutions: 1:50.000 for total or isotype-specific IgM and IgG2b, 1:75.000 for IgG1 and 1:25.000 for IgG2c and IgG3 antibodies. For autoantibody detection, serums were diluted 1:100. Biotin-conjugated detection antibodies (2 µg/ml) in 50 µl of blocking buffer were added for 1 h followed by 50 µl ExtrAvidin-Alkaline phosphatase (1:5.000 dilution) in blocking buffer for 1 h at RT. Between incubation steps, plates were washed with 150 µl of TBST either three times for the steps before or six times after adding the samples. Finally, wells were washed with 150 µl of water followed by incubation with 50 µl of pNPP (0.5 – 1 mg/ml).

OD was measured at 405 nm. All ELISA samples were run in duplicates, OD values were averaged, and blank background was subtracted. Absolute concentrations of total antibody levels were extrapolated from calibration curves prepared by serial dilution of mouse IgM or IgG subclasses from the C57BL/6 immunoglobulin panel. Relative NP-specific antibody levels were extrapolated from reference curves prepared by serial dilution of pooled serum from day 14 after NP-KLH immunisation, and the highest dilution step received an arbitrary value. Absolute concentrations of interleukins were interpolated from calibration curves prepared by serial dilution of recombinant mouse IL-2 and IL-6.

4.21 BCR Signalling and Immunoblotting (II, III)

For analysis of BCR signalling, isolated splenic B cells were starved for 20 min in plain RPMI, and 2.5×10^6 cells in 100 µl of plain RPMI were stimulated in duplicates with $F(ab')_2$ goat anti-mouse IgM antibodies either in solution or bound to the culture dish surface, for 5, 15 and 30 min. After activation, B cells were instantly lysed with

4X Laemmli buffer with β-mercaptoethanol (to a final concentration of 1X) and sonicated for 5 minutes (High, 30 s on/off cycle, Bioruptor). Lysates (30 µl) were run on 10% polyacrylamide gels and transferred to PVDF membranes using a Trans-Blot Turbo Transfer System (BioRad). Membranes were blocked with 5% BSA in TBS for 1 h and incubated with primary antibodies in 5% BSA in TBST O/N at 4 °C. HRP secondary antibodies (1:20.000) were incubated for 1 h at RT in 5% milk in TBST and washed with TBST (5 x 5 min). Membranes were scanned with ChemiDoc MP Imaging System (Bio-Rad) after the addition of Immobilon Western Chemiluminescent HRP Substrate. Raw integrated densities for each band were measured in Image Studio Lite with appropriate background subtraction methods. Values were normalised to the corresponding loading control for each blot.

4.22 Intracellular Ca^{2+} Flux (III)

Splenic B cells were resuspended at a concentration of 5×10^6 cell/ml in RPMI supplemented with 20 mM HEPES and 2.5% FCS and loaded with 1 µM Fluo-4 and 3 µM Fura Red for 45 min (+37 °C, 5% CO_2) with occasional mixing (Sarapulov et al., 2020). After washing with cRPMI, cells were resuspended at 2.5×10^6 cells/ml in calcium buffer. A 30-second baseline reading was recorded for each sample before addition of $F(ab')_2$ goat anti-mouse IgM (5-10 µg/ml). Calcium flux was monitored for a total time of 5 minutes. Samples were acquired on BD LSR Fortessa using Tube mode, and data was analysed with FlowJo software and presented as the ratiometric measurement of Fluo-4/Fura Red geometric mean (GeoMean) intensity levels.

4.23 Transwell migration / Chemotaxis assay (III)

Chemotaxis assays were carried out using 24-well Transwell chambers with 5-µm pore size polycarbonate membranes. B cells (10^7 cells/ml) were labelled with 0.1 µM CFSE or 0.5 µM CTV for 20 minutes in the incubator (37 °C, 5% CO_2). After incubation, cells were washed twice with cRPMI and resuspended in chemotaxis medium to a concentration of 10^7 cells/ml. WT and KO cells were mixed 1:1 ratio, and dye-switched experiments were systematically performed. The chemotaxis medium with or without CXCL13 (1 µg/ml) or CXCL12/SDF-1α (100 ng/mL) was added to the wells of the receiving plate, and 100 µL cell suspension (10^6 cells/sample) was placed in the transwell insert. Samples were incubated for 4 hours at 37 °C in humidified air with 5% CO_2. After 4 hours, transwell inserts were removed, and the migrated cells in the receiving wells were recovered. Recovered cells were stained with Fixable Viability Dye eFluor™ 780 (FVD) and APC anti-mouse CD19 in PBS-2% FCS containing Fc-block for 30 minutes on ice. After 2 washes in PBS-2% FCS, cells were resuspended in 100 µl of PBS. A known volume

of each sample and the initial cell mix were acquired on BD LSR Fortessa equipped with a high-throughput screening system. After excluding cell debris and gating on singlets and $CD19^+$ FVD^- cells, the percentage of migrating cells (migration index) was calculated by dividing the total number of migrated cells in each well by the total number of input cells determined by FACS x 100.

4.24 RNA isolation and RNA sequencing (III)

RNA was extracted using TRIsure™ from B cells isolated from the spleen or the lymph nodes (non-activated cells) or from co-cultures with OT-II T cells as described above (*see* 4.19 OT-II proliferation (III) and sorted using a Sony SH800S Cell Sorter. After RNA isolation, samples were sent to Novegene (Cambridge, UK). After quality check (RIN > 8), messenger RNA was subjected to library construction and sequenced on the Illumina NovaSeq 6000 platform (PE150, 20 M read pairs per sample). Details about library construction, reads mapping and analysis can be found in Supplementary Materials and Methods (Hernández Pérez et al., manuscript; III).

4.25 Statistical analysis and illustrations (I, II, III)

Statistical significances were calculated using unpaired Student's *t*-test assuming a normal distribution of the data unless otherwise stated in the figure legends. Statistical values are denoted as: $*P < 0.05$, $**P < 0.01$, $***P < 0.001$, $****P < 0.0001$. Graphs were created in GraphPad Prism 6/8, and illustrations were created with BioRender. Figure formatting was done on Inkscape 1.0.

5 Results and Discussion

5.1 B cells employ specialised compartments to degrade antigen (I)

The initiation of T-depended (TD) antibody responses by B cells greatly depends on the presentation of specific antigen peptides to T_H cells. To do so, B cells need to recognise a specific antigen via their BCR, internalised it, and process it into peptides for loading onto the MHC II and presentation. Despite the critical importance of these processes, our knowledge has not significantly increased in the last decades.

The MHC II compartment (MIIC), a specialised compartment or group of compartments where the antigen is processed, is defined by the presence of antigen and MHC II, as well as the peptide loading chaperone H2-M and the protease cathepsin S (Adler et al., 2017b). It has been previously shown that MIICs are multivesicular bodies containing late endosome or lysosomal markers. In this work, we set up a systematic microscopy approach to follow the antigen traffic to the MIIC after internalisation and assessed its colocalisation with different vesicular markers to gain further understanding into its formation and maturation.

5.1.1 Antigen trafficking involves atypical vesicles sharing early and late endosomal markers

Mechanisms of membrane trafficking are largely controlled by the Rab family of small GTPases. Because of that, Rab proteins are commonly used to define sub-populations of vesicles with different functions, such as early endosomes, recycling endosomes, or lysosomes. To characterize the antigen compartments in B cells, we used a cell line, A20 D1.3 B cells, that express a transgenic IgM BCR and can be activated using fluorescent anti-IgM as a surrogate antigen. Consistent with the literature (Aluvihare et al., 1997; Siemasko et al., 1998; Tsui et al., 2018; Vascotto et al., 2007b), we found that the anti-IgM/BCR complexes (referred as “antigen” from now on) were quickly internalised after BCR activation and gathered in a cluster in the vicinity of MTOC after 30-60 minutes (**Figure 7A, B**) (**I; Fig. 1**). In addition, we examined the nature of these vesicles using electron microscopy and,

although with great heterogeneity, we observed antigen in multivesicular bodies 15 min after activation (**Figure 7C**) (**I; Fig. 1**).

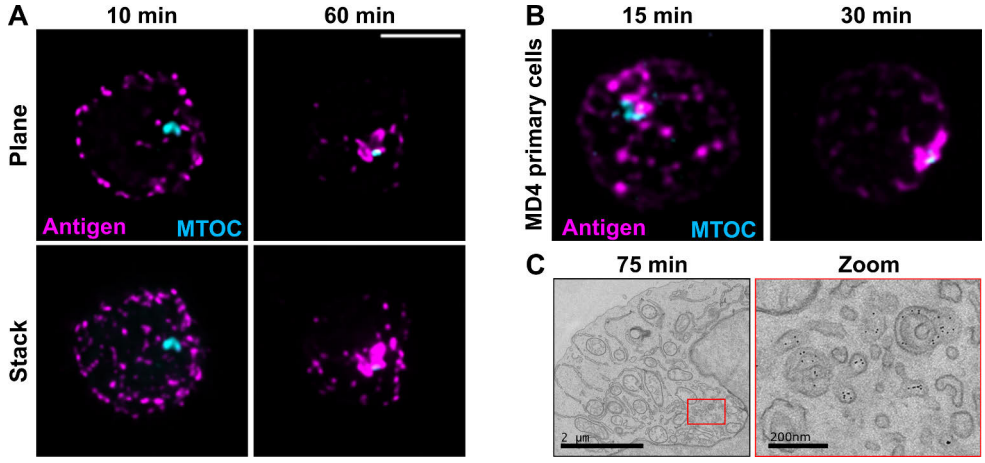

Figure 7. Antigen vesicles traffic to a perinuclear compartment in the vicinity of the MTOC. (**A**) A20 D1.3 B cells were activated with Alexa Fluor-labelled anti-IgM antibodies (antigen, magenta) and stained with anti-PCM-1 (MTOC marker, cyan). Cells were imaged with 3D SDCM and deconvolved. Upper panel, single confocal planes; lower panel, z-projections of 10 µm stacks of representative cells. Scale bar: 5 µm. (**B**) Primary MD4 B cells were activated (antigen, magenta) for different time points and stained with anti-PCM-1 (MTOC, cyan) and imaged as in A. Z-projections of the whole stacks from representative cells are shown. Scale bar: 5 µm. (**C**) A20 D1.3 cells were activated with anti-IgM conjugated to 6 nm colloidal gold particles and imaged using transmission electron microscopy. Adapted from Publication I.

To further examine the nature of these multivesicular structures, we studied the colocalisation of the antigen with Rab5 (EE marker), Rab7 and Rab9 (LE markers), Rab11 (RE marker), and Rab6 (Golgi) as a control. By doing this, we expected to find the antigen in early endosomes ($Rab5^+$) in the early timepoints, followed by a maturation into late endosomes ($Rab7^+$ or $Rab9^+$). However, we detected similar colocalisation of the antigen with the Rab markers, except for the Golgi marker Rab6 (**Figure 8A, B**) (**I; Fig. 2**). This observation could reflect technical challenges to resolve small vesicles close to each other, as vesicles fall under the resolution limit of the optical microscopes (< 200 nm), but it could also suggest the existence of a mixed vesicle population. Intrigued by this, we performed multi-stainings and labelled the same cells with early (Rab5 or EEA1) and late (Rab7, LAMP1 or LysoTracker) markers simultaneously. By doing this, we observed that some of the antigen vesicles were positive for early and late markers (**Figure 8C**). Nevertheless, the markers appeared often partially overlapping and we were still limited by the resolution of light microscopy.

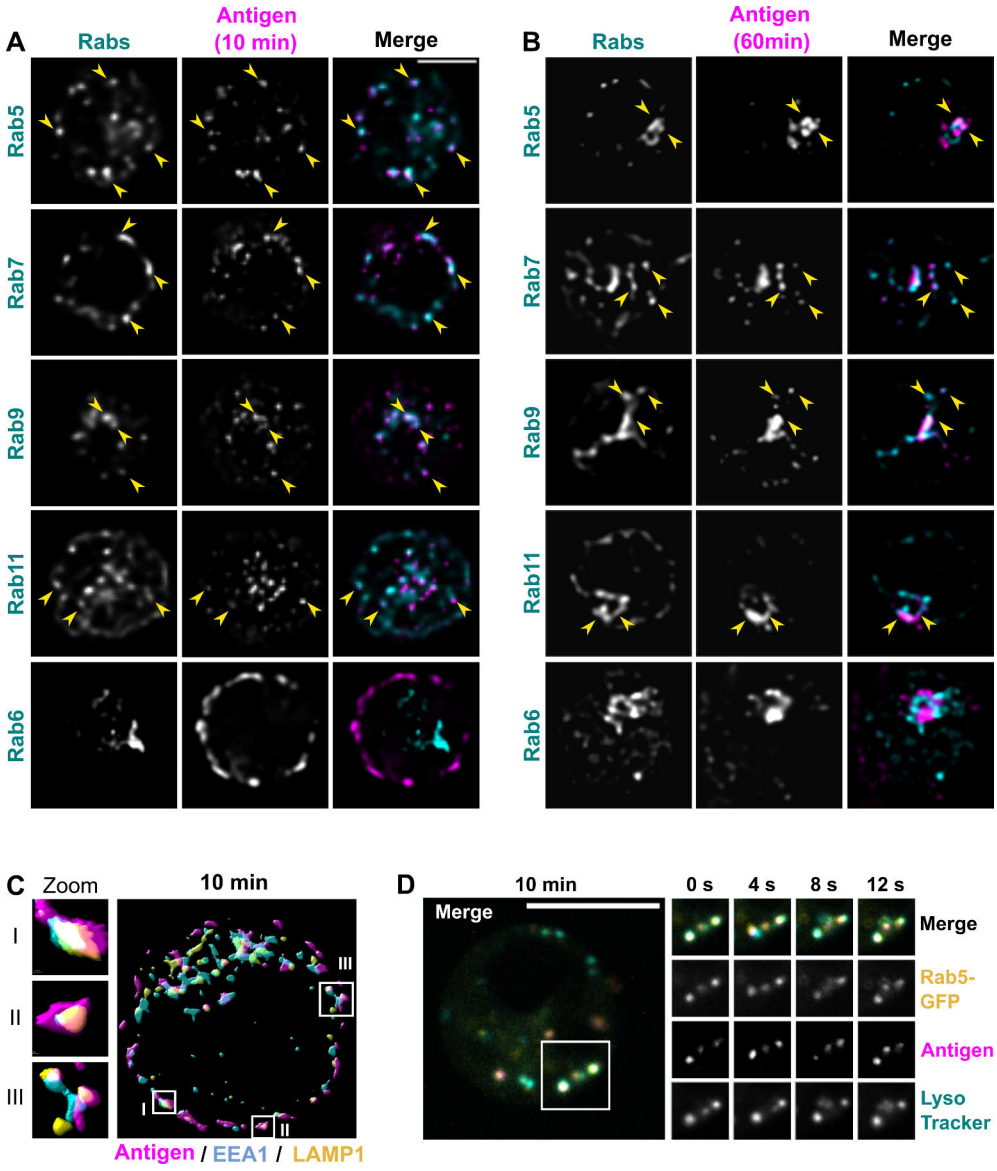

Figure 8. Colocalisation of antigen with early and late endosomal markers. (**A, B**) SDCM imaging of A20 D1.3 cells activated as in Fig. 1 (antigen, magenta) for 10 min (A) or 60 min (B) and immunostained for different Rab proteins (cyan). Single confocal planes from deconvolved images of representative cells are shown, and examples of colocalising vesicles are indicated with yellow arrowheads. Scale bar: 5 µm. (**C**) Surface reconstruction, from the Huygens rendering tool, of SRRF images from samples prepared as in A (antigen, magenta) and immunostained for EEA1 (cyan) and LAMP1 (yellow). (**D**) A20 D1.3 cells were transfected with GFP–Rab5 (yellow), loaded with LysoTracker (cyan) and activated (antigen, magenta). On the left, a merge image of a representative cell after 10 min of activation is shown. On the right, the region in the white square is followed in each channel as a time-lapse for 12 s, starting 10 min after activation. Scale bar: 5 µm. Adapted from Publication I.

Then, we used live imaging to follow the movement of the antigen and its colocalisation with vesicles carrying early and/or late markers ($Rab5^+$/$LysoTracker^+$). Indeed, some of these vesicles were moving together, suggesting that the partial overlap of the markers was not due to the limited resolution, but rather because the compartments were the same or were physically entangled (**Figure 8D**) (**I; Fig. 3**). In addition, the colocalisation with LysoTracker, a dye that labels acidic compartments, hinted that degradation might be possible in these vesicles. These findings indicated that the antigen could traffic in atypical vesicles sharing early and late endosomal features with acidic nature.

5.1.2 Antigen enters degradative compartments shortly after internalisation together with plasma membrane-derived MHC II molecules

Next, we asked the question where and when does the antigen degradation start. To study antigen degradation, we conjugated the antigen to a degradation reporter, DQ-ovalbumin (DQ-OVA). The DQ-OVA reporter is based on self-quenching, as the fluorescent DQ moieties quench each other when the ovalbumin is intact, but they fluoresce upon proteolysis (**Figure 9A**). We detected a clear signal that constantly increased through the analysis period starting at 15-20 minutes using flow cytometry, suggesting that proteolysis can occur relatively fast after antigen uptake (**Figure 9B**). In addition, we investigated the colocalisation of the DQ-OVA signal with cathepsin S, a protease involved in antigen processing, using microscopy. We could detect antigen vesicles positive for CatS as soon as 10 min after activation (**Figure 9C**) (**I; Fig. 4**). These data, together with the finding that antigen could be observed in $LysoTracker^+$ vesicles immediately after internalisation (**Figure 9D, H**) (**I; Fig. 4**), suggested the existence of a specialised and efficient pathway for antigen degradation.

Next, we asked whether these early degradative vesicles might contain MHC II and H2-M to be able to load the processed peptides for presentation. Using spinning disk microscopy and structured illumination microscopy (SIM), a super-resolution technique, we detected antigen vesicles positive for MHC II soon after activation. SIM images showed a remarkable colocalisation between the antigen and MHC II channels, as they almost perfectly overlapped (**Figure 9E**) (**I; Fig. 5A**). In addition, we found H2-M in the antigen vesicles 10 minutes after internalisation, suggesting that indeed these compartments could readily degrade and load the antigen for presentation.

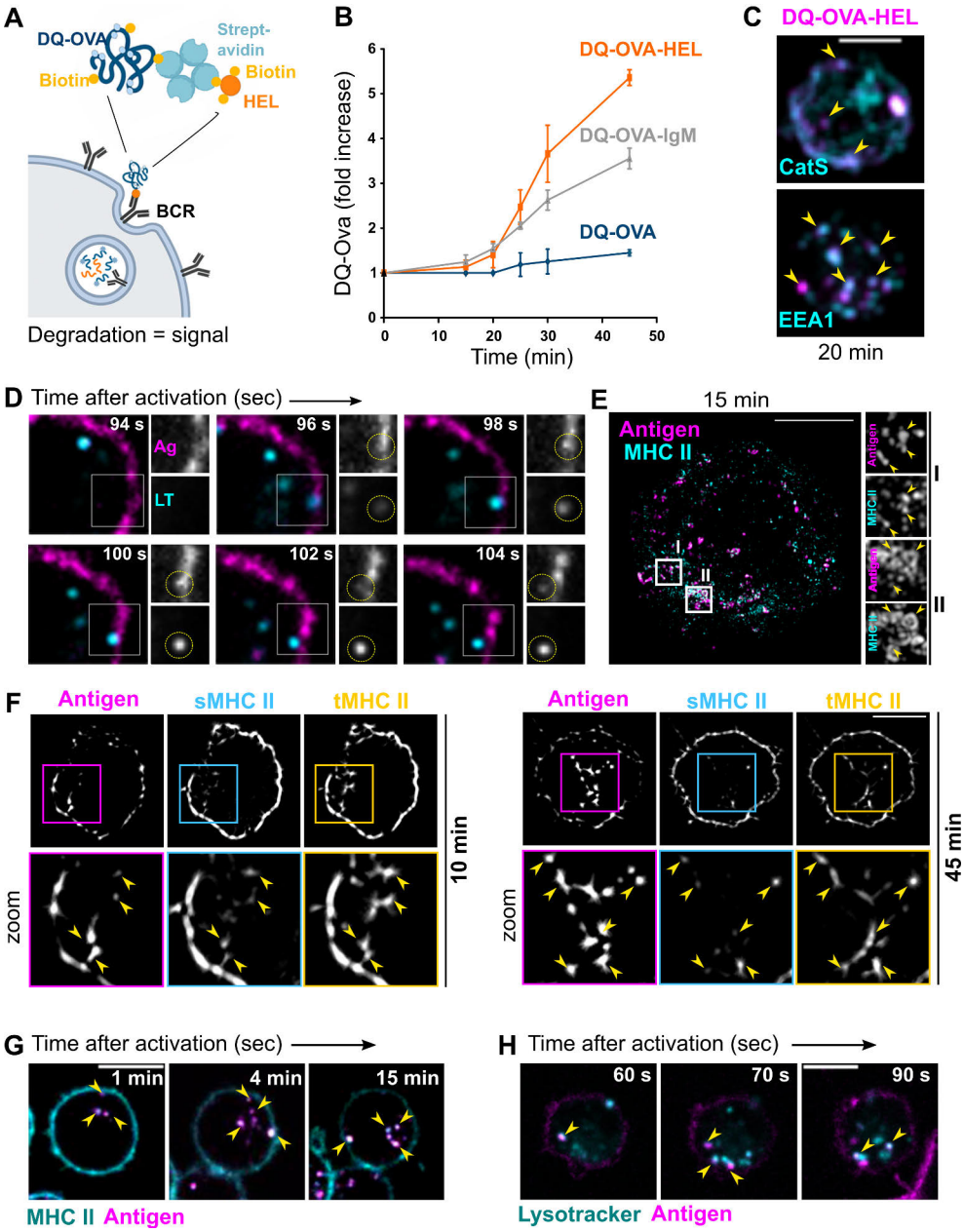

Figure 9. Internalised antigen incorporates into degradative vesicles with low pH and membrane MHC II. (**A**) Schematic view of the DQ-Ova–antigen (lysozyme; HEL) used to probe proteolysis of internalised antigen. (**B**) DQ-Ova and DQ-Ova–antigen (anti-IgM or HEL) degradation as assessed by flow cytometry. Results are shown as fold increase. (**C**) A20 D1.3 cells activated with DQ-Ova–HEL (magenta) for 20 min and stained for EEA1 or CatS (cyan). Images were acquired using SDCM with the EVOLVE (EMCCD) camera. z-projections of representative cells are shown with examples of colocalising vesicles indicated with yellow arrowheads. *Continues.*

Figure 9. Internalised antigen incorporates into degradative vesicles with low pH and membrane MHC II (*continues*). Scale bar: 5 µm. (**D**) A time-lapse of an example movie highlighting a probable fusion event between an internalising antigen (Ag) vesicle and a LysoTracker (LT)-stained vesicle (dashed yellow circle). A white square in the merge image (left) depicts the region shown for the single channels in the right-hand panels. (**E**) SIM imaging of A20 D1.3 cells activated with AF647-anti-IgM (antigen, magenta) for 15 min and stained for MHC II (cyan). Scale bar: 5 µm. (**F**) A20 D1.3 cells (plane image; antigen in magenta) were stained with anti-MHCII (AF488) before activation to label surface-bound MHCII (sMHCII, cyan). After activation for 10 or 45 min at 37°C, cells were fixed and permeabilised and stained with anti-MHCII and a secondary antibody (AF633; tMHCII, yellow). Samples were imaged and post-processed to obtain SRRF super-resolution images. Upper panel: representative cell; lower panel, magnification of the region shown by the coloured square in the upper panel. Examples of colocalising vesicles are indicated with yellow arrowheads. Scale bar: 5 µm. (**G-H**) Live imaging of A20D1.3 stained on ice with (G) AF488-anti-MHCII (cyan) or (H) loaded with LysoTracker and activated with RRx-anti-IgM (antigen, magenta). Samples were imaged every 5 s using SDCM after 1 min at 37°C (ORCA camera). A time-lapse from a representative cell is shown, and examples of colocalising vesicles are indicated with yellow arrowheads. Scale bar: 5 µm. Adapted from Publication I.

To further examine the origin of the MHC II molecules in these compartments, we set up a surface discrimination assay. Prior to activation of the cells at 37 °C, the cells were labelled with fluorescent anti-IgM and anti-MHC II without permeabilization, allowing us to visualise the molecules on the surface of the cell (surface MHC II; sMHCII). After activation at 37 °C and internalisation of the antigen, cells were fixed, permeabilised and stained with anti-MHC II to detect the total MHC II (tMHCII) in a different colour (**I; Fig. 5B**). By studying the signal of the two channels (sMHCII vs tMHCII), we could differentiate between the sMHCII, internalised from the cell surface together with the BCR, or the total MHC II. Interestingly, we observed a strong colocalisation of sMHCII with the antigen vesicles after internalisation in fixed samples and live imaging (**Figure 9F, G**) (**I; Fig. 5C, D**). The colocalisation with the sMHCII was higher soon after internalisation (10 minutes), although some antigen vesicles were still positive for sMHCII after 45 minutes. However, at this timepoint, we observed also antigen vesicles positive for tMHCII but negative for sMHCII, indicating that these MIIC contained MHC II that was not derived from the PM, but some other intracellular compartment, such as newly synthesised MHC II from the trans-Golgi network. Based on these findings, we outlined a model pathway where two different processing routes may play different functions, as discussed in the next section (**Figure 10**).

5.1.3 Discussion and future perspectives (I)

B lymphocytes are unique APCs, as they recognise and present BCR-restricted antigens with striking efficiency. To do so, BCR-antigen complexes need to be internalised to deliver the antigen to the intracellular antigen-processing compartments or MIIC. This process is fundamental as B cells need to present the peptide-MHC II complex to receive T cell help and achieve full activation (Lanzavecchia, 1990). The exact nature and origin of MIIC have been for long a matter of debate. The MIIC is a special lysosome-like compartment characterised by the presence of loading chaperones, such as H2-M, and proteolytic enzymes, such as CatS, together with antigen-BCR complexes and MHC II (Guagliardi et al., 1990; Neefjes et al., 1990; Peters et al., 1991). Interestingly, these compartments are dynamic, as they can change upon BCR stimulation, making their study and classification technically challenging (Aluvihare et al., 1997; Anderson et al., 1999; Cheng et al., 1999a; Lankar et al., 2002; Xu et al., 1996). Some studies reported that peptides can also be loaded on the MHC II in the EEs and possibly even on the PM, questioning the requirement of the MIIC (Arndt et al., 2000; Castellino and Germain, 1995; Pinet and Long, 1998; Pinet et al., 1995).

The early studies of the B cell antigen-processing compartments were conducted using biochemical techniques, such as cell fractionation, radiolabelled antigen, and electron microscopy (Amigorena et al., 1994b; Lankar et al., 2002; West et al., 1994). In our study (I), we revisited these data aiming to verify those findings using modern microscopy and to gain new knowledge about the dynamics and subcellular localisation of the MIICs. Consistent with previous studies, we observed that the localisation of the antigen vesicles changed from dispersed (5-20 min) to clustered in a perinuclear compartment around the MTOC (20-60 min) (Lankar et al., 2002). Our data revealed that antigen-containing vesicles possessed a remarkable heterogeneity, as antigen was found to colocalise with Rab5 (EEs), Rab 7 and 9 (LEs), and Rab11 (REs) (**Figure 7-8**) (**I; Fig. 1-3**). Interestingly, we found that some antigen vesicles partially overlapped with both EE and LE markers. This overlap would suggest that these vesicles do not follow the "Rab conversion" model, where EEs sequentially lose Rab5 and acquire Rab7 to become LEs. Instead, the data would rather fit with the idea that different markers are segregated in different endosomal subdomains and could generate new vesicles from budding (Huotari and Helenius, 2011). However, our study had several limitations. First, the small size of the endosomes was a major challenge for the colocalisation analyses, as the resolution of optical microscopy is limited by the light wavelength (200 nm). Second, the pulse-chase assay used to study the antigen colocalisation with the vesicles also had shortcomings. In this assay, the cell surface was pre-labelled with fluorescent surrogate antigen (anti-IgM antibodies), followed by an activation time at 37 °C. During this time, the antigen was internalised, but part of the labelled antigen (25-

75% depending on the time point) remained on the cell surface (**I; Fig. S2**), artificially modifying the colocalisation coefficients. We addressed this issue in a separate study (II) (Hernández-Pérez and Mattila, 2022). To partially overcome these challenges, we studied the antigen vesicles using live imaging and super-resolution microscopy. We observed that the antigen vesicles positive for EE and LE markers often moved together, indicating that the colocalisation overlap was not only due to the limited resolution of the microscopes, but because of a physical entanglement. In addition, it has also been recently shown that the autophagic machinery is recruited to antigen-containing compartments after BCR internalisation (Martinez-Martin et al., 2017; Schmid et al., 2007; Watanabe and Tsubata, 2009). We have also detected the colocalisation of LC3, an autophagy marker, with the antigen in our B cell line (Runsala et al., unpublished data) and ring-like structures compatible with autophagosomes (**I; Fig. 5A**). This could also explain the vesicle heterogeneity observed in our study, as the autophagy machinery can recruit lysosomes to early endosomes (Fraser et al., 2019), and this idea deserves further investigation.

Next, we investigated the degradative capacity of the antigen vesicles. We observed a very fast acidification process, as the antigen vesicles quickly became Lysotracker^{+}. In addition, these vesicles were able to degrade proteins, as demonstrated by antigen colocalisation with DQ-OVA and CatS (**Figure 9**) (**I; Fig. 4**). These vesicles also possessed MHC II and H2-M, further supporting their classification as MIIC (**Figure 9**) (**I; Fig. 5**). However, we termed these vesicles early MIIC (eMIIC) as, compared to the MIIC classically described in the literature, they appeared soon after antigen internalisation (5-15 min), were dispersed, and additionally colocalised with EE markers. Our results are in line with previous studies showing antigen in LEs after 10 minutes, degradation of the antigen as early as 10-20 minutes after shifting the cells to 37 °C, and peptide presentation after 20 minutes (Aluvihare et al., 1997; Davidson and Watts, 1989). Nevertheless, studies have also shown that, although MHC II can be internalised and recycled from the PM, the majority of the processed antigen was loaded onto newly synthesised MHC II molecules (Aluvihare et al., 1997; Davidson et al., 1991; Reid and Watts, 1992; Roche et al., 1993). However, these studies were done using biochemical approaches together with inhibitors such as cycloheximide, a drug that blocks *de novo* protein synthesis. Hence, to evaluate those findings and examine the origin of the MHC II molecules in the eMIICs, we set up a surface discrimination assay using microscopy. We found that early antigen vesicles (eMIIC, < 20 min) contained MHC II internalised from the PM together with the antigen-BCR complexes. At later time points, some antigen vesicles remained positive for surface MHC II, but a majority of the antigen was found with intracellular MHC II (**Figure 9**) (**I; Fig. 5**). Hence, our data, together with previous reports, suggest that two different processing routes might exist: a fast-track route where antigen is processed in eMIIC and loaded on

MHC II internalised from the PM, and a slow route where antigen is processed in MIIC and loaded on *de novo* synthesised MHC II (**Figure 10**). The different functional outcomes of these routes deserve further investigation. Interestingly, the peptide repertoire seems to differ depending on the compartment where the antigen is processed (Griffin et al., 1997; Lindner and Unanue, 1996). Therefore, these two different pathways might support the presentation of different peptide repertoires to activate different T cell clones. In addition to that, the eMIIC fast route might be needed for prompt activation of the humoral responses, while the MIIC route might support a more sustained activation by delaying peptide presentation.

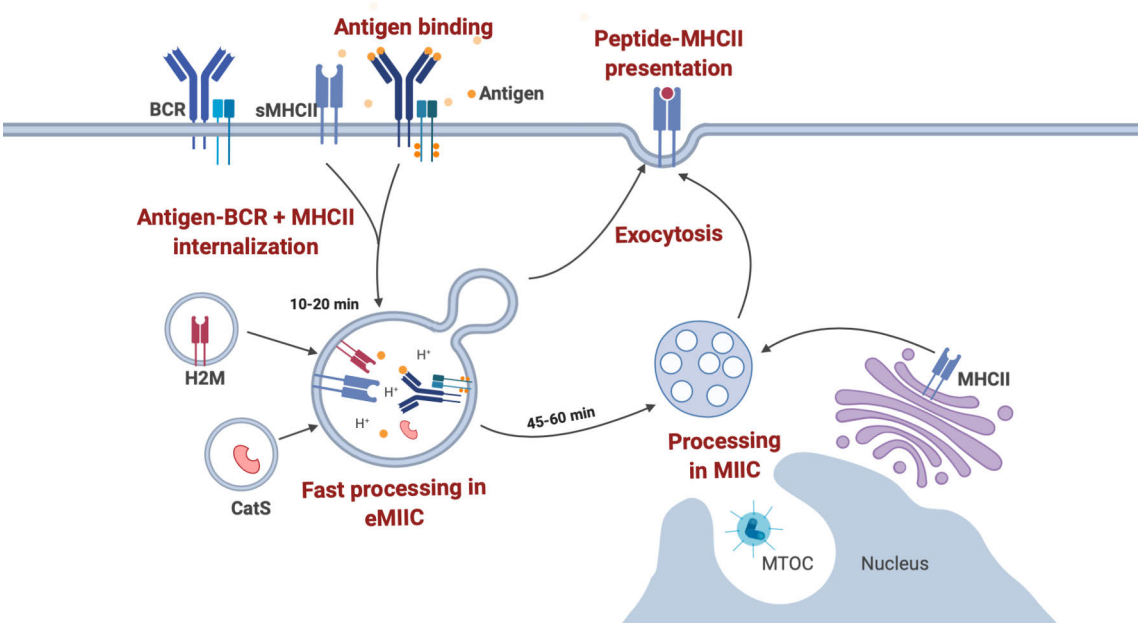

Figure 10. Schematics of the model proposed here for antigen processing in B cells. (e)MIIC: (early) MHC II compartment. MTOC: microtubule organising centre.

5.2 The SHIP system enables improved imaging of internalised antigen in B cells (II)

Facilitated by the latest improvements in microscopy in recent years, our understanding of the complexity and dynamics of the intracellular vesicle trafficking has drastically increased. However, notable challenges remain associated to the use of microscopes have arisen when studying cargo sorting to endosomal compartments. For instance, in small or round cells, such as lymphocytes, super-resolution techniques are needed to discern the internalisation status of the cargo/receptors. However, even with the most modern imaging techniques, analysis of the plasma membrane-bound (outside) or internalised (inside) ligands remains technically challenging. In our previous work, we characterised the antigen processing route in B cells by analysing different vesicle markers using spinning disk confocal microscopy (Hernández-Pérez et al., 2020). However, unambiguous distinction between surface and internalised BCRs was a major obstacle in the study, as inaccurate determination of the extracellular and intracellular cargo can ultimately skew the analyses, misguiding the interpretation of the data.

In 2013, Liu and Johnston developed a method termed specific hybridization internalisation probe (SHIP) assay able to differentiate between internalised and non-internalised material in fixed and live cells (Liu and Johnston, 2013). The SHIP assay utilises a short (20-mer) fluorescent single-stranded DNA (ssDNA), termed fluorescent internalisation probe (FIP), that can be coupled to any ligand of interest, and a complementary ssDNA quenching probe (QP). This elegant assay can be used to analyse the kinetics of cargo internalisation, and it has been applied in the past to the study of nanoparticles, antibody-dependent phagocytosis and MHC II turnover in dendritic cells (Ana-Sosa-Batiz et al., 2017; Liu et al., 2016a; Liu et al., 2016b; Mann et al., 2016). Nevertheless, these studies relied on high-throughput flow cytometry, leaving the great potential of this technique for imaging largely unexplored. Hence, we evaluated how the SHIP assay could be used to study the trafficking of receptor/ligand complexes using modern microscopy and BCR-antigen internalisation as a model system (**Figure 11A**) (**II; Fig. 1B**).

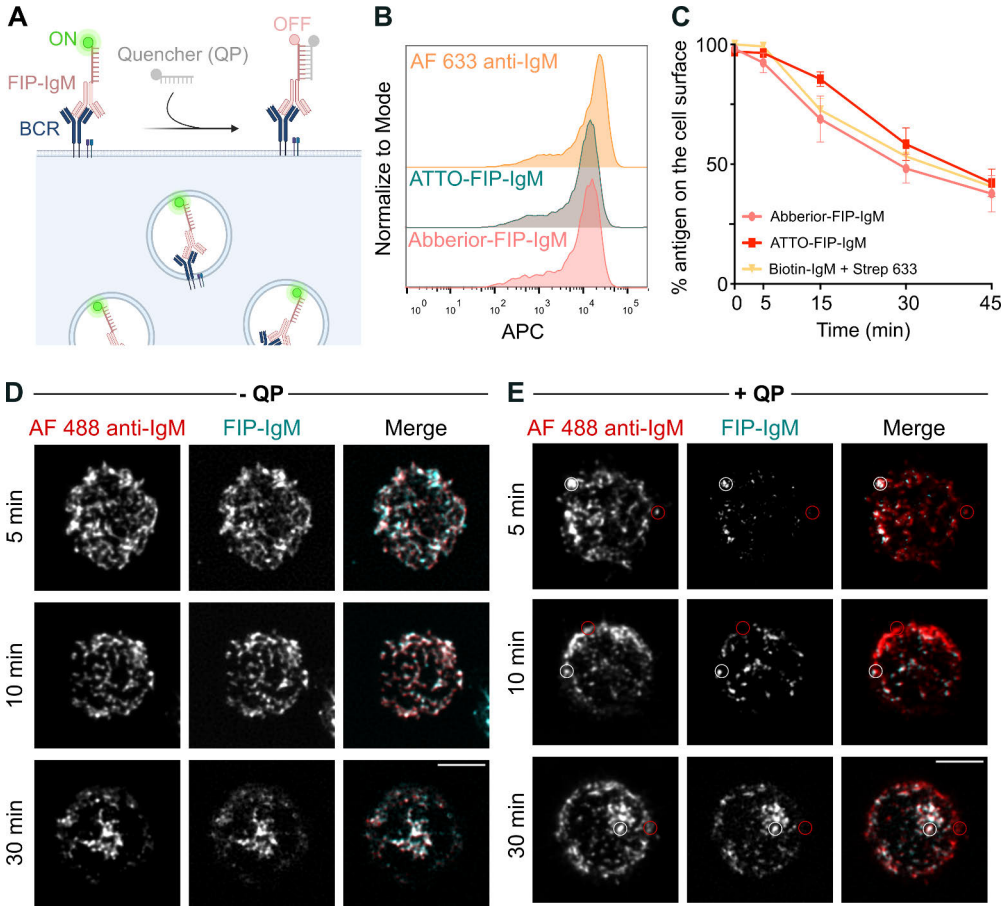

Figure 11. BCR internalization and trafficking is not disturbed by the SHIP assay. (A) Schematic of the SHIP assay. (**B**) B cells were engaged on ice with a commercial AF633 anti-IgM antibody, ATTO-FIP-IgM or Abberior-FIP-IgM and analysed by flow cytometry to verify the labelling and binding of the FIP-labelled antibodies. (**C**) BCR internalisation assay by flow cytometry. B cells were engaged on ice with Abberior-FIP-IgM (Abberior-FIP), ATTO 647N-FIP-IgM (ATTO-FIP) or biotinylated anti-IgM (Biotin-Strep). After the indicated time points, cells were placed on ice and quenched (FIP samples) or stained with Streptavidin 633 (Biotin-Strep samples) to analyse the amount of BCR inside or outside the cell respectively (n = 3; mean ± SEM). (**D, E**) B cells were stained with ATTO-FIP-IgM and anti-IgM Alexa Fluor 488, and activated at different time points. After activation, cells were incubated with (D) PBS or (E) QP for 10 min and fixed. Images were acquired using a SDCM. A representative image of one cell (stack, sum intensity projection) is shown. White and red circles mark examples of internalised and non-internalised antigen, respectively. Scale bar: 5 µm. Adapted from Publication II.

5.2.1 FIP-IgM does not perturb the normal internalisation and traffic of BCR

As a model for BCR-antigen internalisation, we employed anti-IgM antibodies, commonly used in the literature as surrogate antigen, to engage the BCR and trigger robust B cell responses. Due to their size and stability, antibodies are easy to label in-house. We labelled these antibodies with a FIP conjugated to Abberior® STAR 635P (Abberior-FIP-IgM) or ATTO 647N (ATTO-FIP-IgM), two dyes commonly used in super-resolution microscopy. After verification of the labelling (**Figure 11B**), we proceeded to test the system. Labelling with the FIP did not interfere with the antibody-BCR internalisation nor with B cell activation, compared to the equivalent unlabelled antibody. In addition, the internalised cargo was normally delivered to the processing compartments, verifying that the FIP oligo did not interfere with normal BCR trafficking (**Figure 11C**) (**II; Fig. S1**).

5.2.2 The SHIP assay allows for reliable colocalisation analysis in fixed cells

Next, we tested the potential of the SHIP assay to image fixed samples. We labelled the A20 D1.3 cells on ice with the FIP-antigen (ATTO-FIP-IgM) as previously described (**I**) and let them to internalise it. Samples with and without the QP were prepared simultaneously to compare the effect of the quencher and to measure the improvement provided by the SHIP assay. In addition to the ATTO-FIP-IgM, samples were also labelled with a conventional Alexa Fluor 488 (AF488) anti-IgM antibody as a control. As expected, the samples without the quencher (- QP) resembled the conventional setup where the extracellular and internalised ligands could not be differentiated (**Figure 11D**) (**II; Fig. 1C**). The signal from ATTO-FIP-IgM and the AF488 anti-IgM were indistinguishable and we observed a similar amount of antigen (intensity) through the experiment (5-30 min), with only visible changes in the localisation. At 5 minutes, most of the antigen was found in the periphery of the cell, either on the plasma membrane or in vesicles close to the membrane, while at 30 minutes, it trafficked to the perinuclear compartment (as described in **I**). On the contrary, samples treated with the quencher (+ QP) showed remarkable differences (**Figure 11E**) (**II; Fig. 1D**). When comparing the antigen signal at 5 minutes, only few vesicles were visible in the FIP-IgM channel, making apparent that majority of the AF488 anti-IgM signal was clustered on the plasma membrane. However, at later timepoints, most of the antigen found was inside the cell, as evidenced by the high colocalisation between AF488 anti-IgM and FIP-IgM. Nonetheless, even at 30 minutes, some antigen remained on the plasma membrane (non-internalised; AF488 anti-IgM$^+$ / FIP-IgM$^-$), consistently with the quantifications performed by flow cytometry (**II; Fig. S1B**).

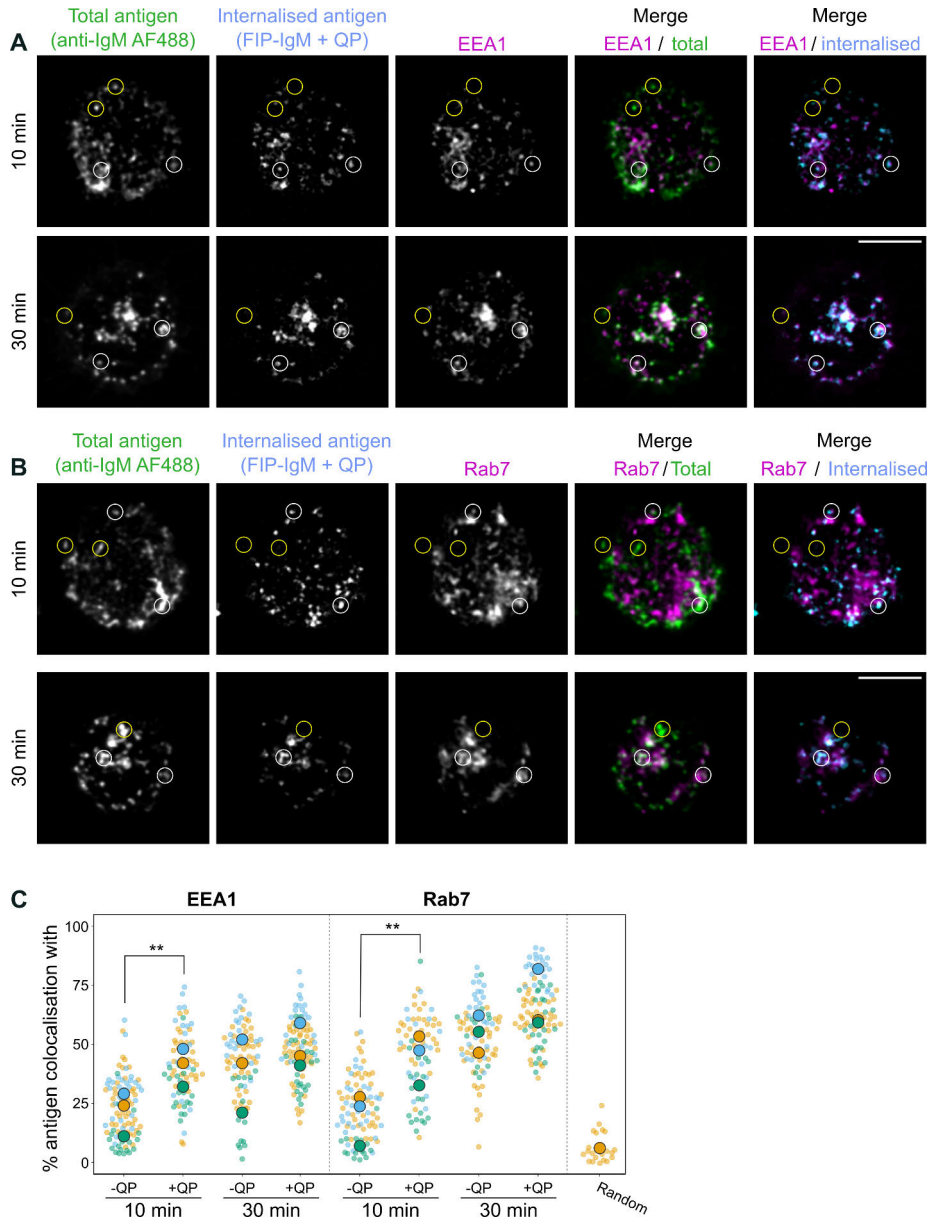

Figure 12. Colocalisation of the antigen with early and late endosomal markers. (A, B) B cells were engaged with ATTO-FIP-IgM and anti-IgM AF488, and activated for 10 or 30 min at 37 °C. After activation, cells were quenched, fixed and stained for (A) EEA1 or (B) Rab7. Images were acquired using a SDCM. A representative image of one cell (stack, sum projection) is shown. The white and yellow circles mark an example of internalised or non-internalised antigen, respectively. Scale bar: 5 µm. **(C)** Colocalisation analysis of the internalised antigen with EEA1 and Rab7. Colocalisation was measured using thresholded Mander's overlap coefficient (tM1 = % of antigen colocalising with EEA1 or Rab7). Different colours represent independent experiments: the mean of each experiments is shown with large symbols, and small symbols show the measured cells. As a control for random colocalisation, one channel was rotated 90° and colocalisation was measured. $^{**}P < 0.01$, paired t-test (n = 3). Adapted from Publication II.

We next proceeded to test the colocalisation of different vesicle markers with the internalised antigen using the conventional (AF488 anti-IgM; total antigen) and the SHIP (FIP-IgM + QP; internalised antigen) systems. As expected, we found that, at 10 minutes, the colocalisation of the internalised antigen with the early endosomal marker EEA1 and the late endosomal marker Rab7 was increased, compared to the total antigen (**Figure 12**) (**II; Fig. 2**). This increase in the colocalisation, measured by Mander´s overlap, was due to the elimination of the background signal (non-internalised antigen on the PM) that cannot colocalise with the vesicles. Hence, the SHIP assay provided an advantageous system to measure precise colocalisation of internalised cargo with intracellular proteins. The benefits of the system were more noticeable in early timepoints, as in the later timepoints (30 minutes), majority of the antigen could be found clearly inside the cell (**Figure 11 and 12**) (**II; Fig. 1 and 2**).

5.2.3 The SHIP system is compatible with live and super-resolution imaging

Since we found no reports demonstrating the use of the SHIP assay in living cells, we next evaluated its potential for live imaging at different timepoints (**Figure 13A**) (**II; Fig. 3**). We observed that only a few seconds after addition of the QP to the cells, the extracellular FIP signal was dramatically quenched under our eyes. Notably, after quenching the non-internalised signal, the visualisation of the internalised vesicles was clearly enhanced, proving the benefit of the SHIP system. In addition to 2D live imaging, we also tested the SHIP system in 3D live imaging. Since the FIP oligo was conjugated to ATTO 647N, a bright and stable fluorophore, we were able to perform constant 3D live imaging over short times (15 minutes) without compromising the image quality (**Figure 13B**). In order to acquire even faster images to improve the temporal resolution, we turned to deep-learning image restoration algorithms, such as Content-Aware Image Restoration (CARE) (von Chamier et al., 2021). Using CARE, we were able to image the whole cell volume in 3D with a temporal resolution of 3-4 seconds (**Figure 13C**) (**II; Fig. 5**). Hence, we demonstrated that the SHIP assay could be successfully applied to the live imaging of internalised cargo in 2D and 3D, defeating once more the conventional imaging without quenching.

Due to the diffraction limit of light, traditional confocal microscopy cannot resolve structures below 200-250 nm. Importantly, many cellular structures, including vesicles, fall below this limit, so researchers are now turning to super-resolution imaging modalities to solve long-standing biological questions. Hence, we tested if the SHIP assay could be used in combination with super-resolution techniques to study the traffic of internalised cargo. We tested the system using different microscopy modalities available to researchers worldwide: stimulated

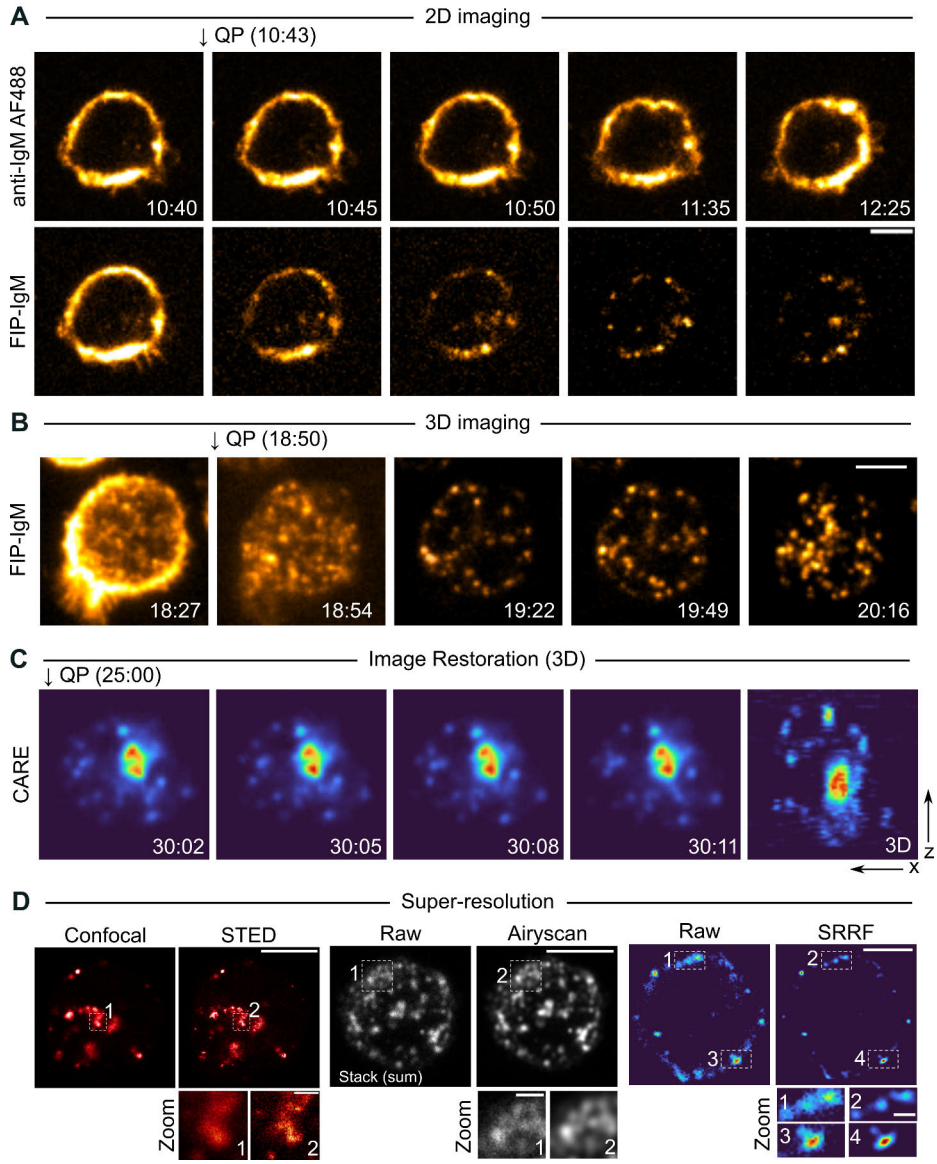

Figure 13. The SHIP assay improves live cell imaging and super-resolution imaging of antigen trafficking. (A) B cells were attached to a fibronectin-coated dish and engaged on ice with ATTO-FIP-IgM and Alexa Fluor 488 anti-IgM. Cells were transferred to 37 °C for 10 min to allow antigen/receptor endocytosis. The recording was started and after 40 s QP was added (arrow) to the cells without interrupting image acquisition. Images were acquired using a SDCM (one slice, one frame every 5 s). (**B**) B cells were attached and activated as described in (A). QP was added to the cells at indicated time point (arrows) after activation without interrupting image acquisition. Images were acquired using a SDCM (49 planes, one stack every 27 s). Scale bar: 5 µm. (**C**) Short acquisition time images (raw image) were acquired using a SDCM (49 planes, one stack every 3.7 s) and restored using CARE. Time in minutes after triggering endocytosis is indicated in the top-left corner. Scale bar: 5 µm. (**D**) Cells were activated as in (A) and imaged with STED, Airyscan or SRFF. Scale bar: 5 µm; scale bar of the inset: 1 µm. Adapted from Publication II.

emission depletion (STED) microscopy, an Airyscan confocal microscope (Huff, 2015; Huff et al., 2017) and super-resolution radial fluctuations (SRRF) on a spinning disk confocal microscope (Gustafsson et al., 2016) (**Figure 13D**) (**II; Fig. 6**). We found that the SHIP assay was compatible with all the tested techniques using fixed samples. The increase in the resolution, especially in STED and SRRF, clearly improved the separation of the vesicles, unveiling also small vesicles locating close to each other.

5.2.4 Discussion and future perspectives (II)

Our study probed the combined potential of the SHIP assay together with multiple imaging modalities, such as live-cell imaging and super-resolution microscopy, to specifically detect and image internalised receptor/ligand complexes in fixed and live cells (**Figure 14**).

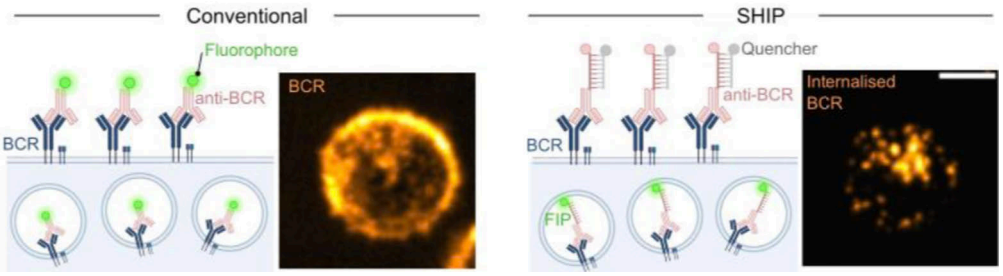

Figure 14. Schematics of the SHIP assay (right) compared to conventional imaging (left). The use of FIP-IgM (anti-BCR) together with the quencher allows for specific imaging of internalised antigen:BCR complexes in B cells.

Hence, although we tested the system using antigen:BCR in lymphocytes, the SHIP assay could be applied in future research to facilitate the study of internalised cargo and receptors in different cell types. The SHIP assay has numerous advantages over traditional imaging: it can clearly distinguish between non-internalised and internalised ligands, and it allows for improved colocalisation analysis in fixed cells and improved cargo tracking in live cells. In addition, the assay is easy to set up in the lab and it allows certain flexibility in the design of the oligos and the choice of fluorophores. In addition, since the SHIP assay is based on the specific recognition of two complementary ssDNA probes, it would be very interesting to expand the system to allow multiple simultaneous labels. At the moment, the SHIP assay has only been used to track the internalisation of one ligand at a time, but two different complementary pairs, such as ATTO647N-FIP/QP-BHQ3 and ATTO488-FIP/QP-BHQ1 could be, in theory, used.

The main drawback of the system is the high cost of the oligo synthesis, as the FIP oligos require of two modifications: a reactive modification for the chemical coupling

to the cargo and the fluorophore modification. Thus, when setting up the system, we decided to label the antibodies using a 2x molar excess of oligo, yielding a degree of labelling (DOL) of 1-2. Although this DOL was good for conventional microscopy, such as spinning disk confocal microscopy, a higher degree of labelling might improve the signal in live imaging and super-resolution imaging. For instance, both Airyscan and SRRF are compatible with live-cell imaging, but these methods require a bright signal to obtain high-quality data. As a result of the limited amount of antigen internalised at early timepoints, and possibly influenced by the low DOL, the low brightness of the samples hampered the acquisition of live super-resolution images (data not shown). Hence, whether a higher DOL would further improve the imaging remains to be tested, as an optimal fluorophore:antibody ratio of 2-8 has been described (Vira et al., 2010). Although this was not a limitation in our study, the size of the reporter (antibody or tag) can be detrimental in more demanding super-resolution experiments, such as in single-molecule localisation microscopy. For instance, a primary antibody together with a labelled secondary antibody add an estimated error of up to 30 nm between the epitope and the reporter (Sahl et al., 2017). The use of smaller epitope-binding fragments, such as nanobodies (5 nm), as secondary antibodies can partially overcome this problem by reducing the error to about 15-20 nm (Pleiner et al., 2015). Here, we directly labelled our primary antibody with a fluorescent oligo (20 nt, about 5 nm), hence reducing the estimated error to 15-20 nm. To further improve this set-up, it would be possible the directly conjugate the DNA oligo to a smaller epitope-binding fragment, such as a Fab fragment (9 nm) or nanobody against the protein of interest, decreasing the error to about 9-15 nm. However, these fragments would need to be produced and purified in the lab, as they are not commonly available.

Although the SHIP system has been only used to study the internalisation of cargo (Ana-Sosa-Batiz et al., 2017; Liu et al., 2016a; Liu et al., 2016b; Mann et al., 2016), it would be interesting to exploit the system to study different biological processes. For example, B lymphocytes need to extract the antigen encountered on the surface of antigen presenting cells in order to get activated (Hoogeboom and Tolar, 2015; Spillane and Tolar, 2017; Spillane and Tolar, 2018; Yuseff et al., 2011). Different set-ups are currently used to investigate antigen extraction. For example, OVA-antigen-coated beads are stained with anti-OVA antibodies and the OVA fluorescence decrease is quantified (Yuseff et al., 2011). However, this approach offers an indirect readout of the antigen extracted by quantifying the antigen that remains still attached to the presenting surface. As an alternative approach, plasma membrane sheets functionalised with fluorescent antigens have been used to image antigen extraction (Nowosad and Tolar, 2017). We hypothesized that the SHIP system could be applied to the study of antigen extraction by coupling the FIP-IgM to the beads or the plasma membrane sheets. The use of the QP would allow for the quenching of the non-extracted antigen, while allowing an easy quantification of the extracted antigen inside the cell using flow cytometry or microscopy.

5.3 Loss of Rab8a leads to hyperactive immune responses (III)

Tight spatiotemporal control of the vesicular traffic inside and outside the cell is critical for maintaining cellular homeostasis and regulating cellular responses to different cues. Rab GTPases are regulators of the secretory and endocytic pathways and, by targeting membrane compartments, they define the structural and functional identity of intracellular organelles (Stenmark, 2009; Stenmark and Olkkonen, 2001; Zerial and McBride, 2001). More than 60 different Rab proteins have been found in humans, controlling not only vesicle trafficking but many other cellular processes. In our previous work, we followed the colocalisation of the internalised antigen with Rab5, 6, 7, 9 and 11 along the endocytic route (Hernández-Pérez et al., 2020). Nevertheless, the role of the small Rab GTPases in B lymphocytes has not been extensively studied. Only a few reports have shown a direct link between Rab GTPases and antibody responses. For instance, Rab7 is needed to regulate AID (activation-induced cytidine deaminase) expression, controlling class-switch recombination (CSR) in T-dependent and T-independent antibody responses (Lam et al., 2016; Pone et al., 2015).

Rab8 (Rab8a and Rab8b) is a ubiquitous small Rab GTPase. Rab8a localises to the endosomal recycling compartment together with Rab11 and Arf6, promoting the polarized transport of newly synthesised proteins (Hattula et al., 2006). There are few studies to date describing the role of Rab8 in immune cells, and studies are exceedingly scarce in B lymphocytes. In T lymphocytes, Rab8 is implicated in TCR recycling and final docking to the immune synapse via its interaction with VAMP3 (Finetti et al., 2015b). In macrophages, Rab8a interacts with PI3Kγ in membrane ruffles and early macropinosome membranes and regulates TLR signalling, inflammation and polarisation using the AKT/mTOR pathway (Luo et al., 2014; Luo et al., 2018; Tong et al., 2021; Wall et al., 2017; Wall et al., 2019). In B cells, Porter et al. hypothesized that Rab8a might be required during activation-induced proliferation and antigen processing, as Rab8a mRNA turnover is regulated in B cells, as its stability increases upon CpG stimulation (Porter et al., 2008). In this work, using a conditional B cell-specific Rab8a knockout mouse model, we comprehensively explored the function of Rab8a in B lymphocytes for the first time *in vivo* and *in vitro*.

5.3.1 Rab8a specifically responds to BCR activation

Little is known about the role of Rab8a in immune cells. Since it has been reported that Rab8 participates in TCR recycling, this prompted us to analyse the colocalization of the internalised antigen-BCR complexes with Rab8a. We detected colocalization of Rab8a with the antigen at all times along the antigen route both in

the A20 D1.3 cell line and primary B cells. Shortly after internalisation, Rab8a colocalised with the antigen close to the PM, while at later time points, Rab8a trafficked together with the antigen to the perinuclear compartment (**Figure 15A, B**) (**III; Fig. 1A, B**).

Next, we addressed whether Rab8 was specifically activated upon BCR stimulation by evaluating its phosphorylation status (Eguchi et al., 2018; Steger et al., 2017). As it has been reported that Rab8a responds to TLR activation in macrophages (Luo et al., 2014), we also tested the LPS response in B lymphocytes. Notably, we detected robust Rab8a phosphorylation (pT72) following BCR (anti-IgM or HEL) but not TLR (LPS) activation in A20 D1.3 cells (**Figure 15C, D**) (**III; Fig. 1D and Fig. S1A**). Altogether, these data suggest that Rab8a might play a role in antigen trafficking and B cell activation.

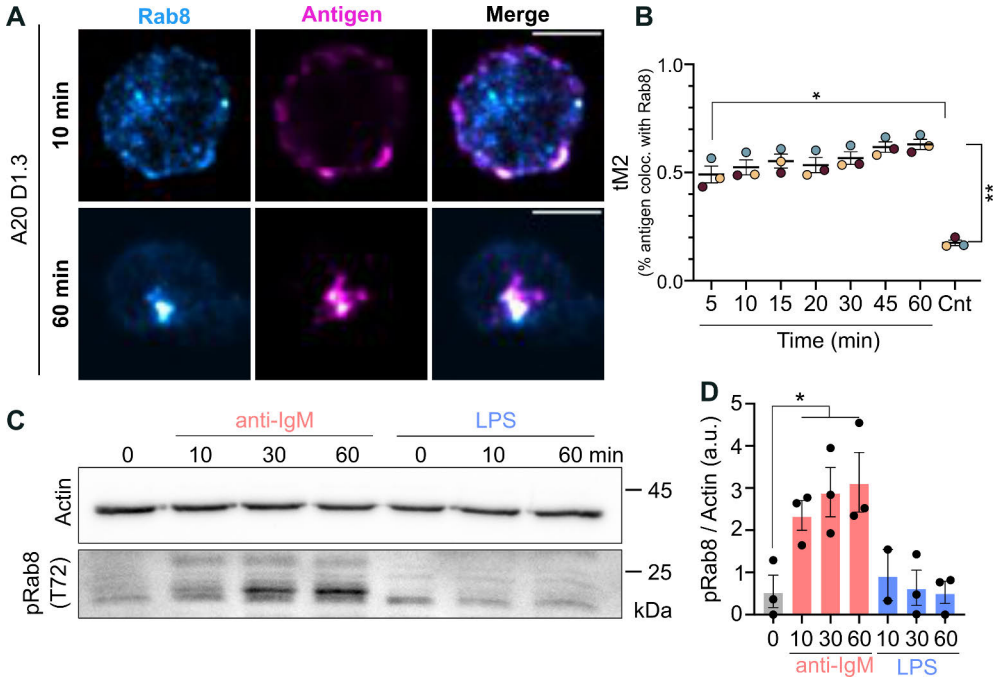

Figure 15. Rab8a is phosphorylated upon BCR activation and recruited to antigen vesicles. **(A)** A20 D1.3 cells activated with anti-IgM (antigen, magenta) and stained with anti-Rab8a (cyan) at different time points. (**B**) Colocalisation of the antigen with Rab8 (tM2) in 3 independent experiments. Each dot represents the mean of one experiment (cells 30-80 per timepoint per experiment). As negative control to evaluate the random colocalization, the Rab8a channel was rotated 90° right. Statistics: unpaired t-test. (**C, D**) Western blot showing Rab8a phosphorylation (T72) after BCR (anti-IgM) or TLR (LPS) stimulation. One representative blot and quantification from n = 3 independent experiments. Statistics: paired t-test, compared to unstimulated control. Adapted from Publication III.

5.3.2 B cells in the Rab8a KO mice develop normally and have no defects on BCR trafficking

To study the role of Rab8a in B cell biology, we generated a B cell conditional Rab8a$^{-/-}$ knock out (KO) by crossing the Rab8a$^{flox/flox}$ strain (Sato et al., 2007) with CD19-Cre knock-in mice (Rickert et al., 1997) (**Figure 16A, B**) (**III; Fig. 2A-B and Fig. S2A**). B cells isolated from the spleen of Rab8a KO mice did not show Rab8a protein expression by Western blot, and importantly Rab8b expression remained unmodified. These results confirmed the specificity of the deletion and ruled out the possibility that increased levels of Rab8b could be compensating for the loss of Rab8a.

After successful establishment of the Rab8a KO model, we investigated the effect of the Rab8a deletion on lymphocyte development. To do so, we extracted the total cell populations from the bone marrow, spleen and lymph nodes of WT and Rab8a KO mice (**III; Fig. 2C, 2D and S3**, respectively) and analysed the different populations using flow cytometry (Sarapulov et al., 2020). We confirmed the normal development of the B cell populations in the Rab8a KO mice, and we found no significant differences, except for a slight increase of marginal zone (MZ) B cells (**Figure 16C**) (**III; Fig. 2D**). These results suggest that Rab8a does not alter the development or maintenance of the B cell populations.

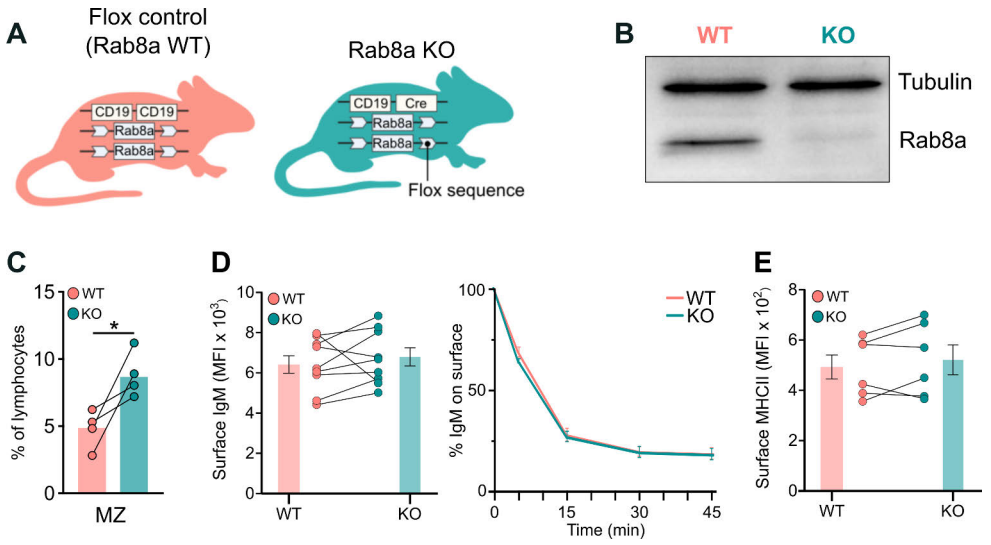

Figure 16. Rab8a does not affect BCR levels and internalization. (**A**) Schematics of the Rab8a conditional KO model (**B**) WB showing Rab8a expression in purified B cells (spleen) in the WT and KO mice. (**C**) Percentage of marginal zone (MZ) B cells in the spleen of WT and KO mice. Statistics: paired t-test. (**D**) Surface BCR (IgM) levels and BCR internalisation in WT and KO mice. (**E**) Surface MHC II levels in WT and KO mice measured by flow cytometry. Adapted from Publication III.

To evaluate the potential role of Rab8a in the BCR traffic, we examined the BCR dynamics in primary B cells isolated from WT and Rab8a KO mice. The levels of surface BCR (IgM), as well as the internalisation rate, remained unmodified (**Figure 16D**) (**III; Fig S2C-D**). In addition, we also tested the levels of MHC II on the cell surface, needed for effective peptide presentation, but no differences were detected (**Figure 16E**) (**III; Fig. S2C**).

5.3.3 Loss of Rab8a increases antibody secretion *in vivo*

To further evaluate the impact of Rab8a on the immune responses, we next evaluated antibody levels in these mice *in vivo*. We analysed the levels of different antibody subclasses – IgM, IgG, IgE and IgA – in the serum of the mice, prior to any antigenic stimuli, using ELISA. The basal antibody in the serum showed increased levels of IgM and IgE antibodies, and decreased levels of IgG1 (**Figure 17A**) (**III; Fig. 3A**). To examine the antibody responses upon vaccination, we selected different model antigens: NP-KLH (T-dependent) (**Figure 17B**), NP-FICOLL (T-independent type II) (**Figure 18A**) and NP-LPS (T-independent type I) (**Figure 18B**). To our surprise, we found that Rab8a KO mice produced more antibodies in response to the immunisations, especially IgG2 and IgG3 antibodies, independent of the type of antigen employed (**Figure 17C and Figure 18C, D**) (**III; Fig. 4 and 5**). We analysed the induction of the germinal centre response and the numbers of antibody secreting cells (ASC) using ELISpot but found no differences between the WT and Rab8a KO mice (**Figure 17D-F**) (**III; Fig. S4**). These data indicate that Rab8a might not affect the numbers of ASC but rather play a role in the efficiency of antibody secretion.
To confirm these results and gain further knowledge into the biological mechanisms, we compared the RNA profiles of WT and Rab8a KO cells in non-activated and activated B cells (**III; Fig. 7 and Fig. S7**). We found few differently expressed genes (DEG) in the Rab8a KO cells compared to the WT cells: 17 in non-activated cells from spleen, 10 in non-activated cells from lymph nodes and 15 DEGs in activated cells. Interestingly, we found a significant increase in AID (Aicda), IgG2b and IgG2c in the activated Rab8a KO B cells, supporting the *in vivo* data showing increased antibody class-switching to these isotypes and increased antibody secretion (**Figure 19A**). Using Gene Ontology (GO), we found that Rab8a KO cells had DEGs in categories such as “inflammatory response”, “production of molecular mediators”, “immunoglobulin production” and “cytokine production” (**Figure 19B**), supporting the increased B cell responses found *in vivo* upon immunisation.

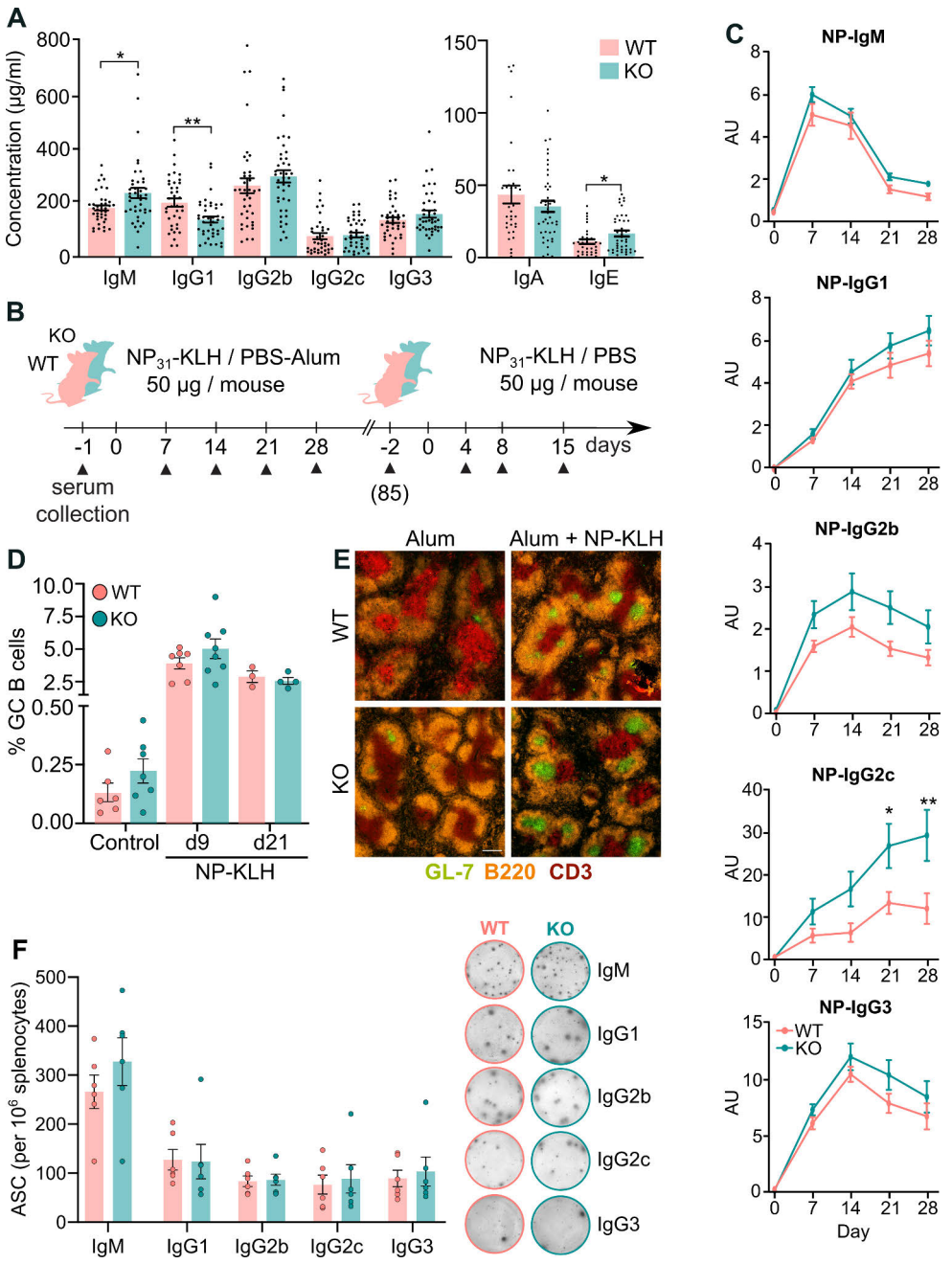

Figure 17. Loss of Rab8a affects TD-antibody production. (A) Basal antibody levels in serum (n = 35-45 mice). Statistics: unpaired t-test. (**B**) Schematics for the NP-KLH immunisation schedule. (**C**) NP-specific antibody levels upon primary immunisation with NP-KLH (n = 5 mice per group). (**D**) Analysis of germinal centre (GC) B cells in the spleen of non-immunised (control) and immunised mice. (**E**) Analysis of germinal centres using immunohistochemistry. (**F**) Analysis of antibody secreting cells (ASCs) using ELISPOT upon NP-KLH immunisation (day 9). Adapted from Publication III

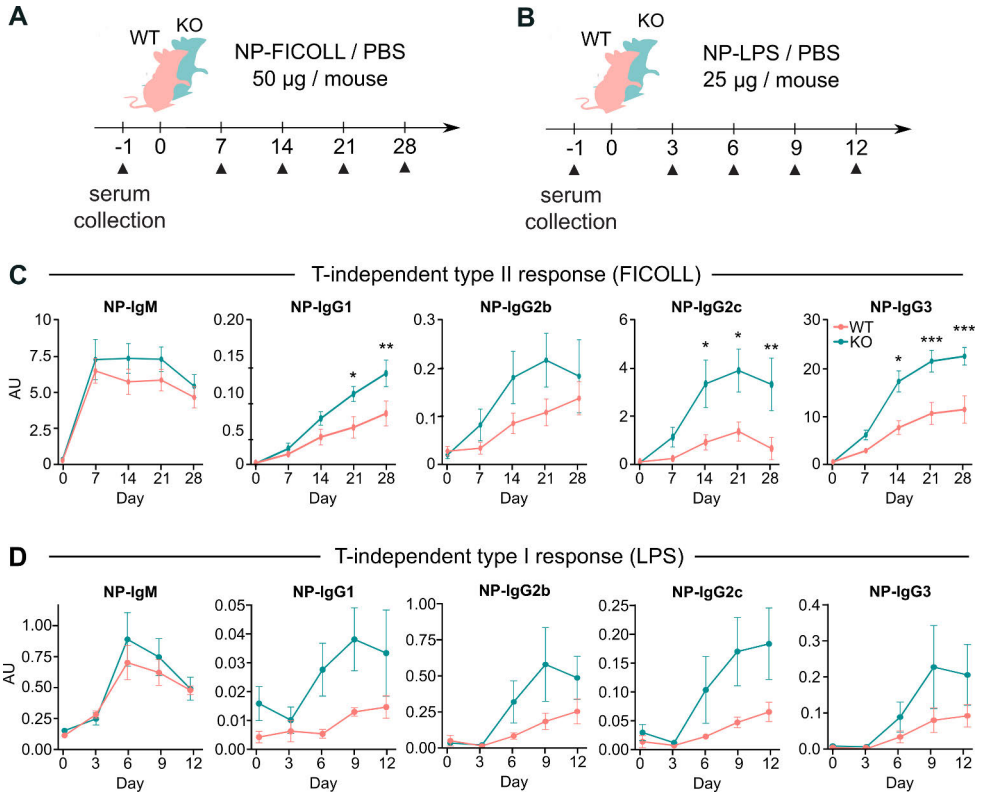

Figure 18. Loss of Rab8a affects TI-antibody production. (A, B) Schematics for the (A) NP-FICOLL and (B) NP-LPS immunisation schedule. (**C**) NP-specific levels (NP_{20}) after NP-FICOLL immunisation (n = 5 mice per group). (**D**) NP-specific antibodies (NP_{20}) after NP-LPS immunisation (n = 5 mice per group). Statistics: multiple t-test (corrected p-value). Adapted from Publication III

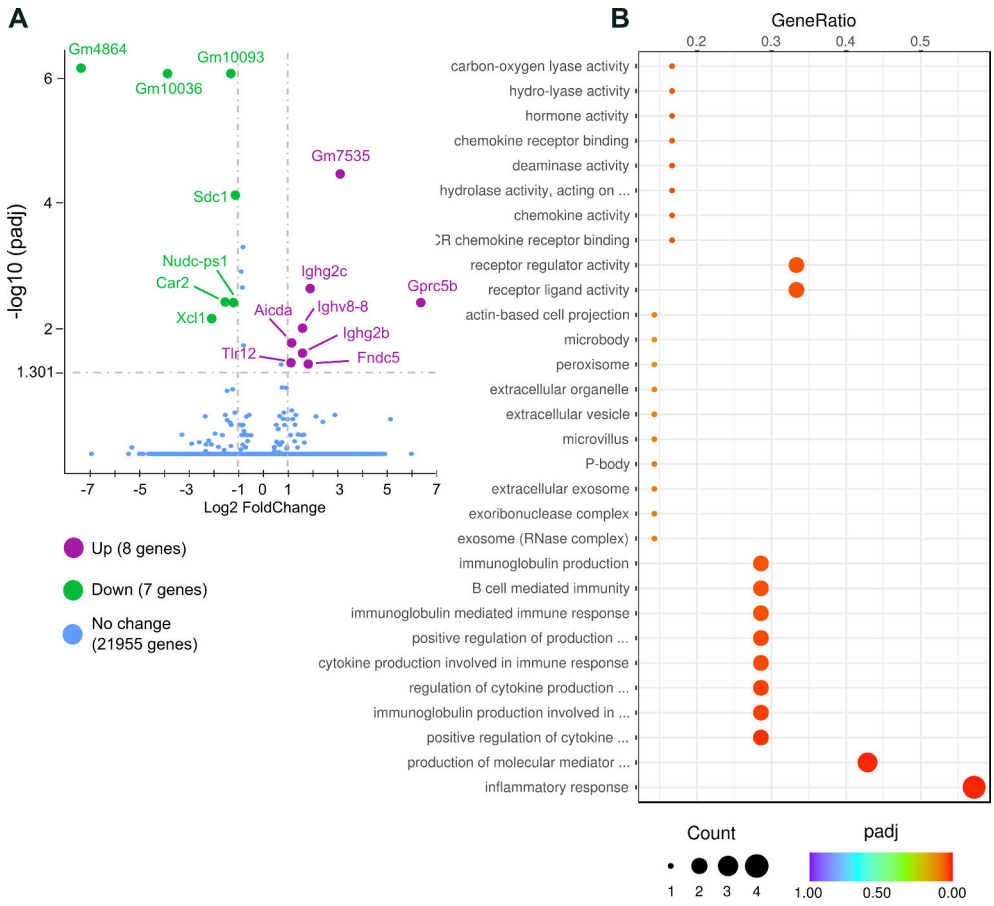

Figure 19. Activated Rab8a KO B cells show an increased activation profile. (A) Volcano plot showing the DEGs in WT/KO B cells activated *in vitro*. Purple: upregulated in Rab8a KO cells. Green: downregulated in Rab8a KO genes. (**B**) GO analysis of the DEGs found in Rab8a KO cells (activated samples). Adapted from Publication III.

5.3.4 Rab8a KO B cells show normal proliferation levels and unaffected antigen presentation

To verify the *in vivo* data, we further studied the antigen responses using B cell isolated from the spleen of the WT and Rab8a KO mice. Isolated B cells were stimulated with anti-IgM, LPS, CD40L, CpG or a combination of those, and proliferation was analysed by flow cytometry after 3 days. We did not detect any differences in B cell proliferation in response to any of these stimuli (**III; Fig.5A**), supporting that the increased antibody responses are not due to increased B cell numbers. To test for antigen presentation, we set up two different systems. The Eα peptide system uses small beads coated with antigen (anti-IgM) and the Eα peptide.

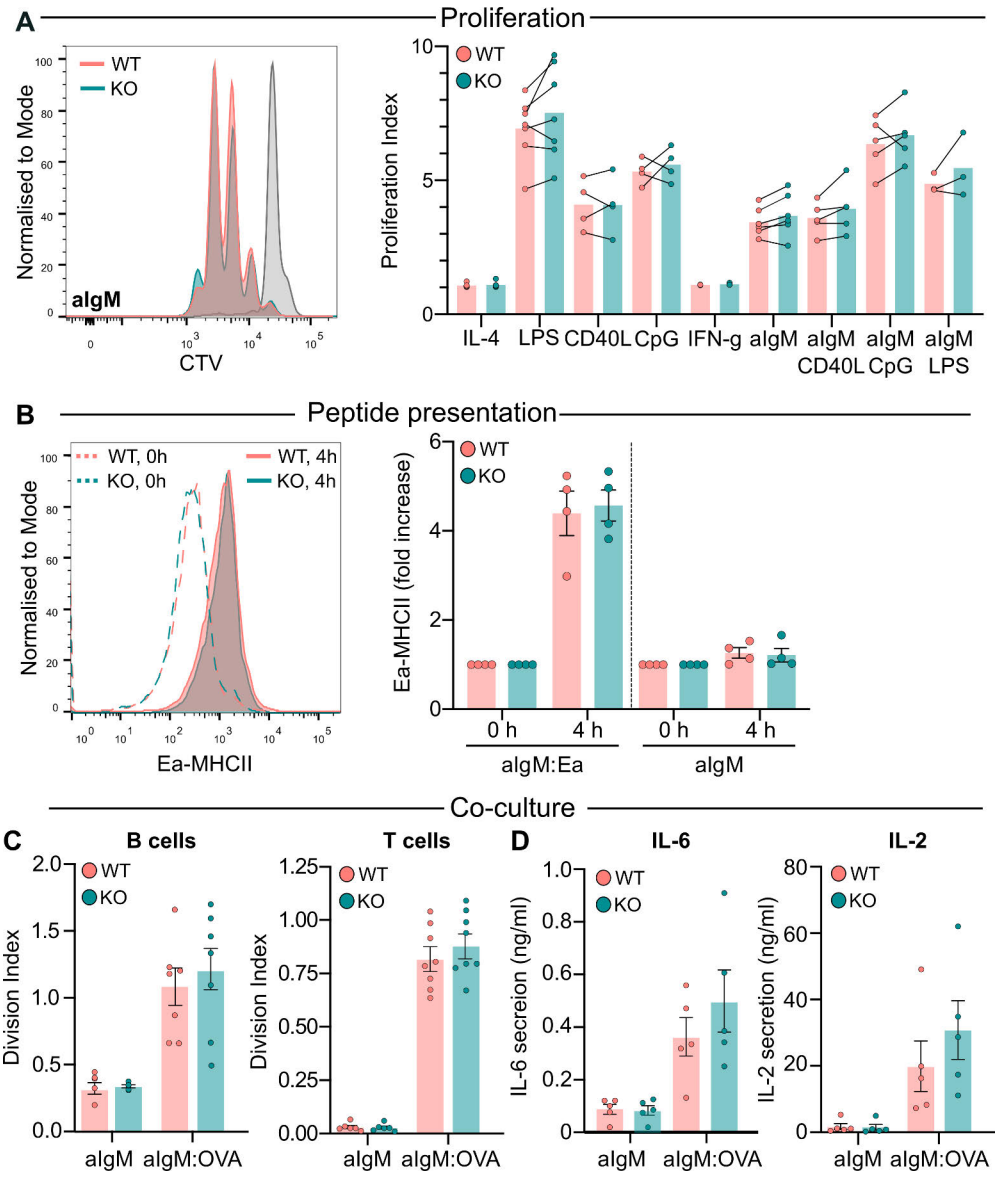

Figure 20. Rab8a KO mouse shows normal B and T proliferation, migration and antigen presentation. (**A**) Analysis of WT or Rab8a KO B cell proliferation in response to different stimuli. Cells were loaded with CTV, and proliferation was analysed after 72 h with flow cytometry. Left: representative plots of anti-IgM activated cells. Right: Proliferation responses measured as proliferation index. Statistics: paired t-test. (**B**) Measure of peptide presentation with the Eα peptide system. Representative plots and data from 4 individual experiments shown as fold increase of the MHCII-Eα signal after 4 hours, compared to 0 hours (arbitrary value of 1). (**C, D**) OT-II proliferation experiments. (C) Proliferation (division index) of B cells and T cells. (D) Amount of IL-6 and IL-2 in the OT-II-B cell co-culture supernatants after 3 days measured by ELISA. Paired t-test. Adapted from Publication III.

These beads are internalised by the B cells and the Eα peptide is presented on the MHC II, and peptide loading can be detected by flow cytometry. In the OT-II co-culture system, T cells that specifically recognise ovalbumin (OVA) peptides are isolated from the spleen of OT-II mice. B cells are activated with beads coated with anti-IgM and OVA and let to interact for 3 days with the T cells to analyse the B and T clonal expansion. However, we did not detect increased antigen presentation, not using the Eα peptide system nor the OT-II co-culture system (**III; Fig. 5C-G**).

5.3.5 Loss of Rab8a alters downstream BCR signalling pathways

Next, we investigated the signalling responses in the Rab8a KO B cells in response to soluble and surface-bound antigen. It has been previously described in the literature that Rab8a affects the organisation of the actin cytoskeleton playing a role in migration and invasion (Bravo-Cordero et al., 2016). However, we found that Rab8a KO B cells were able to form normal immunological synapses, in terms of actin spreading and early BCR responses, in response to antigen-coated surfaces (**Figure 21A**) (**III; Fig. 5A**). We also detected normal proximal tyrosine kinase (Syk, Lyn) (**Figure 21B**) (**III; Fig. 5B**) and calcium signalling (**Figure 21C**) (**III; Fig. 5C**) in response to soluble antigen. Despite the normal early signalling, we found altered levels of pERK1/2, pAKT and pPI3K following BCR activation (**Figure 21D**) (**III; Fig. 5D**). We observed that Rab8a KO B cells had decreased levels of phosphorylated ERK1/2 and AKT and altered PI3K kinetics, as the signalling is not maintained in the KO cells. It has been described that the AKT-PI3K pathway is involved in antibody production, but the exact mechanism remains elusive.

5.3.6 The progression of autoimmunity is not significantly affected by the loss of Rab8a

Due to the increased levels of antibody secretion detected in Rab8a KO B cells, specially of IgG subclasses, we hypothesized that this could enhance the progression of autoimmune diseases such as SLE. In SLE, IgG antibodies are involved in the pathology of the disease, causing autoimmune responses to autoantigens such as DNA and nuclear proteins or deposits in the kidneys (Dema and Charles, 2016). To study the role of Rab8a in SLE, we established an autoimmune model by treating the mice with resiquimod (R848), a TLR7 agonist that can trigger a SLE-like phenotype (Yokogawa et al., 2014) (**Figure 22A**). Indeed, we observed that mice treated with R848 developed splenomegaly, produced autoantibodies and showed profound alterations in the lymphocyte populations in the spleen (**III; Fig. 8B-E**). However, we did not detect any differences between the WT and the Rab8a KO mice, except

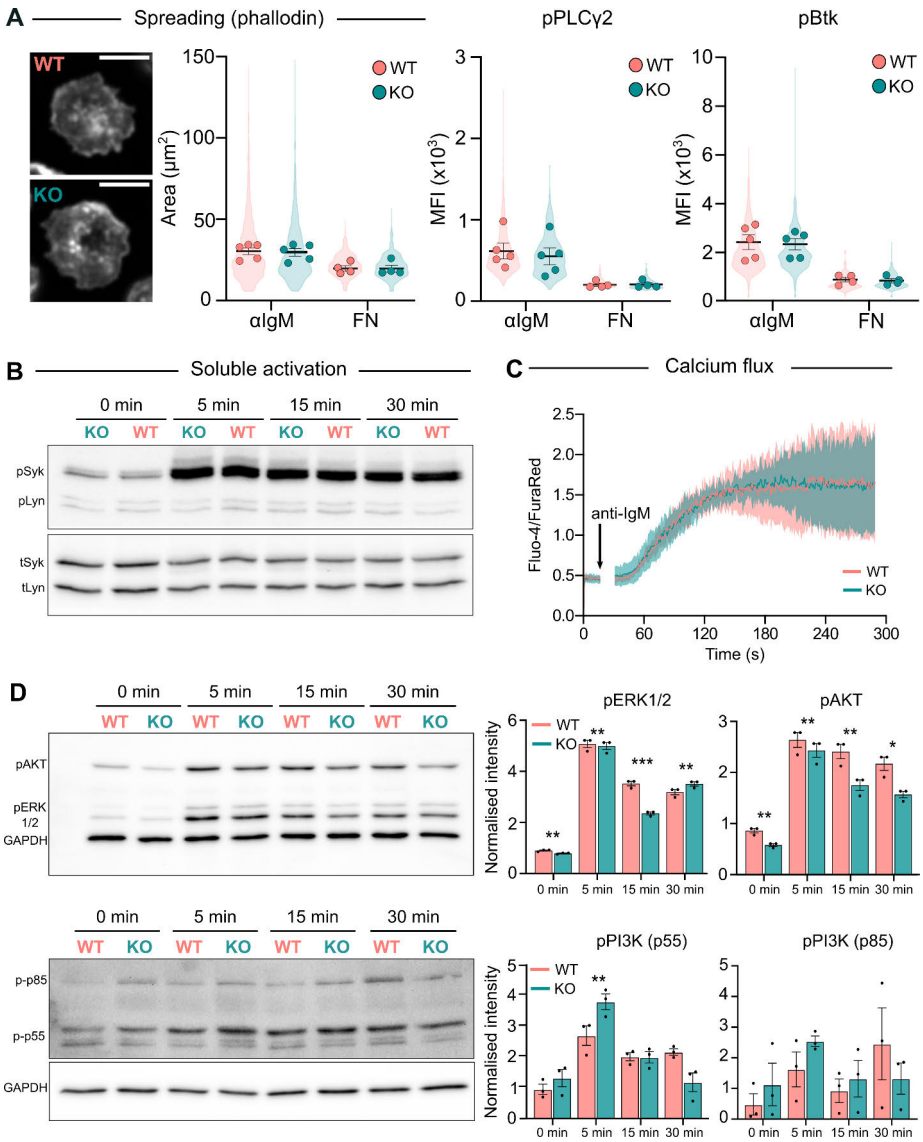

Figure 21. Altered BCR signalling in Rab8a KO mouse. (A) Analysis of B cell activation in response to anti-IgM coated glass for 15 min. Spreading response (measured as the area of the synapse stained with phalloidin; left image) and early BCR signalling measured by phospho-PLCγ$_2$ and phospho-Btk (MFI). The violin plots represent the distribution of the population (all analysed cells, > 100 cells per experiment) and dots represent the mean of individual experiments (n = 4-5). (**B**) Analysis of early BCR signalling in response to anti-IgM by Western blot. Cells were activated with 10 μg/ml of Fab$_2$ anti-IgM in solution for 5, 15 and 30 minutes. (**C**) Calcium flux in WT and Rab8a KO cells in response to 5 μg/ml of Fab$_2$ anti-IgM. The response is measured as the ratio between Fluo-4 and FuraRed GeoMean at each timepoint. The thick line represents the mean, and the shadow area represents the SD of n = 4 independent experiments. The arrow marks the addition of anti-IgM. (**D**) Analysis of downstream BCR signalling in response to anti-IgM by Western blot. Cells were activated with 10 μg/ml of Fab$_2$ anti-IgM in solution for 5, 15 and 30 minutes. Statistics: paired t-test. Adapted from Publication III.

for a slight decrease in the lymphocyte percentage in the KO mice (**Figure 22B**) (**III; Fig. 8E**). In regard to the autoantibody production, we found no differences in anti-DNA IgM antibodies, and only a small, yet not significant, difference in anti-DNA IgG antibodies (**Figure 22C**) (**III; Fig. 8C-D**).

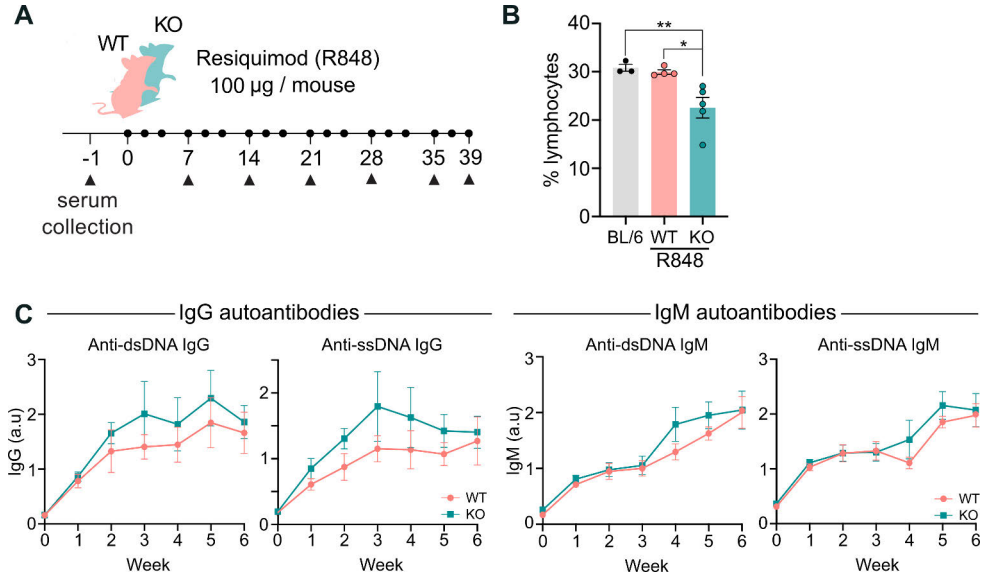

Figure 22. Lack of Rab8a does not impact the development of autoimmunity. (A) Schematic and timeline for the R848 treatment (black dots) and serum collection (black triangles). (**B**) Lymphocyte populations (gated using SSC and FSC) in the spleen of untreated C57BL/6 mice (BL/6) and R848-treated WT and KO mice analysed by flow cytometry. N = 3-5 mice per group (**C**) Measure of IgG and IgM autoantibodies against dsDNA and ssDNA in WT and Rab8a KO mice. N = 4-5 mice per group. Adapted from Publication III.

5.3.7 Discussion and future perspectives (III)

Vesicular traffic is essential for many cell functions. All cells need a tight regulation of the endosomal traffic: however, this is imperative in immune cells. B lymphocytes require an exquisite regulation of their different intracellular pathways as they are involved, among other things, in BCR-antigen internalisation, antigen processing and presentation, cytokine secretion and antibody production. Due to the prominent role of Rab GTPases in the vesicle trafficking, it comes to no surprise that these proteins play several roles in regulating the immune responses (Krzewski and Cullinane, 2013). In addition, alterations in their expression or activity can lead to pathological scenarios, such as autoimmunity (Mitra et al., 2011). For instance, two recent reports showed that Rab7 plays a role in CSR and production of autoantibodies (Lam et al., 2016; Pone et al., 2015).

In this study, we focused on the role of Rab8a in the B cell immune responses. Rab8a is a small GTPase with a wide range of functions in different cell types, including vesicular traffic to the recycling endosomes, traffic to cilia, cell ruffling and migration, neurite outgrowth, TLR signalling and TCR docking at the immune synapse. However, the role of Rab8a in B lymphocytes has not been described to date. When analysing the colocalisation of the antigen vesicles with different Rab proteins (Hernández-Pérez et al., 2020), we observed a high colocalisation of Rab8a with the antigen (**III; Fig. 1**). This fact, together with the information about Rab8a reported in other cell types in the literature, prompted us to study the functions of Rab8a in B cell biology.

To do so, we created a conditional KO mouse model lacking Rab8a in B cells. We showed that Rab8a deletion in B cells did not significantly alter B cell development and B cell populations, except for a slight increase in the numbers of MZ B cells (**III; Fig. 2**). When we analysed the antibody levels in the serum of these mice, we found increased IgM levels, probably supported by the increased numbers of MZ B cells (Appelgren et al., 2018), and increased IgE, but decreased IgG1 levels (**III; Fig. 3A**). Interestingly, upon immunisation with TD and TI antigens, we observed no differences in IgM production, but increased IgG levels (**III; Fig. 3-4**). Notably, we obtained similar data by doing RNAseq of cells activated *in vitro*, confirming the results (**III; Fig. 7**). However, although we hypothesised that Rab8a might participate in antigen internalisation, processing or presentation, this was not supported by our results *in vitro.* We found that Rab8a KO cells internalised the BCR normally and could present peptides to similar levels as the WT control cells. In addition, cells proliferated and migrated normally in response to different stimuli (**III; Fig. 6**).

When analysing the BCR signalling, we observed no differences in proximal tyrosine kinase signalling and calcium signalling, but we found alterations in the downstream interactors (**III; Fig. 5**). Our data suggested that the kinetics of PI3K activation were dysregulated in Rab8a KO cells, and the levels of pERK1/2 and pAKT were decreased. The regulation of PI3K signalling is critical for CSR and the formation of GCs and PCs. However, the regulation of CSR is not completely understood, as B cells express three isoforms of the class I PI3K catalytic subunit (p110α, p110δ, and p110γ) that can exert compensatory functions (Janas et al., 2008). Interestingly, the strength of the signal also plays a role, as one recent study reported that partial inhibition of the PI3K/AKT/mTOR pathway leads to increased CSR, while total inhibition results in decreased CSR (Limon et al., 2014). *In vivo*, two studies have shown controversial results, as mTOR inhibition or activation can decreased plasma cell differentiation in response to antigen, further supporting that a tight regulation or compensation exits (Benhamron and Tirosh, 2011; Zhang et al., 2011). An independent study showed that reduced PI3K activation increased the

expression of AID and CSR via AKT and FoxO (Omori et al., 2006). Supporting this, in addition to the decreased AKT phosphorylation in WB, we observed increased AID expression in the Rab8a KO cells in our RNA sequencing data set. Notably, another study showed that inhibition of AKT promoted IgG1 and IgE CSR in B cells (Chen et al., 2015). These data are partially in line with our results, as we showed decreased basal AKT activation (**III; Fig. 5D**) and increased levels IgE, but not IgG1, in serum before immunisation (**III; Fig. 2A**). Importantly, it has been reported that Rab8a interacts with PI3K in membrane ruffles and early macropinosome membranes in macrophages to regulate inflammation via the PI3K/AKT/mTOR pathway (Luo et al., 2014; Luo et al., 2018; Tong et al., 2021; Wall et al., 2017; Wall et al., 2019). Hence, we speculate that the lack of Rab8a in B lymphocytes decreases AKT signalling, leading to increased CSR and antibody secretion. However, further investigation is needed to support this hypothesis. It would be interesting to analyse the activation of mTOR, PTEN and FoxO in Rab8a KO B cells, as well as to analyse CSR in more detail. In addition to CSR, Rab8a might participate in the secretory pathway, leading to increased levels of antibody secretion in Rab8a KO B cells, or in autophagy. The PI3K/AKT/mTOR signalling pathway is closely related to autophagy and some reports have linked Rab8a to autophagy-related effectors, such as optineurin (Hattula and Peränen, 2000; Nagabhushana et al., 2010). Autophagy can regulate antigen processing and presentation in B cells (Arbogast and Gros, 2018) and it is required for sustainable antibody production (Pengo et al., 2013), but the functions Rab8 in autophagy, especially in the context of B cell activation, are unknown.

The PI3K/AKT/mTOR pathway also participates in the inhibition of apoptosis, cell proliferation and the expression of inflammatory cytokines. Importantly, this pathway is activated in murine SLE (Stylianou et al., 2011). Hence, we asked if Rab8a could protect or contribute to the development of autoimmunity. Using a SLE-induced model, we detected similar levels of auto-antibodies in the Rab8a KO and WT mice, indicating that Rab8a does not alter the progression of autoimmunity (**III; Fig. 8**). These data also suggest that dysregulated signalling alone is not sufficient to trigger autoimmunity, and other factors might be implicated in the progression of the disease.

Altogether, the results of this work demonstrate a role for Rab8a in the regulation of antibody responses, potentially exerting its action via the mTOR/AKT pathway (**Figure 23**). However, further studies are needed to verify the molecular mechanisms involved in this regulation.

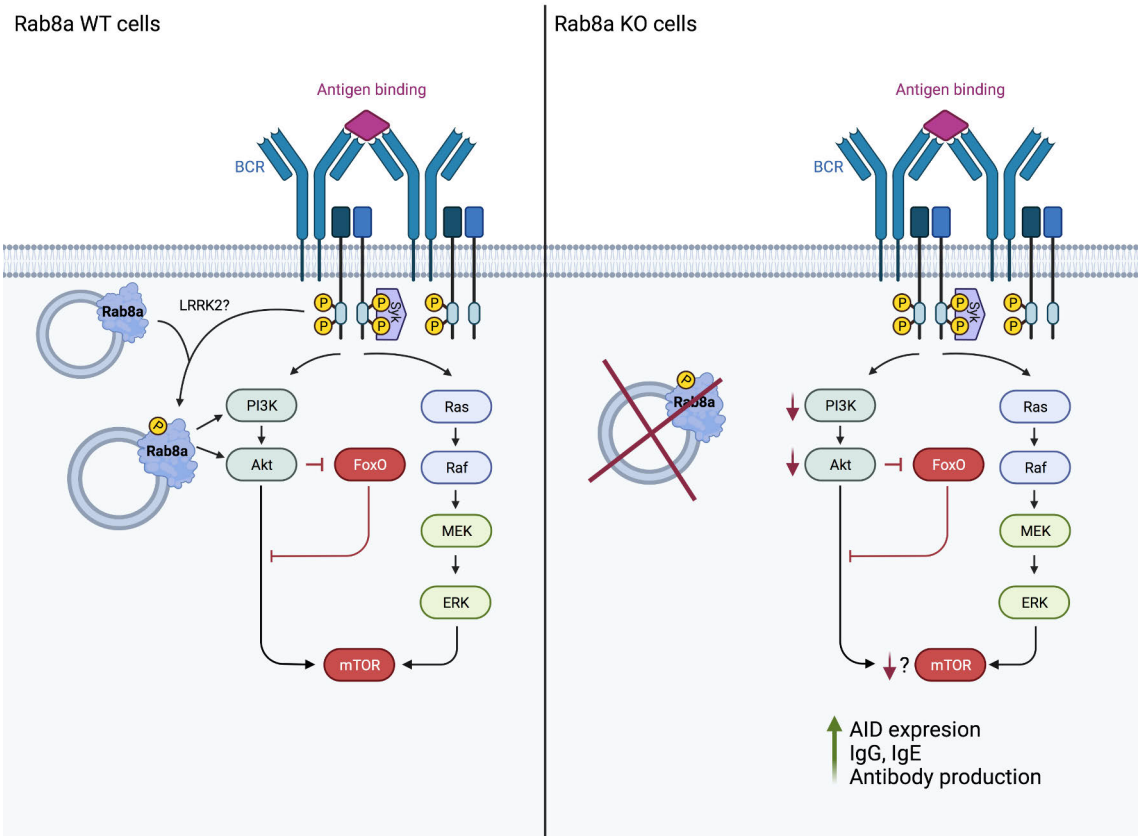

Figure 23. Proposed mechanism of Rab8a in B cells. Rab8a gets phosphorylated upon BCR activation and regulates PI3K/AKT activation. Lack of Rab8a diminishes the activation of the PI3K/AKT/mTOR pathway. This partial inhibition (represented with downwards red arrows) results in increased AID expression and antibody production.

6 Conclusions

Collectively, the results of this thesis contribute to the understanding of the antigen internalisation and trafficking in B cells and addressed the role of a previously uncharacterised small GTPase, Rab8a, in the antibody responses in B lymphocytes.

The main findings of the studies listed in this thesis are as follows:

I. We contributed to the definition of the antigen processing compartments in B cells, shedding light on the characteristics and complexity of different vesicle populations.

II. A Specific Hybridisation Internalisation Probe (SHIP) can fully harness the potential of microscopy to study antigen:BCR internalisation in B lymphocytes.

III. Rab8a is redundant for BCR trafficking but regulates antibody production and secretion.

A better understanding of the mechanisms of antigen processing and presentation, as well as the role of Rab GTPases in the immune response, can provide new avenues for vaccine design. These studies can also advance our knowledge of antibody-mediated autoimmune diseases, such as systemic lupus erythematosus. The development of new powerful techniques, such as the SHIP assay, can unveil new biological information relevant not only in immunological studies, but also important in other diseases, such as receptor trafficking in cancer cells.

Acknowledgements

Conducting research is by no means easy. The completion of this thesis has been possible thanks to the support of many different people. This work has been carried out during the years 2018-2022 at the University of Turku, Finland, in the Lymphocyte Cytoskeleton group led by Dr Pieta Mattila. Thus, I would first like to thank the University of Turku for accepting me as a PhD candidate. I deeply enjoyed working in Biocity, a terrific place for research, and being part of such a lively community. This work would not be possible without the excellent research facilities at the Medicity Research Laboratory of the Faculty of Medicine and Turku Bioscience, also supported by Euro-Bioimaging Finland (Turku Bioimaging) and InFLAMES. Big thanks to each one of the people working hard every day to keep our research centre up and running. Special thanks to the CIC Core for taking such great care of our microscopes and flow cytometers and for your patience in troubleshooting: thank you, Markku Saari, Jouko Sandholm, Markus Peurla, and Ketlin Adel. Big thanks to all the mice that contributed to these studies (except you, R848#33). A warm applause to the great people working in the UTU Central Animal Laboratory: this work will not be possible without you, thank you for taking good care of the animals and helping the researchers.

Thanks to the TuDMM graduate school and the Faculty of Medicine – especially to Eeva Valve and Outi Irjala – and my follow-up committee members, Dr Jukka Alinikula and Dr Marko Salmi. Big thanks to the preliminary examiners, Dr Leonardo Almeida de Souza and Dr Nuria Martínez Martín, for taking the time to read and improve my thesis, and to my opponent, Dr Balbino Alarcón, for what I am sure will be a very interesting defence.

In addition, I am deeply grateful to all the funding bodies that have supported my research over the course of these years: EDUFI, Turun Yliopistosäätiö, the TuDMM graduate school and the Finnish Cultural Foundation.

My deepest gratitude goes to my supervisor, Dr Pieta Mattila. I have been extremely lucky to be guided by you. Thank you very much for your endless support and patience, as well as the independence given to pursue my idea(l)s. Your kindness, enthusiasm, and encouragement throughout these years have enormously contributed to my development as a scientist.

I would like to thank my co-workers and co-authors as well for the mutual advice and help. Thanks also to all our collaborators, especially to Dr Yolanda Carrasco and Dr Gabriele Fischer von Mollard for making a little bit of time and space for me in their labs, and to Dr María Isabel Yuseff for being an inspiration. I warmly thank all the past and present members of the Lymphocyte Cytoskeleton group. Thanks to all my lab babies – Vilma Paavola, Sofia Forstén, Eveliina Uski, and Elmeri Kiviluoto – it was a pleasure supervising teaching you, and I learned something from every one of you.

Special thanks to some of you, my antibuddies, who I have the pleasure to call not only lab mates but also friends:

Thank you, Dr Alexey Sarapulov, for all the wisdom in and outside the lab. I will take with me all the ingenious tricks that you showed to me and teach them to future generations. Thank you very much for all your help and support with the animals, I was very lucky to learn from the best.

Thank you, Dr Petar Petrov, for all your support and the mutual ranting in the office 5089. The little she misses you.

Thank you, Diogo Cunha, for adding Portuguese sauce to our lives. I enjoyed a lot working with you, I am very proud of everything that you have accomplished, and I cannot wait to see you shine. The experiments will not always work (since I will not be around), but it is what it is, and you will overcome everything. Quero-te.

Thank you, Blanca Tejeda González, for bringing a bit of the Spanish warmth to the lab and always being willing to grab a beer after work. Thanks for all the fun plans, games, and educational conversations. I wish you many batches of good attaching cells and sharp micropatterns.

Thank you, Amna Music, for all the good laughs and angry faces. Thank you for all the hugs when you sense that I am sad (you witch) and for always having an honest answer.

Thank you, Özge Balcı, for your tireless efforts in the lab and your endless joy.

Thank you, Felipe del Valle Batalla, for crossing the world to come to Turku for a research visit (thank you so much, academic Twitter). You have been a great support in this last stage of my PhD, inside and outside the lab.

Big thanks to all my Turku friends: some of you I found very late, but I hope that our friendship continues throughout the years and we see each other again to share food, drinks, and laughs. Special mention to Natasa Mantziari: te quiero, amiga. Thank you very much for all the support and for making the Finnish language – a bit – more enjoyable. Thank you to the Cryparty group - Inês Félix (& Archie), Rahul Biradar, Emilie Rydgren, Bárbara Ramos Artigot, Sadaf Fazeli, Iman Farahani and Giulia Sultana – for all the fun plans outside the lab.

I would also like to thank all those others that have made my days better, either by quickly chatting in the corridors of the building, sharing some drinks outside the

lab, discussing experiments, or inspiring me to be a better scientist. You are many, and for sure I am missing many names here, but I hope you recognise yourselves along these lines. Just to mention a few, thanks to Dr Francisco López Picón, Dado Tokic, Veera Ojala, Tiina Lehtiniemi, Sina Tadayon, Dr Sheyla Cisneros Montalvo, Nataliia Petruk, Aleksi Isomursu, Jasmin Kaivola, Dr Pia Rantakari, Dr Guillaume Jacquemet, and Dr Johanna Ivaska.

Last but not least, thanks to my Spanish people that support me from the distance. Thanks to my former supervisor, Dr Pedro Roda Navarro, for his critical support at the beginning of my scientific career. Thanks to my little biochemist troupe, especially Cristina Segovia Falquina and Nerea Jiménez Téllez. I warmly thank my best (and non-scientific) friends, Alejandra Pardo García-Pardo and Fernando Ortiz Fernández, and my family. I know you may not understand everything I say, but you love me and support me anyway. My most special thanks to Dr Juan Palacios Ortega for sharing this adventure in the cold lands of Finland and for always being there for me. I definitely could not have made it without you.

Thank you all for your endless support.

June 2022
Sara Hernández Pérez

References

Adler, L. N., Jiang, W., Bhamidipati, K., Millican, M., Macaubas, C., Hung, S. chen and Mellins, E. D. (2017a). The other function: Class II-restricted antigen presentation by B cells. *Front. Immunol.* **8**,.

Adler, L. N., Jiang, W., Bhamidipati, K., Millican, M., Macaubas, C., Hung, S. chen and Mellins, E. D. (2017b). The other function: Class II-restricted antigen presentation by B cells. *Front. Immunol.* **8**, 1.

Adorini, L., Guéry, J. C., Fuchs, S., Ortiz-Navarrete, V., Hämmerling, G. J. and Momburg, F. (1993). Processing of endogenously synthesized hen egg-white lysozyme retained in the endoplasmic reticulum or in secretory form gives rise to a similar but not identical set of epitopes recognized by class II-restricted T cells. *J. Immunol.* **151**, 3576–86.

Allen, C. D. C., Okada, T. and Cyster, J. G. (2007). Germinal-Center Organization and Cellular Dynamics. *Immunity* **27**, 190–202.

Aluvihare, V. R., Khamlichi, A. A., Williams, G. T., Adorini, L. and Neuberger, M. S. (1997). Acceleration of intracellular targeting of antigen by the B-cell antigen receptor: Importance depends on the nature of the antigen-antibody interaction. *EMBO J.* **16**, 3553–3562.

Amigorena, S., Drake, J. R., Webster, P. and Mellman, I. (1994a). Transient accumulation of new class II MHC molecules in a novel endocytic compartment in B lymphocytes. *Nature* **369**, 113–120.

Amigorena, S., Drake, J. R., Webster, P. and Mellman, I. (1994b). Transient accumulation of new class II MHC molecules in a novel endocytic compartment in B lymphocytes. *Nature* **369**, 113–120.

Ana-Sosa-Batiz, F., Johnston, A. P. R., Hogarth, P. M., Wines, B. D., Barr, I., Wheatley, A. K. and Kent, S. J. (2017). Antibody-dependent phagocytosis (ADP) responses following trivalent inactivated influenza vaccination of younger and older adults. *Vaccine* **35**, 6451–6458.

Anderson, H. A., Bergstralh, D. T., Kawamura, T., Blauvelt, A. and Roche, P. A. (1999). Phosphorylation of the invariant chain by protein kinase C regulates MHC class II trafficking to antigen-processing compartments. *J. Immunol.* **163**, 5435–43.

Appelgren, D., Eriksson, P., Ernerudh, J. and Segelmark, M. (2018). Marginal-Zone B-Cells are main producers of IgM in humans, and are reduced in patients with autoimmune vasculitis. *Front. Immunol.* **9**, 2242.

Arana, E., Vehlow, A., Harwood, N. E., Vigorito, E., Henderson, R., Turner, M., Tybulewicz, V. L. L. J. and Batista, F. D. (2008). Activation of the Small GTPase Rac2 via the B Cell Receptor Regulates B Cell Adhesion and Immunological-Synapse Formation. *Immunity* **28**, 88–99.

Arbogast, F. and Gros, F. (2018). Lymphocyte Autophagy in Homeostasis, Activation, and Inflammatory Diseases. *Front. Immunol.* **9**,.

Arbogast, F., Arnold, J., Hammann, P., Kuhn, L., Chicher, J., Murera, D., Weishaar, J., Muller, S., Fauny, J. D. and Gros, F. (2019). ATG5 is required for B cell polarization and presentation of particulate antigens. *Autophagy* **15**, 280–294.

Arndt, S. O., Vogt, A. B., Markovic-Plese, S., Martin, R., Moldenhauer, G., Wölpl, A., Sun, Y., Schadendorf, D., Hämmerling, G. J. and Kropshofer, H. (2000). Functional HLA-DM on the surface of B cells and immature dendritic cells. *EMBO J.* **19**, 1241–1251.

Arnold, J., Murera, D., Arbogast, F., Fauny, J. D., Muller, S. and Gros, F. (2016). Autophagy is dispensable for B-cell development but essential for humoral autoimmune responses. *Cell Death Differ.* **23**, 853–864.

Arulraj, T., Binder, S. C., Robert, P. A. and Meyer-Hermann, M. (2021). Germinal Centre Shutdown. *Front. Immunol.* **12**, 2730.

Avalos, A. M. and Ploegh, H. L. (2014). Early BCR events and antigen capture, processing, and loading on MHC class II on B cells. *Front. Immunol.* **5**,.

Baba, Y. and Kurosaki, T. (2015). Role of calcium signaling in B cell activation and biology. *Curr. Top. Microbiol. Immunol.* **393**, 143–174.

Bakke, O. and Dobberstein, B. (1990). MHC class II-associated invariant chain contains a sorting signal for endosomal compartments. *Cell* **63**, 707–716.

Banton, M. C., Inder, K. L., Valk, E., Rudd, C. E. and Schneider, H. (2014). Rab8 Binding to Immune Cell-Specific Adaptor LAX Facilitates Formation of trans -Golgi Network-Proximal CTLA-4 Vesicles for Surface Expression . *Mol. Cell. Biol.* **34**, 1486–1499.

Barlow, A. K., He, X. and Janeway, C. (1998). Exogenously provided peptides of a self-antigen can be processed into forms that are recognized by self-T cells. *J. Exp. Med.* **187**, 1403–1415.

Barnden, M. J., Allison, J., Heath, W. R. and Carbone, F. R. (1998). Defective TCR expression in transgenic mice constructed using cDNA- based α- and β-chain genes under the control of heterologous regulatory elements. *Immunol. Cell Biol.* **76**, 34–40.

Baron, R. A. and Seabra, M. C. (2008). Rab geranylgeranylation occurs preferentially via the pre-formed REP-RGGT complex and is regulated by geranylgeranyl pyrophosphate. *Biochem. J.* **415**, 67–75.

Barr, F. A. (2013). Rab GTPases and membrane identity: Causal or inconsequential? *J. Cell Biol.* **202**, 191–199.

Barr, F. and Lambright, D. G. (2010). Rab GEFs and GAPs. *Curr. Opin. Cell Biol.* **22**, 461–470.

Barral, D. C., Ramalho, J. S., Anders, R., Hume, A. N., Knapton, H. J., Tolmachova, T., Collinson, L. M., Goulding, D., Authi, K. S. and Seabra, M. C. (2002). Functional redundancy of Rab27 proteins and the pathogenesis of Griscelli syndrome. *J. Clin. Invest.* **110**, 247–257.

Barrett, J. C., Hansoul, S., Nicolae, D. L., Cho, J. H., Duerr, R. H., Rioux, J. D., Brant, S. R., Silverberg, M. S., Taylor, K. D., Barmada, M. M., et al. (2008). Genome-wide association defines more than 30 distinct susceptibility loci for Crohn's disease. *Nat. Genet.* **40**, 955–962.

Barroso, M., Tucker, H., Drake, L., Nichol, K. and Drake, J. R. (2015). Antigen-B cell receptor complexes associate with intracellular major histocompatibility complex (MHC) class II molecules. *J. Biol. Chem.* **290**, 27101–27112.

Batista, F. D. and Neuberger, M. S. (1998). Affinity dependence of the B cell response to antigen: A threshold, a ceiling, and the importance of off-rate. *Immunity* **8**, 751–759.

Batista, F. D., Iber, D. and Neuberger, M. S. (2001). B cells acquire antigen from target cells after synapse formation. *Nature* **411**, 489–494.

Bem, D., Yoshimura, S. I., Nunes-Bastos, R., Bond, F. F., Kurian, M. A., Rahman, F., Handley, M. T. W., Hadzhiev, Y., Masood, I., Straatman-Iwanowska, A. A., et al. (2011). Loss-of-function mutations in RAB18 cause Warburg micro syndrome. *Am. J. Hum. Genet.* **88**, 499–507.

Benado, A., Nasagi-Atiya, Y. and Sagi-Eisenberg, R. (2009). Protein trafficking in immune cells. *Immunobiology* **214**, 507–525.

Benhamron, S. and Tirosh, B. (2011). Direct activation of mTOR in B lymphocytes confers impairment in B-cell maturation andloss of marginal zone B cells. *Eur. J. Immunol.* **41**, 2390–2396.

Berek, C., Berger, A. and Apel, M. (1991). Maturation of the immune response in germinal centers. *Cell* **67**, 1121–1129.

Bergtold, A., Desai, D. D., Gavhane, A. and Clynes, R. (2005). Cell surface recycling of internalized antigen permits dendritic cell priming of B cells. *Immunity* **23**, 503–514.

Bertram, E. M., Hawley, R. G. and Watts, T. H. (2002). Overexpression of rab7 enhances the kinetics of antigen processing and presentation with MHC class II molecules in B cells. *Int. Immunol.* **14**, 309–318.

Beutler, B. (2004). Innate immunity: An overview. *Mol. Immunol.* **40**, 845–859.

Bianchi, M. E. (2007). DAMPs, PAMPs and alarmins: all we need to know about danger. *J. Leukoc. Biol.* **81**, 1–5.

Blacque, O. E., Scheidel, N. and Kuhns, S. (2018). Rab GTPases in cilium formation and function. *Small GTPases* **9**, 76–94.

Blonska, M. and Lin, X. (2010). NF-κB signaling pathways regulated by CARMA family of scaffold proteins. *Cell Res. 2011 211* **21**, 55–70.

Borbet, T. C., Hines, M. J. and Koralov, S. B. (2021). MicroRNA regulation of B cell receptor signaling. *Immunol. Rev.* **304**, 111–125.

Borchers, A. C., Langemeyer, L. and Ungermann, C. (2021). Who's in control? Principles of Rab GTPase activation in endolysosomal membrane trafficking and beyond. *J. Cell Biol.* **220**,.

Boucrot, E., Ferreira, A. P. A., Almeida-Souza, L., Debard, S., Vallis, Y., Howard, G., Bertot, L., Sauvonnet, N. and McMahon, H. T. (2015). Endophilin marks and controls a clathrin-independent endocytic pathway. *Nature* **517**, 460–465.

Bravo-Cordero, J. J., Marrero-Diaz, R., Megías, D., Genís, L., García-Grande, A., García, M. A., Arroyo, A. G. and Montoya, M. C. (2007). MT1-MMP proinvasive activity is regulated by a novel Rab8-dependent exocytic pathway. *EMBO J.* **26**, 1499–1510.

Bravo-Cordero, J. J., Cordani, M., Soriano, S. F., Díez, B., Muñoz-Agudo, C., Casanova-Acebes, M., Boullosa, C., Guadamillas, M. C., Ezkurdia, I., González-Pisano, D., et al. (2016). A novel high-content analysis tool reveals Rab8-driven cytoskeletal reorganization through Rho GTPases, calpain and MT1-MMP. *J. Cell Sci.* **129**, 1734–1749.

Brown, B. K. and Song, W. (2001). The actin cytoskeleton is required for the trafficking of the B cell antigen receptor to the late endosomes. *Traffic* **2**, 414–427.

Brown, J. H., Jardetzky, T. S., Gorga, J. C., Stern, L. J., Urban, R. G., Strominger, J. L. and Wiley, D. C. (1993). Three-dimensional structure of the human class II histocompatibility antigen HLA-DR1. *Nature* **364**, 33–39.

Burbage, M., Keppler, S. J., Gasparrini, F., Martínez-Martín, N., Gaya, M., Feest, C., Domart, M. C., Brakebusch, C., Collinson, L., Bruckbauer, A., et al. (2015). Cdc42 is a key regulator of b cell differentiation and is required for antiviral humoral immunity. *J. Exp. Med.* **212**, 53–72.

Burbage, M., Keppler, S. J., Montaner, B., Mattila, P. K. and Batista, F. D. (2017). The Small Rho GTPase TC10 Modulates B Cell Immune Responses. *J. Immunol.* **199**, 1682–1695.

Busman-Sahay, K., Sargent, E., Harton, J. A. and Drake, J. R. (2011). The Ia.2 Epitope Defines a Subset of Lipid Raft-Resident MHC Class II Molecules Crucial to Effective Antigen Presentation. *J. Immunol.* **186**, 6710–6717.

Busman-Sahay, K., Drake, L., Sitaram, A., Marks, M. and Drake, J. R. (2013). Cis and Trans Regulatory Mechanisms Control AP2-Mediated B Cell Receptor Endocytosis via Select Tyrosine-Based Motifs. *PLoS One* **8**,.

Buzas, E. I., György, B., Nagy, G., Falus, A. and Gay, S. (2014). Emerging role of extracellular vesicles in inflammatory diseases. *Nat. Rev. Rheumatol.* **10**, 356–364.

Calis, J. J. A. and Rosenberg, B. R. (2014). Characterizing immune repertoires by high throughput sequencing: Strategies and applications. *Trends Immunol.* **35**, 581–590.

Calvo, V. and Izquierdo, M. (2021). Role of Actin Cytoskeleton Reorganization in Polarized Secretory Traffic at the Immunological Synapse. *Front. Cell Dev. Biol.* **9**, 629097.

Cancro, M. P. and Tomayko, M. M. (2021). Memory B cells and plasma cells: The differentiative continuum of humoral immunity. *Immunol. Rev.* **303**, 72–82.

Carpier, J. M., Zucchetti, A. E., Bataille, L., Dogniaux, S., Shafaq-Zadah, M., Bardin, S., Lucchino, M., Maurin, M., Joannas, L. D., Magalhaes, J. G., et al. (2018). Rab6-dependent retrograde traffic of LAT controls immune synapse formation and T cell activation. *J. Exp. Med.* **215**, 1245–1265.

Carrasco, Y. R. (2010). Molecular and cellular dynamics at the early stages of antigen encounter: The B-cell immunological synapse. *Curr. Top. Microbiol. Immunol.* **340**, 51–62.

Carrasco, Y. R. and Batista, F. D. (2006a). B cell recognition of membrane-bound antigen: an exquisite way of sensing ligands. *Curr. Opin. Immunol.* **18**, 286–291.

Carrasco, Y. R. and Batista, F. D. (2006b). B-cell activation by membrane-bound antigens is facilitated by the interaction of VLA-4 with VCAM-1. *EMBO J.* **25**, 889–899.

Carrasco, Y. R. and Batista, F. D. (2007). B Cells Acquire Particulate Antigen in a Macrophage-Rich Area at the Boundary between the Follicle and the Subcapsular Sinus of the Lymph Node. *Immunity* **27**, 160–171.

Castellino, F. and Germain, R. N. (1995). Extensive trafficking of MHC class II-invariant chain complexes in the endocytic pathway and appearance of peptide-loaded class II in multiple compartments. *Immunity* **2**, 73–88.

Cerutti, A., Cols, M. and Puga, I. (2013). Marginal zone B cells: virtues of innatelike antibody-producing lymphocytes. *Nat. Rev. Immunol.* **13**, 118.

Chaturvedi, A., Martz, R., Dorward, D., Waisberg, M. and Pierce, S. K. (2011). Endocytosed BCRs sequentially regulate MAPK and Akt signaling pathways from intracellular compartments. *Nat. Immunol.* **12**, 1119–1126.

Chavrier, P., Gorvel, J. P., Stelzer, E., Simons, K., Gruenberg, J. and Zerial, M. (1991). Hypervariable C-termmal domain of rab proteins acts as a targeting signal. *Nature* **353**, 769–772.

Chen, X. and Jensen, P. E. (2008). The role of B lymphocytes as antigen-presenting cells. *Arch. Immunol. Ther. Exp. (Warsz).* **56**, 77–83.

Chen, Z. and Wang, J. H. (2021). How the Signaling Crosstalk of B Cell Receptor (BCR) and Co-Receptors Regulates Antibody Class Switch Recombination: A New Perspective of Checkpoints of BCR Signaling. *Front. Immunol.* **12**,.

Chen, Z., Getahun, A., Chen, X., Dollin, Y., Cambier, J. C. and Wang, J. H. (2015). Imbalanced PTEN and PI3K Signaling Impairs Class Switch Recombination. *J. Immunol.* **195**, 5461–5471.

Cheng, P. C., Steele, C. R., Gu, L., Song, W. and Pierce, S. K. (1999a). MHC class II antigen processing in B cells: accelerated intracellular targeting of antigens. *J. Immunol.* **162**, 7171–80.

Cheng, P. C., Dykstra, M. L., Mitchell, R. N. and Pierce, S. K. (1999b). A role for lipid rafts in B cell antigen receptor signaling and antigen targeting. *J. Exp. Med.* **190**, 1549–1560.

Cinamon, G., Zachariah, M. A., Lam, O. M., Foss, F. W. and Cyster, J. G. (2008). Follicular shuttling of marginal zone B cells facilitates antigen transport. *Nat. Immunol.* **9**, 54–62.

Colonne, P. M., Winchell, C. G. and Voth, D. E. (2016). Hijacking host cell highways: Manipulation of the host actin cytoskeleton by obligate intracellular bacterial pathogens. *Front. Cell. Infect. Microbiol.* **6**, 107.

Comrie, W. A., Faruqi, A. J., Price, S., Zhang, Y., Rao, V. K., Su, H. C. and Lenardo, M. J. (2018). RELA haploinsufficiency in CD4 lymphoproliferative disease with autoimmune cytopenias. *J. Allergy Clin. Immunol.* **141**, 1507-1510.e8.

Cooper, M. D. (2015). The early history of B cells. *Nat. Rev. Immunol.* **15**, 191–197.

Cruz, F. M., Colbert, J. D. and Rock, K. L. (2020). The GTP ase Rab39a promotes phagosome maturation into MHC -I antigen-presenting compartments. *EMBO J.* **39**,.

Culley, S., Albrecht, D., Jacobs, C., Pereira, P. M., Leterrier, C., Mercer, J. and Henriques, R. (2018a). Quantitative mapping and minimization of super-resolution optical imaging artifacts. *Nat. Methods* **15**, 263–266.

Culley, S., Tosheva, K. L., Matos Pereira, P. and Henriques, R. (2018b). SRRF: Universal live-cell super-resolution microscopy. *Int. J. Biochem. Cell Biol.* **101**, 74–79.

Davidson, H. W. and Watts, C. (1989). Epitope-directed processing of specific antigen by B lymphocytes. *J. Cell Biol.* **109**, 85–92.

Davidson, H. W., Reid, P. A., Lanzavecchia, A. and Watts, C. (1991). Processed antigen binds to newly synthesized mhc class II molecules in antigen-specific B lymphocytes. *Cell* **67**, 105–116.

Davis, D. M., Chiu, I., Fassett, M., Cohen, G. B., Mandelboim, O. and Strominger, J. L. (1999). The human natural killer cell immune synapse. *Proc. Natl. Acad. Sci. U. S. A.* **96**, 15062–15067.

De Silva, N. S. and Klein, U. (2015). Dynamics of B cells in germinal centres. *Nat. Rev. Immunol.* **15**, 137–148.

del Valle Batalla, F., Lennon-Dumenil, A. M. and Yuseff, M. I. (2018). Tuning B cell responses to antigens by cell polarity and membrane trafficking. *Mol. Immunol.* **101**, 140–145.

Delevoye, C., Marks, M. S. and Raposo, G. (2019). Lysosome-related organelles as functional adaptations of the endolysosomal system. *Curr. Opin. Cell Biol.* **59**, 147–158.

Dema, B. and Charles, N. (2016). Autoantibodies in SLE: Specificities, isotypes and receptors. *Antibodies* **5**, 1–30.

Denzin, L. K., Hammond, C. and Cresswell, P. (1996). HLA-DM interactions with intermediates in HLA-DR maturation and a role for HLA-DM in stabilizing empty HLA-DR molecules. *J. Exp. Med.* **184**, 2153–2165.

Denzin, L. K., Fallas, J. L., Prendes, M. and Yi, W. (2005). Right place, right time, right peptide: DO keeps DM focused. *Immunol. Rev.* **207**, 279–292.

Depoil, D., Fleire, S., Treanor, B. L., Weber, M., Harwood, N. E., Marchbank, K. L., Tybulewicz, V. L. J. and Batista, F. D. (2008). CD19 is essential for B cell activation by promoting B cell receptor-antigen microcluster formation in response to membrane-bound ligand. *Nat. Immunol.* **9**, 63–72.

Depoil, D., Weber, M., Treanor, B., Fleire, S. J., Carrasco, Y. R., Harwood, N. E. and Batista, F. D. (2009). Early events of B cell activation by antigen. *Sci. Signal.* **2**,.

Derby, M. C. and Gleeson, P. A. (2007). New insights into membrane trafficking and protein sorting. *Int. Rev. Cytol.* **261**, 47–116.

Derré, I. (2017). Hijacking of membrane contact sites by intracellular bacterial pathogens. *Adv. Exp. Med. Biol.* **997**, 211–223.

Di Pietro, S. M. and Dell'Angelica, E. C. (2005). The cell biology of Hermansky-Pudlak syndrome: Recent advances. *Traffic* **6**, 525–533.

Dinarello, C. A., Simon, A. and Van Der Meer, J. W. M. (2012). Treating inflammation by blocking interleukin-1 in a broad spectrum of diseases. *Nat. Rev. Drug Discov. 2012 118* **11**, 633–652.

Drake, L., McGovern-Brindisi, E. M. and Drake, J. R. (2006). BCR ubiquitination controls BCR-mediated antigen processing and presentation. *Blood* **108**, 4086–4093.

Dupont, N., Jiang, S., Pilli, M., Ornatowski, W., Bhattacharya, D. and Deretic, V. (2011). Autophagy-based unconventional secretory pathway for extracellular delivery of IL-1β. *EMBO J.* **30**, 4701–4711.

Duque, G. A. and Descoteaux, A. (2014). Macrophage cytokines: Involvement in immunity and infectious diseases. *Front. Immunol.* **5**, 491.

Dustin, M. L. and Shaw, A. S. (1999). Costimulation: Building an immunological synapse. *Science (80-.).* **283**, 649–650.

Dykstra, M., Cherukuri, A., Sohn, H. W., Tzeng, S. J. and Pierce, S. K. (2003). Location is everything: Lipid rafts and immune cell signaling. *Annu. Rev. Immunol.* **21**, 457–481.

Eguchi, T., Kuwahara, T., Sakurai, M., Komori, T., Fujimoto, T., Ito, G., Yoshimura, S. I., Harada, A., Fukuda, M., Koike, M., et al. (2018). LRRK2 and its substrate Rab GTPases are sequentially targeted onto stressed lysosomes and maintain their homeostasis. *Proc. Natl. Acad. Sci. U. S. A.* **115**, E9115–E9124.

Ehlers, M., Fukuyama, H., McGaha, T. L., Aderem, A. and Ravetch, J. V. (2006). TLR9/MyD88 signaling is required for class switching to pathogenic IgG2a and 2b autoantibodies in SLE. *J. Exp. Med.* **203**, 553–561.

Elstak, E. D., Neeft, M., Nehme, N. T., Voortman, J., Cheung, M., Goodarzifard, M., Gerritsen, H. C., Van Bergen En Henegouwen, P. M. P., Callebaut, I., De Saint Basile, G., et al. (2011). The munc13-4-rab27 complex is specifically required for tethering secretory lysosomes at the plasma membrane. *Blood* **118**, 1570–1578.

Engels, N., Wollscheid, B. and Wienands, J. (2001). Association of SLP-65/BLNK with the B cell antigen receptor through a non-ITAM tyrosine of Ig-α. *Eur. J. Immunol.* **31**, 2126–2134.

Enzler, T., Bonizzi, G., Silverman, G. J. J., Otero, D. C., Widhopf, G. F. F., Anzelon-Mills, A., Rickert, R. C. C. and Karin, M. (2006). Alternative and Classical NF-κB Signaling Retain Autoreactive B Cells in the Splenic Marginal Zone and Result in Lupus-like Disease. *Immunity* **25**, 403–415.

Eskelinen, E. L. and Saftig, P. (2009). Autophagy: A lysosomal degradation pathway with a central role in health and disease. *Biochim. Biophys. Acta - Mol. Cell Res.* **1793**, 664–673.

Feldmann, J., Callebaut, I., Raposo, G., Certain, S., Bacq, D., Dumont, C., Lambert, N., Ouachée-Chardin, M., Chedeville, G., Tamary, H., et al. (2003). Munc13-4 Is Essential for Cytolytic Granules Fusion and Is Mutated in a Form of Familial Hemophagocytic Lymphohistiocytosis (FHL3). *Cell* **115**, 461–473.

Ferguson, A. R., Youd, M. E. and Corley, R. B. (2004). Marginal zone B cells transport and deposit IgM-containing immune complexes onto follicular dendritic cells. *Int. Immunol.* **16**, 1411–1422.

Finetti, F., Onnis, A. and Baldari, C. T. (2015a). Regulation of vesicular traffic at the T cell immune synapse: Lessons from the primary cilium. *Traffic* **16**, 241–249.

Finetti, F., Patrussi, L., Galgano, D., Cassioli, C., Perinetti, G., Pazour, G. J. and Baldari, C. T. (2015b). The small GTPase Rab8 interacts with VAMP-3 to regulate the delivery of recycling T-cell receptors to the immune synapse. *J. Cell Sci.* **128**, 2541–2552.

Flajnik, M. F. and Kasahara, M. (2010). Origin and evolution of the adaptive immune system: genetic events and selective pressures. *Nat. Rev. Genet.* **11**, 47.

Flaswinkel, H. and Reth, M. (1994). Dual role of the tyrosine activation motif of the Ig-α protein during signal transduction via the B cell antigen receptor. *EMBO J.* **13**, 83–89.

Fleire, S. J., Goldman, J. P., Carrasco, Y. R., Weber, M., Bray, D. and Batista, F. D. (2006). B cell ligand discrimination through a spreading and contraction response. *Science (80-.).* **312**, 738–741.

Fraser, J., Simpson, J., Fontana, R., Kishi-Itakura, C., Ktistakis, N. T. and Gammoh, N. (2019). Targeting of early endosomes by autophagy facilitates EGFR recycling and signalling. *EMBO Rep.* **20**,.

Freeman, S. A., Lei, V., Dang-Lawson, M., Mizuno, K., Roskelley, C. D. and Gold, M. R. (2011). Cofilin-Mediated F-Actin Severing Is Regulated by the Rap GTPase and Controls the Cytoskeletal Dynamics That Drive Lymphocyte Spreading and BCR Microcluster Formation. *J. Immunol.* **187**, 5887–5900.

Gallo, R. L. and Nizet, V. (2008). Innate barriers against infection and associated disorders. *Drug Discov. Today. Dis. Mech.* **5**, 145.

García De Vinuesa, C., Cook, M. C., Ball, J., Drew, M., Sunners, Y., Cascalho, M., Wabl, M., Klaus, G. G. B. and MacLennan, I. C. M. (2000). Germinal centers without T cells. *J. Exp. Med.* **191**, 485–493.

Gardet, A., Benita, Y., Li, C., Sands, B. E., Ballester, I., Stevens, C., Korzenik, J. R., Rioux, J. D., Daly, M. J., Xavier, R. J., et al. (2010). LRRK2 Is Involved in the IFN-γ Response and Host Response to Pathogens. *J. Immunol.* **185**, 5577–5585.

Gasteiger, G., D'osualdo, A., Schubert, D. A., Weber, A., Bruscia, E. M. and Hartl, D. (2017). Cellular Innate Immunity: An Old Game with New Players. *J. Innate Immun.* **9**, 111–125.

Gazumyan, A., Reichlin, A. and Nussenzweig, M. C. (2006). Igβ tyrosine residues contribute to the control of B cell receptor signaling by regulating receptor internalization. *J. Exp. Med.* **203**, 1785–1794.

Gerwert, K., Mann, D. and Kötting, C. (2017). Common mechanisms of catalysis in small and heterotrimeric GTPases and their respective GAPs. *Biol. Chem.* **398**, 523–533.

Ghosh, D., Jiang, W., Mukhopadhyay, D. and Mellins, E. D. (2021). New insights into B cells as antigen presenting cells. *Curr. Opin. Immunol.* **70**, 129–137.

Giannandrea, M., Bianchi, V., Mignogna, M. L., Sirri, A., Carrabino, S., D'Elia, E., Vecellio, M., Russo, S., Cogliati, F., Larizza, L., et al. (2010). Mutations in the Small GTPase Gene RAB39B Are Responsible for X-linked Mental Retardation Associated with Autism, Epilepsy, and Macrocephaly. *Am. J. Hum. Genet.* **86**, 185–195.

Gilbert, S. C. (2012). T-cell-inducing vaccines – what's the future. *Immunology* **135**, 19.

Ginsberg, S. D., Alldred, M. J., Counts, S. E., Cataldo, A. M., Neve, R. L., Jiang, Y., Wuu, J., Chao, M. V., Mufson, E. J., Nixon, R. A., et al. (2010). Microarray analysis of hippocampal CA1 neurons implicates early endosomal dysfunction during Alzheimer's disease progression. *Biol. Psychiatry* **68**, 885–893.

Gioseffi, A., Edelmann, M. J. and Kima, P. E. (2021). Intravacuolar Pathogens Hijack Host Extracellular Vesicle Biogenesis to Secrete Virulence Factors. *Front. Immunol.* **12**,.

Glazier, K. S., Hake, S. B., Tobin, H. M., Chadburn, A., Schattner, E. J. and Denzin, L. K. (2002). Germinal center B cells regulate their capability to present antigen by modulation of HLA-DO. *J. Exp. Med.* **195**, 1063–1069.

Glick, B. (1955). Growth and Function of the Bursa of Fabricius.

Glick, B. (1956). Normal Growth of the Bursa of Fabricius in Chickens. *Poult. Sci.* **35**, 843–851.

Glick, B., Chang, T. S. and Jaap, R. G. (1956). The Bursa of Fabricius and Antibody Production. *Poult. Sci.* **35**, 224–225.

Gold, M. R. and Reth, M. G. (2019). Antigen Receptor Function in the Context of the Nanoscale Organization of the B Cell Membrane. *https://doi.org/10.1146/annurev-immunol-042718-041704* **37**, 97–123.

Goldrath, A. W. and Bevan, M. J. (1999). Selecting and maintaining a diverse T-cell repertoire. *Nature* **402**, 6–13.

Gonzalez-Juarrero, M., Kingry, L. C., Ordway, D. J., Henao-Tamayo, M., Harton, M., Basaraba, R. J., Hanneman, W. H., Orme, I. M. and Slayden, R. A. (2009). Immune response to mycobacterium tuberculosis and identification of molecular markers of disease. *Am. J. Respir. Cell Mol. Biol.* **40**, 398–409.

Good, K. L., Avery, D. T. and Tangye, S. G. (2009). Resting Human Memory B Cells Are Intrinsically Programmed for Enhanced Survival and Responsiveness to Diverse Stimuli Compared to Naive B Cells. *J. Immunol.* **182**, 890–901.

Gourbal, B., Pinaud, S., Beckers, G. J. M., Van Der Meer, J. W. M., Conrath, U. and Netea, M. G. (2018). Innate immune memory: An evolutionary perspective. *Immunol. Rev.* **283**, 21–40.

Grakoui, A., Bromley, S. K., Sumen, C., Davis, M. M., Shaw, A. S., Allen, P. M. and Dustin, M. L. (1999). The immunological synapse: A molecular machine controlling T cell activation. *Science (80-.).* **285**, 221–227.

Greaves, S. A., Peterson, J. N., Torres, R. M. and Pelanda, R. (2018). Activation of the MEK-ERK pathway is necessary but not sufficient for breaking central B cell tolerance. *Front. Immunol.* **9**, 707.

Gretz, J. E., Norbury, C. C., Anderson, A. O., Proudfoot, A. E. I. and Shaw, S. (2000). Lymph-borne chemokines and other low molecular weight molecules reach high endothelial venules via specialized conduits while a functional barrier limits access to the lymphocyte microenvironments in lymph node cortex. *J. Exp. Med.* **192**, 1425–1439.

Grey, H. M. and Chesnut, R. (1985). Antigen processing and presentation to T cells. *Immunol. Today* **6**, 101–106.

Griffin, J. P., Chu, R. and Harding, C. V (1997). Early endosomes and a late endocytic compartment generate different peptide-class II MHC complexes via distinct processing mechanisms. *J. Immunol.* **158**, 1523–32.

Grosshans, B. L., Ortiz, D. and Novick, P. (2006). Rabs and their effectors: Achieving specificity in membrane traffic. *Proc. Natl. Acad. Sci. U. S. A.* **103**, 11821–11827.

Gruenberg, J. (2001). The endocytic pathway: A mosaic of domains. *Nat. Rev. Mol. Cell Biol.* **2**, 721–730.

Guagliardi, L. E., Koppelman, B., Blum, J. S., Marks, M. S., Cresswell, P. and Brodsky, F. M. (1990). Co-localization of molecules involved in antigen processing and presentation in an early endocytic compartment. *Nature* **343**, 133–139.

Guinamard, R., Okigaki, M., Schlessinger, J. and Ravetch, J. V. (2000). Absence of marginal zone B cells in Pyk-2-deficient mice defines their role in the humoral response. *Nat. Immunol.* **1**, 31–36.

Gustafsson, N., Culley, S., Ashdown, G., Owen, D. M., Pereira, P. M. and Henriques, R. (2016). Fast live-cell conventional fluorophore nanoscopy with ImageJ through super-resolution radial fluctuations. *Nat. Commun.* **7**, 1–9.

Gutierrez, M. G. (2013). Functional role(s) of phagosomal Rab GTPases. *Small GTPases* **4**, 148.

Hakimi, M., Selvanantham, T., Swinton, E., Padmore, R. F., Tong, Y., Kabbach, G., Venderova, K., Girardin, S. E., Bulman, D. E., Scherzer, C. R., et al. (2011). Parkinson's disease-linked LRRK2 is expressed in circulating and tissue immune cells and upregulated following recognition of microbial structures. *J. Neural Transm.* **118**, 795–808.

Hartley, S. B., Crosbie, J., Brink, R., Kantor, A. B., Basten, A. and Goodnow, C. C. (1991). Elimination from peripheral lymphoid tissues of self-reactive B lymphocytes recognizing membrane-bound antigens. *Nature* **353**, 765–769.

Harwood, N. E. and Batista, F. D. (2010). Early events in B cell activation. *Annu. Rev. Immunol.* **28**, 185–210.

Hattula, K. and Peränen, J. (2000). FIP-2, a coiled-coil protein, links Huntingtin to Rab8 and modulates, cellular morphogenesis. *Curr. Biol.* **10**, 1603–1606.

Hattula, K., Furujelm, J., Tikkanen, J., Tanhuanpää, K., Laakkonen, P. and Peränen, J. (2006). Characterization of the Rab8-specific membrane traffic route linked to protrusion formation. *J. Cell Sci.* **119**, 4866–4877.

Heath, W. R., Kato, Y., Steiner, T. M. and Caminschi, I. (2019). *Antigen presentation by dendritic cells for B cell activation*. Curr Opin Immunol.

Heesters, B. A., Myers, R. C. and Carroll, M. C. (2014). Follicular dendritic cells: Dynamic antigen libraries. *Nat. Rev. Immunol.* **14**, 495–504.

Heesters, B. A., Lindqvist, M., Vagefi, P. A., Scully, E. P., Schildberg, F. A., Altfeld, M., Walker, B. D., Kaufmann, D. E. and Carroll, M. C. (2015). Follicular Dendritic Cells Retain Infectious HIV in Cycling Endosomes. *PLoS Pathog.* **11**,.

Herlands, R. A., William, J., Hershberg, U. and Shlomchik, M. J. (2007). Anti-chromatin antibodies drive in vivo antigen-specific activation and somatic hypermutation of rheumatoid factor B cells at extrafollicular sites. *Eur. J. Immunol.* **37**, 3339–3351.

Hernández-Pérez, S. and Mattila, P. K. (2022). A specific hybridisation internalisation probe (SHIP) enables precise live-cell and super-resolution imaging of internalized cargo. *Sci. Rep.* **12**, 1–15.

Hernández-Pérez, S., Vainio, M., Kuokkanen, E., Šuštar, V., Petrov, P., Forstén, S., Paavola, V., Rajala, J., Awoniyi, L. O., Sarapulov, A. V., et al. (2020). B cells rapidly target antigen and surface-derived MHCII into peripheral degradative compartments. *J. Cell Sci.* **133**,.

Hewitt, E. W. (2003). The MHC class I antigen presentation pathway: strategies for viral immune evasion. *Immunology* **110**, 163–169.

Hillion, S., Arleevskaya, M. I., Blanco, P., Bordron, A., Brooks, W. H., Cesbron, J. Y., Kaveri, S., Vivier, E. and Renaudineau, Y. (2020). The Innate Part of the Adaptive Immune System. *Clin. Rev. Allergy Immunol.* **58**, 151–154.

Hogan, P. G., Lewis, R. S. and Rao, A. (2010). Molecular basis of calcium signaling in lymphocytes: STIM and ORAI. *Annu. Rev. Immunol.* **28**, 491–533.

Holthusen, K., Talaty, P. and Everly, D. N. (2015). Regulation of Latent Membrane Protein 1 Signaling through Interaction with Cytoskeletal Proteins. *J. Virol.* **89**, 7277–7290.

Hombach, J., Tsubata, T., Leclercq, L., Stappert, H. and Reth, M. (1990). Molecular components of the B-cell antigen receptor complex of the IgM class. *Nature* **343**, 760–762.

Hoogeboom, R. and Tolar, P. (2015). Molecular mechanisms of B cell antigen gathering and endocytosis. *Curr. Top. Microbiol. Immunol.* **393**, 45–63.

Hou, P., Araujo, E., Zhao, T., Zhang, M., Massenburg, D., Veselits, M., Doyle, C., Dinner, A. R. and Clark, M. R. (2006). B cell antigen receptor signaling and internalization are mutually exclusive events. *PLoS Biol.* **4**, 1147–1158.

Hsu, M. C., Toellner, K. M., Vinuesa, C. G. and MacLennan, I. C. M. (2006). B cell clones that sustain long-term plasmablast growth in T-independent extrafollicular antibody responses. *Proc. Natl. Acad. Sci. U. S. A.* **103**, 5905–5910.

Huber, L. A., Pimplikar, S., Parton, R. G., Virta, H., Zerial, M. and Simons, K. (1993). Rab8, a small GTPase involved in vesicular traffic between the TGN and the basolateral plasma membrane. *J. Cell Biol.* **123**, 35–45.

Huff, J. (2015). The Airyscan detector from ZEISS: confocal imaging with improved signal-to-noise ratio and super-resolution. *Nat. Methods* **12**, i–ii.

Huff, J., Bergter, A., Birkenbeil, J., Kleppe, I., Engelmann, R. and Krzic, U. (2017). The new 2D Superresolution mode for ZEISS Airyscan. *Nat. Methods* **14**, 1223–1223.

Huizing, M. and Gahl, W. (2005). Disorders of Vesicles of Lysosomal Lineage: The Hermansky-Pudlak Syndromes. *Curr. Mol. Med.* **2**, 451–467.

Huotari, J. and Helenius, A. (2011). Endosome maturation. *EMBO J.* **30**, 3481–3500.

Iwasaki, A. and Medzhitov, R. (2015). Control of adaptive immunity by the innate immune system. *Nat. Immunol.* **16**, 343–353.

Jackson, K. J. L., Kidd, M. J., Wang, Y. and Collins, A. M. (2013). The shape of the lymphocyte receptor repertoire: Lessons from the B cell receptor. *Front. Immunol.* **4**, 263.

Jacob, J., Kassir, R. and Kelsoe, G. (1991). In situ studies of the primary immune response to (4-hydroxy-3-nitrophenyl)acetyl. I. The architecture and dynamics of responding cell populations. *J. Exp. Med.* **173**, 1165–1175.

Janas, M. L., Hodson, D., Stamataki, Z., Hill, S., Welch, K., Gambardella, L., Trotman, L. C., Pandolfi, P. P., Vigorito, E. and Turner, M. (2008). The Effect of Deleting p110δ on the Phenotype and Function of PTEN-Deficient B Cells. *J. Immunol.* **180**, 739–746.

Janeway, C. A. (1989). Approaching the asymptote? Evolution and revolution in immunology. In *Cold Spring Harbor Symposia on Quantitative Biology*, pp. 1–13.

Jenkins, D., Seelow, D., Jehee, F. S., Perlyn, C. A., Alonso, L. G., Bueno, D. F., Donnai, D., Josifiova, D., Mathijssen, I. M. J., Morton, J. E. V., et al. (2007). RAB23 mutations in carpenter syndrome imply an unexpected role for Hedgehog signaling in cranial-suture development and obesity. *Am. J. Hum. Genet.* **80**, 1162–1170.

Jiang, W., Strohman, M. J., Somasundaram, S., Ayyangar, S., Hou, T., Wang, N. and Mellins, E. D. (2015). PH-susceptibility of HLA-DO tunes DO/DM ratios to regulate HLA-DM catalytic activity. *Sci. Rep.* **5**, 1–13.

Jin, H., Tang, Y., Yang, L., Peng, X., Li, B., Fan, Q., Wei, S., Yang, S., Li, X., Wu, B., et al. (2021). Rab GTPases: Central Coordinators of Membrane Trafficking in Cancer. *Front. Cell Dev. Biol.* **9**,.

Kabak, S., Skaggs, B. J., Gold, M. R., Affolter, M., West, K. L., Foster, M. S., Siemasko, K., Chan, A. C., Aebersold, R. and Clark, M. R. (2002). The Direct Recruitment of BLNK to Immunoglobulin α Couples the B-Cell Antigen Receptor to Distal Signaling Pathways. *Mol. Cell. Biol.* **22**, 2524–2535.

Katkere, B., Rosa, S., Caballero, A., Repasky, E. A. and Drake, J. R. (2010). Physiological-Range Temperature Changes Modulate Cognate Antigen Processing and Presentation Mediated by Lipid Raft-Restricted Ubiquitinated B Cell Receptor Molecules. *J. Immunol.* **185**, 5032–5039.

Katkere, B., Rosa, S. and Drake, J. R. (2012). The syk-binding ubiquitin ligase c-Cbl mediates signaling-dependent B cell receptor ubiquitination and B cell receptor-mediated antigen processing and presentation. *J. Biol. Chem.* **287**, 16636–16644.

Kim, B., Yang, M. S., Choi, D., Kim, J. H., Kim, H. S., Seol, W., Choi, S., Jou, I., Kim, E. Y. and Joe, E. hye (2012). Impaired inflammatory responses in murine lrrk2-knockdown brain microglia. *PLoS One* **7**, e34693.

Kiral, F. R., Kohrs, F. E., Jin, E. J. and Hiesinger, P. R. (2018). Rab GTPases and Membrane Trafficking in Neurodegeneration. *Curr. Biol.* **28**, R471–R486.

Klaus, G. G. B., Humphrey, J. H., Kunkl, A. and Dongworth, D. W. (1980). The Follicular Dendritic Cell: Its Role in Antigen Presentation in the Generation of Immunological Memory. *Immunol. Rev.* **53**, 3–28.

Knödler, A., Feng, S., Zhang, J., Zhang, X., Das, A., Peränen, J. and Guo, W. (2010). Coordination of Rab8 and Rab11 in primary ciliogenesis. *Proc. Natl. Acad. Sci. U. S. A.* **107**, 6346–6351.

Koopman, G., Parmentier, H. K., Schuurman, H. J., Newman, W., Meijer, C. J. L. M. and Pals, S. T. (1991). Adhesion of human B cells to follicular dendritic cells involves both the lymphocyte function-associated antigen 1/intercellular adhesion molecule 1 and very late antigen 4/vascular cell adhesion molecule 1 pathways. *J. Exp. Med.* **173**, 1297–1304.

Krzewski, K. and Cullinane, A. R. (2013). Evidence for defective Rab GTPase-dependent cargo traffic in immune disorders. *Exp. Cell Res.* **319**, 2360–2367.

Kumari, S., Swetha, M. and Mayor, S. (2010). Endocytosis unplugged: multiple ways to enter the cell. *Cell Res. 2010 203* **20**, 256–275.

Kurosaki, T. (2002). Regulation of B-cell signal transduction by adaptor proteins. *Nat. Rev. Immunol.* **2**, 354–363.

Kurosaki, T. (2011). Regulation of BCR signaling. *Mol. Immunol.* **48**, 1287–1291.

Kurosaki, T. and Hikida, M. (2009). Tyrosine kinases and their substrates in B lymphocytes. *Immunol. Rev.* **228**, 132–148.

Kypri, E., Falkenstein, K. and De Lozanne, A. (2013). Antagonistic Control of Lysosomal Fusion by Rab14 and the Lyst-Related Protein LvsB. *Traffic* **14**, 599–609.

Lai, Y., Kondapalli, C., Lehneck, R., Procter, J. B., Dill, B. D., Woodroof, H. I., Gourlay, R., Peggie, M., Macartney, T. J., Corti, O., et al. (2015). Phosphoproteomic screening identifies Rab GTP ases as novel downstream targets of PINK 1 . *EMBO J.* **34**, 2840–2861.

Lam, T., Kulp, D. V., Wang, R., Lou, Z., Taylor, J., Rivera, C. E., Yan, H., Zhang, Q., Wang, Z., Zan, H., et al. (2016). Small Molecule Inhibition of Rab7 Impairs B Cell Class Switching and Plasma Cell Survival To Dampen the Autoantibody Response in Murine Lupus. *J. Immunol.* **197**, 3792–3805.

Lankar, D., Vincent-Schneider, H., Briken, V., Yokozeki, T., Raposo, G. and Bonnerot, C. (2002). Dynamics of major histocompatibility complex class II compartments during B cell receptor-mediated cell activation. *J. Exp. Med.* **195**, 461–472.

Lanzavecchia, A. (1985). Antigen-specific interaction between T and B cells. *Nature* **314**, 537–539.

Lanzavecchia, A. (1990). Receptor-mediated antigen uptake and its effect on antigen presentation to class II-restricted T lymphocytes. *Annu. Rev. Immunol.* **8**, 773–793.

Le Floc'H, A. and Huse, M. (2015). Molecular mechanisms and functional implications of polarized actin remodeling at the T cell immunological synapse. *Cell. Mol. Life Sci.* **72**, 537–556.

Lee, H., Flynn, R., Sharma, I., Haberman, E., Carling, P. J., Nicholls, F. J., Stegmann, M., Vowles, J., Haenseler, W., Wade-Martins, R., et al. (2020). LRRK2 Is Recruited to Phagosomes and Co-recruits RAB8 and RAB10 in Human Pluripotent Stem Cell-Derived Macrophages. *Stem Cell Reports* **14**, 940–955.

Lentz, V. M. and Manser, T. (2001). Cutting Edge: Germinal Centers Can Be Induced in the Absence of T Cells. *J. Immunol.* **167**, 15–20.

Leung, K. F., Baron, R. and Seabra, M. C. (2006). Geranylgeranylation of Rab GTPases. *J. Lipid Res.* **47**, 467–475.

Li, G. and Marlin, M. C. (2015). Rab family of GTpases. *Methods Mol. Biol.* **1298**, 1–15.

Li, P., Bademosi, A. T., Luo, J. and Meunier, F. A. (2018). Actin Remodeling in Regulated Exocytosis: Toward a Mesoscopic View. *Trends Cell Biol.* **28**, 685–697.

Li, J., Yin, W., Jing, Y., Kang, D., Yang, L., Cheng, J., Yu, Z., Peng, Z., Li, X., Wen, Y., et al. (2019). The coordination between B cell receptor signaling and the actin cytoskeleton during B cell activation. *Front. Immunol.* **10**, 3096.

Lian, H., Jiang, K., Tong, M., Chen, Z., Liu, X., Galán, J. E. and Gao, X. (2021). The Salmonella effector protein SopD targets Rab8 to positively and negatively modulate the inflammatory response. *Nat. Microbiol.* **6**, 658–671.

Limon, J. J., So, L., Jellbauer, S., Chiu, H., Corado, J., Sykes, S. M., Raffatellu, M. and Fruman, D. A. (2014). MTOR kinase inhibitors promote antibody class switching via mTORC2 inhibition. *Proc. Natl. Acad. Sci. U. S. A.* **111**, E5076–E5085.

Lindner, R. and Unanue, E. R. (1996). Distinct antigen MHC class II complexes generated by separate processing pathways. *EMBO J.* **15**, 6910–6920.

Liu, H. and Johnston, A. P. R. (2013). A programmable sensor to probe the internalization of proteins and nanoparticles in live cells. *Angew. Chemie - Int. Ed.* **52**, 5744–5748.

Liu, Y. J., Joshua, D. E., Williams, G. T., Smith, C. A., Gordon, J. and MacLennan, I. C. M. (1989). Mechanism of antigen-driven selection in germinal centres. *Nature* **342**, 929–931.

Liu, H., Rhodes, M., Wiest, D. L. and Vignali, D. A. A. (2000). On the dynamics of TCR:CD3 complex cell surface expression and downmodulation. *Immunity* **13**, 665–675.

Liu, H., Dumont, C., Johnston, A. P. R. and Mintern, J. D. (2016a). Analysis of intracellular trafficking of dendritic cell receptors for antigen targeting. *Methods Mol. Biol.* **1423**, 199–209.

Liu, H., Jain, R., Guan, J., Vuong, V., Ishido, S., La Gruta, N. L., Gray, D. H., Villadangos, J. A. and Mintern, J. D. (2016b). Ubiquitin ligase MAR CH 8 cooperates with CD83 to control surface MHC II expression in thymic epithelium and CD4 T cell selection. *J. Exp. Med.* **213**, 1695–1703.

Lu, Q. and Westlake, C. J. (2021). CLEM Characterization of Rab8 and Associated Membrane Trafficking Regulators at Primary Cilium Structures. In *Methods in Molecular Biology*, pp. 91–103. Methods Mol Biol.

Luo, L., Wall, A. A., Yeo, J. C., Condon, N. D., Norwood, S. J., Schoenwaelder, S., Chen, K. W., Jackson, S., Jenkins, B. J., Hartland, E. L., et al. (2014). Rab8a interacts directly with PI3Kγ to modulate TLR4-driven PI3K and mTOR signalling. *Nat. Commun.* **5**, 1–13.

Luo, L., Wall, A. A., Tong, S. J., Hung, Y., Xiao, Z., Tarique, A. A., Sly, P. D., Fantino, E., Marzolo, M. P. and Stow, J. L. (2018). TLR Crosstalk Activates LRP1 to Recruit Rab8a and PI3Kγ for Suppression of Inflammatory Responses. *Cell Rep.* **24**, 3033–3044.

Ma, H., Yankee, T. M., Hu, J., Asai, D. J., Harrison, M. L. and Geahlen, R. L. (2001). Visualization of Syk-Antigen Receptor Interactions Using Green Fluorescent Protein: Differential Roles for Syk and Lyn in the Regulation of Receptor Capping and Internalization. *J. Immunol.* **166**, 1507–1516.

Malhotra, S., Kovats, S., Zhang, W. and Coggeshall, K. M. (2009). B cell antigen receptor endocytosis and antigen presentation to T cells require Vav and dynamin. *J. Biol. Chem.* **284**, 24088–24097.

Malinova, D., Wasim, L., Newman, R., Martínez-Riaño, A., Engels, N. and Tolar, P. (2021). Endophilin A2 regulates B-cell endocytosis and is required for germinal center and humoral responses. *EMBO Rep.* **22**, e51328.

Mandel, M. A. (1980). Establishment and characterization of BALB/c lymphoma lines with B cell properties. *Plast. Reconstr. Surg.* **66**, 812.

Mañes, S., Del Real, G. and Martínez-A, C. (2003). Pathogens: raft hijackers. *Nat. Rev. Immunol.* **3**, 557–568.

Mann, S. K., Czuba, E., Selby, L. I., Such, G. K. and Johnston, A. P. R. (2016). Quantifying Nanoparticle Internalization Using a High Throughput Internalization Assay. *Pharm. Res.* **33**, 2421–2432.

Margiotta, A., Frei, D. M., Sendstad, I. H., Janssen, L., Neefjes, J. and Bakke, O. (2021). Invariant chain regulates endosomal fusion and maturation through an interaction with the SNARE Vti1b. *J. Cell Sci.* **133**,.

Martin, W. D., Hicks, G. G., Mendiratta, S. K., Leva, H. I., Ruley, H. E. and Van Kaer, L. (1996). H2-M mutant mice are defective in the peptide loading of class II molecules, antigen presentation, and T cell repertoire selection. *Cell* **84**, 543–550.

Martinez-Martin, N., Maldonado, P., Gasparrini, F., Frederico, B., Aggarwal, S., Gaya, M., Tsui, C., Burbage, M., Keppler, S. J., Montaner, B., et al. (2017). A switch from canonical to noncanonical autophagy shapes B cell responses. *Science (80-.).* **355**, 641–647.

Mattila, P. K., Feest, C., Depoil, D., Treanor, B., Montaner, B., Otipoby, K. L., Carter, R., Justement, L. B., Bruckbauer, A. and Batista, F. D. (2013). The Actin and Tetraspanin Networks Organize Receptor Nanoclusters to Regulate B Cell Receptor-Mediated Signaling. *Immunity* **38**, 461–474.

McHeyzer-Williams, M. G., McLean, M. J., Lalor, P. A. and Nossal, G. J. V. (1993). Antigen-driven B cell differentiation in vivo. *J. Exp. Med.* **178**, 295–307.

McMahon, H. T. and Boucrot, E. (2011). Molecular mechanism and physiological functions of clathrin-mediated endocytosis. *Nat. Rev. Mol. Cell Biol.* **12**, 517–533.

Ménasché, G., Pastural, E., Feldmann, J., Certain, S., Ersoy, F., Dupuis, S., Wulffraat, N., Bianchi, D., Fischer, A., Le Deist, F., et al. (2000). Mutations in RAB27A cause Griscelli syndrome associated with haemophagocytic syndrome. *Nat. Genet.* **25**, 173–176.

Mettlen, M., Chen, P. H., Srinivasan, S., Danuser, G. and Schmid, S. L. (2018). Regulation of Clathrin-Mediated Endocytosis. *Annu. Rev. Biochem.* **87**, 871–896.

Mili, S., Moissoglu, K. and Macara, I. G. (2008). Genome-wide screen reveals APC-associated RNAs enriched in cell protrusions. *Nature* **453**, 115–119.

Miller, J. F. and Mitchell, G. F. (1968). Cell to cell interaction in the immune response. I. Hemolysin-forming cells in neonatally thymectomized mice reconstituted with thymus or thoracic duct lymphocytes. *J. Exp. Med.* **128**, 801–820.

Mitchell, G. F. and Miller, J. F. (1968). Cell to cell interaction in the immune response. II. The source of hemolysin-forming cells in irradiated mice given bone marrow and thymus or thoracic duct lymphocytes. *J. Exp. Med.* **128**, 821–837.

Mitra, S., Cheng, K. W. and Mills, G. B. (2011). Rab GTPases implicated in inherited and acquired disorders. *Semin. Cell Dev. Biol.* **22**, 57–68.

Mizuno-Yamasaki, E., Rivera-Molina, F. and Novick, P. (2012). GTPase networks in membrane traffic. *Annu. Rev. Biochem.* **81**, 637–659.

Mizushima, N. and Komatsu, M. (2011). Autophagy: renovation of cells and tissues. *Cell* **147**, 728–741.

Moehle, M. S., Webber, P. J., Tse, T., Sukar, N., Standaert, D. G., Desilva, T. M., Cowell, R. M. and West, A. B. (2012). LRRK2 inhibition attenuates microglial inflammatory responses. *J. Neurosci.* **32**, 1602–1611.

Mond, J. J., Vos, Q., Lees, A. and Snapper, C. M. (1995a). T cell independent antigens. *Curr. Opin. Immunol.* **7**, 349–354.

Mond, J. J., Lees, A. and Snapper, C. M. (1995b). T cell-independent antigens type 2. *Annu. Rev. Immunol.* **13**, 655–692.

Monks, C. R. F., Freiberg, B. A., Kupfer, H., Sciaky, N. and Kupfer, A. (1998). Three-dimensional segregation of supramolecular activation clusters in T cells. *Nature* **395**, 82–86.

Moretta, A., Marcenaro, E., Parolini, S., Ferlazzo, G. and Moretta, L. (2007). NK cells at the interface between innate and adaptive immunity. *Cell Death Differ. 2008 152* **15**, 226–233.

Mosyak, L., Zaller, D. M. and Wiley, D. C. (1998). The structure of HLA-DM, the peptide exchange catalyst that loads antigen onto class II MHC molecules during antigen presentation. *Immunity* **9**, 377–383.

Nagabhushana, A., Chalasani, M. L., Jain, N., Radha, V., Rangaraj, N., Balasubramanian, D. and Swarup, G. (2010). Regulation of endocytic trafficking of transferrin receptor by optineurin and its impairment by a glaucoma-associated mutant. *BMC Cell Biol.* **11**,.

Nakayama, M. (2015). Antigen Presentation by MHC-Dressed Cells. *Front. Immunol.* **5**,.

Natkanski, E., Lee, W. Y., Mistry, B., Casal, A., Molloy, J. E. and Tolar, P. (2013). B cells use mechanical energy to discriminate antigen affinities. *Science (80-.).* **340**, 1587–1590.

Neefjes, J. J. and Ploegh, H. L. (1992). Inhibition of endosomal proteolytic activity by leupeptin blocks surface expression of MHC Class II molecules and their conversion to SDS resistant αβ heterodimers in endosomes. *EMBO J.* **11**, 411–416.

Neefjes, J. J., Stollorz, V., Peters, P. J., Geuze, H. J. and Ploegh, H. L. (1990). The biosynthetic pathway of MHC class II but not class I molecules intersects the endocytic route. *Cell* **61**, 171–183.

Netea, M. G., Quintin, J. and Van Der Meer, J. W. M. (2011). Trained immunity: A memory for innate host defense. *Cell Host Microbe* **9**, 355–361.

Nicholson, L. B. (2016). The immune system. *Essays Biochem.* **60**, 275–301.

Nielsen, C. T., Østergaard, O., Stener, L., Iversen, L. V., Truedsson, L., Gullstrand, B., Jacobsen, S. and Heegaard, N. H. H. (2012). Increased IgG on cell-derived plasma microparticles in systemic lupus erythematosus is associated with autoantibodies and complement activation. *Arthritis Rheum.* **64**, 1227–1236.

Nimmo, E. R., Sanders, P. G., Padua, R. A., Hughes, D., Williamson, R. and Johnson, K. J. (1991). The MEL gene: A new member of the RAB/YPT class of RAS-related genes. *Oncogene* **6**, 1347–1351.

Nishikimi, A., Ishihara, S., Ozawa, M., Etoh, K., Fukuda, M., Kinashi, T. and Katagiri, K. (2014). Rab13 acts downstream of the kinase Mst1 to deliver the integrin LFA-1 to the cell surface for lymphocyte trafficking. *Sci. Signal.* **7**,.

Nottingham, R. M. and Pfeffer, S. R. (2009). Defining the boundaries: Rab GEFs and GAPs. *Proc. Natl. Acad. Sci. U. S. A.* **106**, 14185–14186.

Nowosad, C. R. and Tolar, P. (2017). Plasma membrane sheets for studies of B cell antigen internalization from immune synapses. In *Methods in Molecular Biology*, pp. 77–88. Humana Press, New York, NY.

Nowosad, C. R., Spillane, K. M. and Tolar, P. (2016). Germinal center B cells recognize antigen through a specialized immune synapse architecture. *Nat. Immunol.* **17**, 870–877.

Nutt, S. L., Hodgkin, P. D., Tarlinton, D. M. and Corcoran, L. M. (2015). The generation of antibody-secreting plasma cells. *Nat. Rev. Immunol.* **15**, 160–171.

Obukhanych, T. V. and Nussenzweig, M. C. (2006). T-independent type II immune responses generate memory B cells. *J. Exp. Med.* **203**, 305–310.

Ohira, M., Oshitani, N., Hosomi, S., Watanabe, K., Yamagami, H., Tominaga, K., Watanabe, T., Fujiwara, Y., Maeda, K., Hirakawa, K., et al. (2009). Dislocation of Rab13 and vasodilator-stimulated phosphoprotein in inactive colon epithelium in patients with Crohn's disease. *Int. J. Mol. Med.* **24**, 829–835.

Okada, T., Maeda, A., Iwamatsu, A., Gotoh, K. and Kurosaki, T. (2000). BCAP: The tyrosine kinase substrate that connects B cell receptor to phosphoinositide 3-kinase activation. *Immunity* **13**, 817–827.

Omori, S. A., Cato, M. H., Anzelon-Mills, A., Puri, K. D., Shapiro-Shelef, M., Calame, K. and Rickert, R. C. (2006). Regulation of class-switch recombination and plasma cell differentiation by phosphatidylinositol 3-kinase signaling. *Immunity* **25**, 545–557.

Onnis, A., Finetti, F., Patrussi, L., Gottardo, M., Cassioli, C., Spanò, S. and Baldari, C. T. (2015). The small GTPase Rab29 is a common regulator of immune synapse assembly and ciliogenesis. *Cell Death Differ.* **22**, 1687–1699.

Onnis, A., Finetti, F. and Baldari, C. T. (2016). Vesicular trafficking to the immune synapse: How to assemble receptor-tailored pathways from a basic building set. *Front. Immunol.* **7**, 50.

Ostrowski, M., Carmo, N. B., Krumeich, S., Fanget, I., Raposo, G., Savina, A., Moita, C. F., Schauer, K., Hume, A. N., Freitas, R. P., et al. (2010). Rab27a and Rab27b control different steps of the exosome secretion pathway. *Nat. Cell Biol.* **12**, 19–30.

Packard, T. A. and Cambier, J. C. (2013). B lymphocyte antigen receptor signaling: Initiation, amplification, and regulation. *F1000Prime Rep.* **5**,.

Paludan, C., Schmid, D., Landthaler, M., Vockerodt, M., Kube, D., Tuschl, T. and Münz, C. (2005). Endogenous MHC class II processing of a viral nuclear antigen after autophagy. *Science (80-.).* **307**, 593–596.

Paludan, S. R., Pradeu, T., Masters, S. L. and Mogensen, T. H. (2020). Constitutive immune mechanisms: mediators of host defence and immune regulation. *Nat. Rev. Immunol. 2020 213* **21**, 137–150.

Pape, K. A., Kouskoff, V., Nemazee, D., Tang, H. L., Cyster, J. G., Tze, L. E., Hippen, K. L., Behrens, T. W. and Jenkins, M. K. (2003). Visualization of the genesis and fate of isotype-switched B cells during a primary immune response. *J. Exp. Med.* **197**, 1677–1687.

Pape, K. A., Catron, D. M., Itano, A. A. and Jenkins, M. K. (2007). The Humoral Immune Response Is Initiated in Lymph Nodes by B Cells that Acquire Soluble Antigen Directly in the Follicles. *Immunity* **26**, 491–502.

Patino-Lopez, G., Dong, X., Ben-Aissa, K., Bernot, K. M., Itoh, T., Fukuda, M., Kruhlak, M. J., Samelson, L. E. and Shaw, S. (2008). Rab35 and its GAP EPI64C in T cells regulate receptor recycling and immunological synapse formation. *J. Biol. Chem.* **283**, 18323–18330.

Pei, G., Bronietzki, M. and Gutierrez, M. G. (2012). Immune regulation of Rab proteins expression and intracellular transport. *J. Leukoc. Biol.* **92**, 41–50.

Pengo, N., Scolari, M., Oliva, L., Milan, E., Mainoldi, F., Raimondi, A., Fagioli, C., Merlini, A., Mariani, E., Pasqualetto, E., et al. (2013). Plasma cells require autophagy for sustainable immunoglobulin production. *Nat. Immunol.* **14**, 298–305.

Peränen, J. (2011). Rab8 GTPase as a regulator of cell shape. *Cytoskeleton* **68**, 527–539.

Peränen, J., Auvinen, P., Virta, H., Wepf, R. and Simons, K. (1996). Rab8 promotes polarized membrane transport through reorganization of actin and microtubules in fibroblasts. *J. Cell Biol.* **135**, 153–167.

Peters, P. J., Neefjes, J. J., Oorschot, V., Ploegh, H. L. and Geuze, H. J. (1991). Segregation of MHC class II molecules from MHC class I molecules in the Golgi complex for transport to lysosomal compartments. *Nature* **349**, 669–676.

Phan, T. G., Grigorova, I., Okada, T. and Cyster, J. G. (2007). Subcapsular encounter and complement-dependent transport of immune complexes by lymph node B cells. *Nat. Immunol.* **8**, 992–1000.

Pieper, K., Grimbacher, B. and Eibel, H. (2013). B-cell biology and development. *J. Allergy Clin. Immunol.* **131**, 959–971.

Pinet, V. M. and Long, E. O. (1998). Peptide loading onto recycling HLA-DR molecules occurs in early endosomes. *Eur. J. Immunol.* **28**, 799–804.

Pinet, V., Vergelli, M., Martini, R., Bakke, O. and Long, E. O. (1995). Antigen presentation mediated by recycling of surface HLA-DR molecules. *Nature* **375**, 603–606.

Pleiner, T., Bates, M., Trakhanov, S., Lee, C. T., Schliep, J. E., Chug, H., Böhning, M., Stark, H., Urlaub, H. and Görlich, D. (2015). Nanobodies: Site-specific labeling for super-resolution imaging, rapid epitope- mapping and native protein complex isolation. *Elife* **4**,.

Plotz, P. H. (2003). The autoantibody repertoire: Searching for order. *Nat. Rev. Immunol.* **3**, 73–78.

Pollard, A. J. and Bijker, E. M. (2020). A guide to vaccinology: from basic principles to new developments. *Nat. Rev. Immunol. 2020 212* **21**, 83–100.

Pond, L. and Watts, C. (1999). Functional early endosomes are required for maturation of major histocompatibility complex class II molecules in human B lymphoblastoid cells. *J. Biol. Chem.* **274**, 18049–18054.

Pone, E. J., Lam, T., Lou, Z., Wang, R., Chen, Y., Liu, D., Edinger, A. L., Xu, Z. and Casali, P. (2015). B Cell Rab7 Mediates Induction of Activation-Induced Cytidine Deaminase Expression and Class-Switching in T-Dependent and T-Independent Antibody Responses. *J. Immunol.* **194**, 3065–3078.

Porter, J. F., Vavassori, S. and Covey, L. R. (2008). A Polypyrimidine Tract-Binding Protein-Dependent Pathway of mRNA Stability Initiates with CpG Activation of Primary B Cells. *J. Immunol.* **181**, 3336–3345.

Prashar, A., Schnettger, L., Bernard, E. M. and Gutierrez, M. G. (2017). Rab GTPases in immunity and inflammation. *Front. Cell. Infect. Microbiol.* **7**, 435.

Qiu, Y., Xu, X., Wandinger-Ness, A., Dalke, D. P. and Pierce, S. K. (1994). Separation of subcellular compartments containing distinct functional forms of MHC class II. *J. Cell Biol.* **125**, 595–605.

Raposo, G., Marks, M. S. and Cutler, D. F. (2007). Lysosome-related organelles: driving post-Golgi compartments into specialisation. *Curr. Opin. Cell Biol.* **19**, 394–401.

Ratajczak, W., Niedźwiedzka-Rystwej, P., Tokarz-Deptuła, B. and DeptuŁa, W. (2018). Immunological memory cells. *Cent. J. Immunol.* **43**, 194.

Recchi, C. and Seabra, M. C. (2012). Novel functions for Rab GTPases in multiple aspects of tumour progression. In *Biochemical Society Transactions*, pp. 1398–1403. Biochem Soc Trans.

Redpath, G. M. I., Betzler, V. M., Rossatti, P. and Rossy, J. (2020). Membrane Heterogeneity Controls Cellular Endocytic Trafficking. *Front. cell Dev. Biol.* **8**,.

Reid, P. A. and Watts, C. (1992). Constitutive endocytosis and recycling of major histocompatibility complex class II glycoproteins in human B-lymphoblastoid cells. *Immunology* **77**, 539–42.

Reth, M. (1989). Antigen receptor tail clue. *Nature* **338**, 383–384.

Reth, M. and Wienands, J. (1997). Initiation and processing of signals from the B cell antigen receptor. *Annu. Rev. Immunol.* **15**, 453–479.

Revelo, N. H., Ter Beest, M. and van den Bogaart, G. (2019). Membrane trafficking as an active regulator of constitutively secreted cytokines. *J. Cell Sci.* **133**,.

Rickert, R. C., Roes, J. and Rajewsky, K. (1997). B lymphocyte-specific, Cre-mediated mutagenesis in mice. *Nucleic Acids Res.* **25**, 1317–1318.

Riese, R. J. and Chapman, H. A. (2000). Cathepsins and compartmentalization in antigen presentation. *Curr. Opin. Immunol.* **12**, 107–113.

Robbins, P. D. and Morelli, A. E. (2014). Regulation of immune responses by extracellular vesicles. *Nat. Rev. Immunol.* **14**, 195–208.

Roberts, A. D., Davenport, T. M., Dickey, A. M., Ahn, R., Sochacki, K. A. and Taraska, J. W. (2020). Structurally distinct endocytic pathways for B cell receptors in B lymphocytes. *Mol. Biol. Cell* **31**, 2826–2840.

Roche, P. A. and Cresswell, P. (1990). Invariant chain association with HLA-DR molecules inhibits immunogenic peptide binding. *Nature* **345**, 615–618.

Roche, P. A. and Furuta, K. (2015). The ins and outs of MHC class II-mediated antigen processing and presentation. *Nat. Rev. Immunol.* **15**, 203–216.

Roche, P. A., Teletski, C. L., Stang, E., Bakke, O. and Long, E. O. (1993). Cell surface HLA-DR-invariant chain complexes are targeted to endosomes by rapid internalization. *Proc. Natl. Acad. Sci. U. S. A.* **90**, 8581–8585.

Roco, J. A., Mesin, L., Binder, S. C., Nefzger, C., Gonzalez-Figueroa, P., Canete, P. F., Ellyard, J., Shen, Q., Robert, P. A., Cappello, J., et al. (2019). Class-Switch Recombination Occurs Infrequently in Germinal Centers. *Immunity* **51**, 337-350.e7.

Roozendaal, R., Mempel, T. R., Pitcher, L. A., Gonzalez, S. F., Verschoor, A., Mebius, R. E., von Andrian, U. H. and Carroll, M. C. (2009). Conduits Mediate Transport of Low-Molecular-Weight Antigen to Lymph Node Follicles. *Immunity* **30**, 264–276.

Rowland, S. L., DePersis, C. L., Torres, R. M. and Pelanda, R. (2010). Ras activation of Erk restores impaired tonic BCR signaling and rescues immature B cell differentiation. *J. Exp. Med.* **207**, 607–621.

Russell, D. M., Dembić, Z., Morahan, G., Miller, J. F. A. P., BÜrki, K. and Nemazee, D. (1991). Peripheral deletion of self-reactive B cells. *Nature* **354**, 308–311.

Sáenz-Cuesta, M., Osorio-Querejeta, I. and Otaegui, D. (2014). Extracellular vesicles in multiple sclerosis: What are they telling us? *Front. Cell. Neurosci.* **8**, 100.

Sahl, S. J., Hell, S. W. and Jakobs, S. (2017). Fluorescence nanoscopy in cell biology. *Nat. Rev. Mol. Cell Biol.* **18**, 685–701.

Saito, K., Tolias, K. F., Saci, A., Koon, H. B., Humphries, L. A., Scharenberg, A., Rawlings, D. J., Kinet, J. P. and Carpenter, C. L. (2003). BTK regulates PtdIns-4,5-P2 synthesis: Importance for calcium signaling and PI3K activity. *Immunity* **19**, 669–677.

Salisbury, J. L., Condeelis, J. S. and Satir, P. (1980). Role of coated vesicles, microfilaments, and calmodulin in receptor-mediated endocytosis by cultured B lymphoblastoid cells. *J. Cell Biol.* **87**, 132–141.

Salminen, A. and Novick, P. J. (1987). A ras-like protein is required for a post-Golgi event in yeast secretion. *Cell* **49**, 527–538.

Sanchez, M., Misulovin, Z., Burkhardt, A. L., Mahajan, S., Costa, T., Franke, R., Bolen, J. B. and Nussenzweig, M. (1993). Signal transduction by immunoglobulin is mediated through Igα and Igβ. *J. Exp. Med.* **178**, 1049–1055.

Sarapulov, A. V., Petrov, P., Hernández-Pérez, S., Šuštar, V., Kuokkanen, E., Cords, L., Samuel, R. V. M., Vainio, M., Fritzsche, M., Carrasco, Y. R., et al. (2020). Missing-in-Metastasis/Metastasis Suppressor 1 Regulates B Cell Receptor Signaling, B Cell Metabolic Potential, and T Cell-Independent Immune Responses. *Front. Immunol.* **11**, 599.

Sato, T., Mushiake, S., Kato, Y., Sato, K., Sato, M., Takeda, N., Ozono, K., Miki, K., Kubo, Y., Tsuji, A., et al. (2007). The Rab8 GTPase regulates apical protein localization in intestinal cells. *Nature* **448**, 366–369.

Sato, T., Iwano, T., Kunii, M., Matsuda, S., Mizuguchi, R., Jung, Y., Hagiwara, H., Yoshihara, Y., Yuzaki, M., Harada, R., et al. (2014). Rab8a and Rab8b are essential for several apical transport pathways but insufficient for ciliogenesis. *J. Cell Sci.* **127**, 422–431.

Savitskiy, S. and Itzen, A. (2021). SopD from Salmonella specifically inactivates Rab8. *Biochim. Biophys. Acta - Proteins Proteomics* **1869**, 140661.

Schamel, W. W. A. and Reth, M. (2000). Monomeric and oligomeric complexes of the B cell antigen receptor. *Immunity* **13**, 5–14.

Schmid, D., Pypaert, M. and Münz, C. (2007). Antigen-Loading Compartments for Major Histocompatibility Complex Class II Molecules Continuously Receive Input from Autophagosomes. *Immunity* **26**, 79–92.

Schmitt, H. D., Wagner, P., Pfaff, E. and Gallwitz, D. (1986). The ras-related YPT1 gene product in yeast: A GTP-binding protein that might be involved in microtubule organization. *Cell* **47**, 401–412.

Scita, G. and Di Fiore, P. P. (2010). The endocytic matrix. *Nature* **463**, 464–473.

Segev, N., Mulholland, J. and Botstein, D. (1988). The yeast GTP-binding YPT1 protein and a mammalian counterpart are associated with the secretion machinery. *Cell* **52**, 915–924.

Sellam, J., Proulle, V., Jüngel, A., Ittah, M., Miceli Richard, C., Gottenberg, J. E., Toti, F., Benessiano, J., Gay, S., Freyssinet, J. M., et al. (2009). Increased levels of circulating microparticles in primary Sjögren's syndrome, systemic lupus erythematosus and rheumatoid arthritis and relation with disease activity. *Arthritis Res. Ther.* **11**,.

Sharma, S., Orlowski, G. and Song, W. (2009). Btk Regulates B Cell Receptor-Mediated Antigen Processing and Presentation by Controlling Actin Cytoskeleton Dynamics in B Cells. *J. Immunol.* **182**, 329–339.

Shaw, A. S. and Dustin, M. L. (1997). Making the T cell receptor go the distance: A topological view of T cell activation. *Immunity* **6**, 361–369.

Shen, F. and Seabra, M. C. (1996). Mechanism of digeranylgeranylation of rab proteins: Formation of a complex between Monogeranylgeranyl-Rab and Rab escort protein. *J. Biol. Chem.* **271**, 3692–3698.

Shinde, S. R. and Maddika, S. (2018). Post translational modifications of Rab GTPases. *Small GTPases* **9**, 49–56.

Siegers, G. M., Yang, J., Duerr, C. U., Nielsen, P. J., Reth, M. and Schamel, W. W. A. (2006). Identification of disulfide bonds in the Ig-α/Ig-β component of the B cell antigen receptor using the Drosophila S2 cell reconstitution system. *Int. Immunol.* **18**, 1385–1396.

Siemasko, K., Eisfelder, B. J., Williamson, E., Kabak, S. and Clark, M. R. (1998). Cutting edge: signals from the B lymphocyte antigen receptor regulate MHC class II containing late endosomes. *J. Immunol.* **160**, 5203–8.

Siemasko, K., Eisfelder, B. J., Stebbins, C., Kabak, S., Sant, A. J., Song, W. and Clark, M. R. (1999). Ig alpha and Ig beta are required for efficient trafficking to late endosomes and to enhance antigen presentation. *J. Immunol.* **162**, 6518–25.

Siemasko, K., Skaggs, B. J., Kabak, S., Williamson, E., Brown, B. K., Song, W. and Clark, M. R. (2002). Receptor-Facilitated Antigen Presentation Requires the Recruitment of B Cell Linker Protein to Igα. *J. Immunol.* **168**, 2127–2138.

Silmon De Monerri, N. C. and Kim, K. (2014). Pathogens Hijack the Epigenome: A New Twist on Host-Pathogen Interactions. *Am. J. Pathol.* **184**, 897–911.

Simitsek, P. D., Campbell, D. G., Lanzavecchia, A., Fairweather, N. and Watts, C. (1995). Modulation of antigen processing by bound antibodies can boost or suppress class II major histocompatibility complex presentation of different T cell determinants. *J. Exp. Med.* **181**, 1957–1963.

Sloan, V. S., Cameron, P., Porter, G., Gammon, M., Amaya, M. and Zaller, D. M. (1995). Mediation by HLA-DM of dissociation of peptides from HLA-DR. *Nature* **375**, 802–806.

Soares, H., Henriques, R., Sachse, M., Ventimiglia, L., Alonso, M. A., Zimmer, C., Thoulouze, M. I. and Alcover, A. (2013). Regulated vesicle fusion generates signaling nanoterritories that control T cell activation at the immunological synapse. *J. Exp. Med.* **210**, 2415–2433.

Song, W., Cho, H., Cheng, P. and Pierce, S. K. (1995). Entry of B cell antigen receptor and antigen into class II peptide-loading compartment is independent of receptor cross-linking. *J. Immunol.* **155**, 4255–63.

Sönnichsen, B., De Renzis, S., Nielsen, E., Rietdorf, J. and Zerial, M. (2000). Distinct membrane domains on endosomes in the recycling pathway visualized by multicolor imaging of Rab4, Rab5, and Rab11. *J. Cell Biol.* **149**, 901–913.

Sorkin, A. and Von Zastrow, M. (2009). Endocytosis and signalling: intertwining molecular networks. *Nat. Rev. Mol. Cell Biol.* **10**, 609–622.

Spanò, S. and Galán, J. E. (2018). Taking control: Hijacking of Rab GTPases by intracellular bacterial pathogens. *Small GTPases* **9**, 182–191.

Spillane, K. M. and Tolar, P. (2017). B cell antigen extraction is regulated by physical properties of antigen-presenting cells. *J. Cell Biol.* **216**, 217–230.

Spillane, K. M. and Tolar, P. (2018). Mechanics of antigen extraction in the B cell synapse. *Mol. Immunol.* **101**, 319–328.

Spinosa, M. R., Progida, C., De Luca, A., Colucci, A. M. R., Alifano, P. and Bucci, C. (2008). Functional characterization of Rab7 mutant proteins associated with Charcot-Marie-Tooth type 2B disease. *J. Neurosci.* **28**, 1640–1648.

Sprent, J. (1995). Antigen-Presenting Cells: Professionals and amateurs. *Curr. Biol.* **5**, 1095–1097.

Srikanth, S., Woo, J. S. and Gwack, Y. (2017). A large Rab GTPase family in a small GTPase world. *Small GTPases* **8**, 43–48.

Stavnezer, J., Guikema, J. E. J. and Schrader, C. E. (2008). Mechanism and regulation of class switch recombination. *Annu. Rev. Immunol.* **26**, 261–292.

Stefan, C. J., Trimble, W. S., Grinstein, S., Drin, G., Reinisch, K., De Camilli, P., Cohen, S., Valm, A. M., Lippincott-Schwartz, J., Levine, T. P., et al. (2017). Membrane dynamics and organelle biogenesis-lipid pipelines and vesicular carriers. *BMC Biol.* **15**, 1–24.

Steger, M., Tonelli, F., Ito, G., Davies, P., Trost, M., Vetter, M., Wachter, S., Lorentzen, E., Duddy, G., Wilson, S., et al. (2016). Phosphoproteomics reveals that Parkinson's disease kinase LRRK2 regulates a subset of Rab GTPases. *Elife* **5**,.

Steger, M., Diez, F., Dhekne, H. S., Lis, P., Nirujogi, R. S., Karayel, O., Tonelli, F., Martinez, T. N., Lorentzen, E., Pfeffer, S. R., et al. (2017). Systematic proteomic analysis of LRRK2-mediated rab GTPase phosphorylation establishes a connection to ciliogenesis. *Elife* **6**,.

Stenmark, H. (2009). Rab GTPases as coordinators of vesicle traffic. *Nat. Rev. Mol. Cell Biol.* **10**, 513–525.

Stenmark, H. and Olkkonen, V. M. (2001). The Rab GTPase family. *Genome Biol.* **2**, reviews3007.1.

Stinchcombe, J. C., Barral, D. C., Mules, E. H., Booth, S., Hume, A. N., Machesky, L. M., Seabra, M. C. and Griffiths, G. M. (2001). Rab27a is required for regulated secretion in cytotoxic T lymphocytes. *J. Cell Biol.* **152**, 825–833.

Stoddart, A., Dykstra, M. L., Brown, B. K., Song, W., Pierce, S. K. and Brodsky, F. M. (2002). Lipid rafts unite signaling cascades with clathrin to regulate BCR internalization. *Immunity* **17**, 451–462.

Stoddart, A., Jackson, A. P. and Brodsky, F. M. (2005). Plasticity of B cell receptor internalization upon conditional depletion of clathrin. *Mol. Biol. Cell* **16**, 2339–2348.

Stögerer, T. and Stäger, S. (2020). Innate Immune Sensing by Cells of the Adaptive Immune System. *Front. Immunol.* **11**,.

Stylianou, K., Petrakis, I., Mavroeidi, V., Stratakis, S., Vardaki, E., Perakis, K., Stratigis, S., Passam, A., Papadogiorgaki, E., Giannakakis, K., et al. (2011). The PI3K/Akt/mTOR pathway is activated in murine lupus nephritis and downregulated by rapamycin. *Nephrol. Dial. Transplant.* **26**, 498–508.

Šuštar, V., Vainio, M. and Mattila, P. K. (2018). Visualization and quantitative analysis of the actin cytoskeleton upon B cell activation. In *Methods in Molecular Biology*, pp. 243–257. Humana Press Inc.

Suzuki, K., Grigorova, I., Phan, T. G., Kelly, L. M. and Cyster, J. G. (2009). Visualizing B cell capture of cognate antigen from follicular dendritic cells. *J. Exp. Med.* **206**, 1485–1493.

Takahashi, Y., Dutta, P. R., Cerasoli, D. M. and Kelsoe, G. (1998). In situ studies of the primary immune response to (4-hydroxy-3- nitrophenyl)acetyl. v. affinity maturation develops in two stages of clonal selection. *J. Exp. Med.* **187**, 885–895.

Takemori, T., Tarlinton, D., Hiepe, F. and Andreas, R. (2015). B Cell Memory and Plasma Cell Development. *Mol. Biol. B Cells Second Ed.* 227–249.

Tanaka, S. and Baba, Y. (2020). B Cell Receptor Signaling. In *Advances in Experimental Medicine and Biology*, pp. 23–36. Springer, Singapore.

Tarlinton, D. and Good-Jacobson, K. (2013). Diversity among memory B cells: Origin, consequences, and utility. *Science (80-.).* **341**, 1205–1211.

Tellier, J. and Nutt, S. L. (2019). Plasma cells: The programming of an antibody-secreting machine. *Eur. J. Immunol.* **49**, 30–37.

Tew, J. G., Phipps, R. P. and Mandel, T. E. (1980). The Maintenance and Regulation of the Humoral Immune Response: Persisting Antigen and the Role of Follicular Antigen-Binding Dendritic Cells as Accessory Cells. *Immunol. Rev.* **53**, 175–201.

Thaunat, O., Granja, A. G., Barral, P., Filby, A., Montaner, B., Collinson, L., Martinez-Martin, N., Harwood, N. E., Bruckbauer, A. and Batista, F. D. (2012). Asymmetric segregation of polarized antigen on B cell division shapes presentation capacity. *Science (80-.).* **335**, 457–479.

Toellner, K. M., Gulbranson-Judge, A., Taylor, D. R., Sze, D. M. Y. and MacLennan, I. C. M. (1996). Immunoglobulin switch transcript production in vivo related to the site and time of antigen-specific B cell activation. *J. Exp. Med.* **183**, 2303–2312.

Tong, S. J., Wall, A. A., Hung, Y., Luo, L. and Stow, J. L. (2021). Guanine nucleotide exchange factors activate Rab8a for Toll-like receptor signalling. *Small GTPases* **12**, 27–43.

Treanor, B. (2012). B-cell receptor: From resting state to activate. *Immunology* **136**, 21–27.

Trepel, F. (1974). Number and distribution of lymphocytes in man. A critical analysis. *Klin. Wochenschr.* **52**, 511–515.

Trück, J. and van der Burg, M. (2020). Development of adaptive immune cells and receptor repertoires from infancy to adulthood. *Curr. Opin. Syst. Biol.* **24**, 51–55.

Tsui, C., Martinez-Martin, N., Gaya, M., Maldonado, P., Llorian, M., Legrave, N. M., Rossi, M., MacRae, J. I., Cameron, A. J., Parker, P. J., et al. (2018). Protein Kinase C-β Dictates B Cell Fate by Regulating Mitochondrial Remodeling, Metabolic Reprogramming, and Heme Biosynthesis. *Immunity* **48**, 1144-1159.e5.

Tsukuba, T., Yamaguchi, Y. and Kadowaki, T. (2021). Large rab gtpases: Novel membrane trafficking regulators with a calcium sensor and functional domains. *Int. J. Mol. Sci.* **22**, 7691.

Tulp, A., Verwoerd, D., Dobberstein, B., Ploegh, H. L. and Pieters, J. (1994). Isolation and characterization of the intracellular MHC class II compartment. *Nature* **369**, 120–126.

Ullal, A. J., Reich, C. F., Clowse, M., Criscione-Schreiber, L. G., Tochacek, M., Monestier, M. and Pisetsky, D. S. (2011). Microparticles as antigenic targets of antibodies to DNA and nucleosomes in systemic lupus erythematosus. *J. Autoimmun.* **36**, 173–180.

Ulloa, R., Corrales, O., Cabrera-Reyes, F., Jara-Wilde, J., Saez, J. J., Rivas, C., Lagos, J., Härtel, S., Quiroga, C., Yuseff, M. I., et al. (2022). B Cells Adapt Their Nuclear Morphology to Organize the Immune Synapse and Facilitate Antigen Extraction. *Front. Immunol.* **12**, 2021.04.20.440571.

Ullrich, O., Stenmark, H., Alexandrov, K., Huber, L. A., Kaibuchi, K., Sasaki, T., Takai, Y. and Zerial, M. (1993). Rab GDP dissociation inhibitor as a general regulator for the membrane association of rab proteins. *J. Biol. Chem.* **268**, 18143–18150.

Upasani, V., Rodenhuis-Zybert, I. and Cantaert, T. (2021). Antibody-independent functions of B cells during viral infections. *PLoS Pathog.* **17**,.

Vascotto, F., Le Roux, D., Lankar, D., Faure-André, G., Vargas, P., Guermonprez, P. and Lennon-Duménil, A. M. (2007a). Antigen presentation by B lymphocytes: how receptor signaling directs membrane trafficking. *Curr. Opin. Immunol.* **19**, 93–98.

Vascotto, F., Lankar, D., Faure-André, G., Vargas, P., Diaz, J., Le Roux, D., Yuseff, M. I., Sibarita, J. B., Boes, M., Raposo, G., et al. (2007b). The actin-based motor protein myosin II regulates MHC class II trafficking and BCR-driven antigen presentation. *J. Cell Biol.* **176**, 1007–1019.

Venkitaraman, A. R., Williams, G. T., Dariavach, P. and Neuberger, M. S. (1991). The B-cell antigen receptor of the five immunoglobulin classes. *Nature* **352**, 777–781.

Verhoeven, K., De Jonghe, P., Coen, K., Verpoorten, N., Auer-Grumbach, M., Kwon, J. M., FitzPatrick, D., Schmedding, E., De Vriendt, E., Jacobs, A., et al. (2003). Mutations in the small GTP-ase late endosomal protein RAB7 cause Charcot-Marie-Tooth type 2B neuropathy. *Am. J. Hum. Genet.* **72**, 722–727.

Vidal-Quadras, M., Holst, M. R., Francis, M. K., Larsson, E., Hachimi, M., Yau, W. L., Peränen, J., Martín-Belmonte, F. and Lundmark, R. (2017). Endocytic turnover of Rab8 controls cell polarization. *J. Cell Sci.* **130**, 1147–1157.

Vidard, L., Kovacsovics-Bankowski, M., Kraeft, S. K., Chen, L. B., Benacerraf, B. and Rock, K. L. (1996). Analysis of MHC class II presentation of particulate antigens of B lymphocytes. *J. Immunol.* **156**, 2809–18.

Vieira, P. and Rajewsky, K. (1988). The half-lives of serum immunoglobulins in adult mice. *Eur. J. Immunol.* **18**, 313–316.

Vira, S., Mekhedov, E., Humphrey, G. and Blank, P. S. (2010). Fluorescent-labeled antibodies: Balancing functionality and degree of labeling. *Anal. Biochem.* **402**, 146–150.

Viville, S., Neefjes, J., Lotteau, V., Dierich, A., Lemeur, M., Ploegh, H., Benoist, C. and Mathis, D. (1993). Mice lacking the MHC class II-associated invariant chain. *Cell* **72**, 635–648.

von Chamier, L., Laine, R. F., Jukkala, J., Spahn, C., Krentzel, D., Nehme, E., Lerche, M., Hernández-Pérez, S., Mattila, P. K., Karinou, E., et al. (2021). Democratising deep learning for microscopy with ZeroCostDL4Mic. *Nat. Commun.* **12**, 1–18.

Voss, S., Li, F., Rätz, A., Röger, M. and Wu, Y. W. (2019). Spatial Cycling of Rab GTPase, Driven by the GTPase Cycle, Controls Rab's Subcellular Distribution. *Biochemistry* **58**, 276–285.

Vyas, J. M., Van Der Veen, A. G. and Ploegh, H. L. (2008). The known unknowns of antigen processing and presentation. *Nat. Rev. Immunol.* **8**, 607–618.

Wall, A. A., Luo, L., Hung, Y., Tong, S. J., Condon, N. D., Blumenthal, A., Sweet, M. J. and Stow, J. L. (2017). Small GTPase Rab8a-recruited phosphatidylinositol 3-kinase γ regulates signaling and cytokine outputs from endosomal toll-like receptors. *J. Biol. Chem.* **292**, 4411–4422.

Wall, A. A., Condon, N. D., Luo, L. and Stow, J. L. (2019). Rab8a localisation and activation by Toll-like receptors on macrophage macropinosomes. *Philos. Trans. R. Soc. B Biol. Sci.* **374**, 20180151.

Wallings, R. L. and Tansey, M. G. (2019). LRRK2 regulation of immune-pathways and inflammatory disease. *Biochem. Soc. Trans.* **47**, 1581–1595.

Wandinger-Ness, A. and Zerial, M. (2014). Rab proteins and the compartmentalization of the endosomal system. *Cold Spring Harb. Perspect. Biol.* **6**, a022616.

Wang, Y., Huynh, W., Skokan, T. D., Lu, W., Weiss, A. and Vale, R. D. (2019). CRACR2a is a calcium-activated dynein adaptor protein that regulates endocytic traffic. *J. Cell Biol.* **218**, 1619–1633.

Wardemann, H., Yurasov, S., Schaefer, A., Young, J. W., Meffre, E. and Nussenzweig, M. C. (2003). Predominant autoantibody production by early human B cell precursors. *Science (80-.).* **301**, 1374–1377.

Watanabe, S. and Boucrot, E. (2017). Fast and ultrafast endocytosis. *Curr. Opin. Cell Biol.* **47**, 64–71.

Watanabe, K. and Tsubata, T. (2009). Autophagy connects antigen receptor signaling to costimulatory signaling in B lymphocytes. *Autophagy* **5**, 108–110.

Watts, C., West, M. A., Reid, P. A. and Davidson, H. W. (1989). Processing of immunoglobulin-associated antigen in B lymphocytes. In *Cold Spring Harbor Symposia on Quantitative Biology*, pp. 345–352. Cold Spring Harb Symp Quant Biol.

Wei, A. H. and Li, W. (2013). Hermansky–Pudlak syndrome: pigmentary and non-pigmentary defects and their pathogenesis. *Pigment Cell Melanoma Res.* **26**, 176–192.

Weigert, M., Schmidt, U., Boothe, T., Müller, A., Dibrov, A., Jain, A., Wilhelm, B., Schmidt, D., Broaddus, C., Culley, S., et al. (2018). Content-aware image restoration: pushing the limits of fluorescence microscopy. *Nat. Methods* **15**, 1090–1097.

Wennerberg, K., Rossman, K. L. and Der, C. J. (2005). The Ras superfamily at a glance. *J. Cell Sci.* **118**, 843–846.

West, M. A., Lucocq, J. M. and Watts, C. (1994). Antigen processing and class II MHC peptide-loading compartments in human B-lymphoblastoid cells. *Nature* **369**, 147–151.

Westlake, C. J., Baye, L. M., Nachury, M. V., Wright, K. J., Ervin, K. E., Phu, L., Chalouni, C., Beck, J. S., Kirkpatrick, D. S., Slusarski, D. C., et al. (2011). Primary cilia membrane assembly is initiated by Rab11 and transport protein particle II (TRAPPII) complex-dependent trafficking of Rabin8 to the centrosome. *Proc. Natl. Acad. Sci. U. S. A.* **108**, 2759–2764.

Williams, G. T., Peaker, C. J. G., Patel, K. J. and Neuberger, M. S. (1994). The α/β sheath and its cytoplasmic tyrosines are required for signaling by the B-cell antigen receptor but not for capping or for serine/threonine- kinase recruitment. *Proc. Natl. Acad. Sci. U. S. A.* **91**, 474–478.

Witoelar, A., Jansen, I. E., Wang, Y., Desikan, R. S., Gibbs, J. R., Blauwendraat, C., Thompson, W. K., Hernandez, D. G., Djurovic, S., Schork, A. J., et al. (2017). Genome-wide pleiotropy between Parkinson disease and autoimmune diseases. *JAMA Neurol.* **74**, 780–792.

Wu, L. G., Hamid, E., Shin, W. and Chiang, H. C. (2014). Exocytosis and Endocytosis: Modes, Functions, and Coupling Mechanisms*. *http://dx.doi.org/10.1146/annurev-physiol-021113-170305* **76**, 301–331.

Wykes, M., Pombo, A., Jenkins, C. and MacPherson, G. G. (1998). Dendritic cells interact directly with naive B lymphocytes to transfer antigen and initiate class switching in a primary T-dependent response. *J. Immunol.* **161**, 1313–9.

Xu, X., Press, B., Wagle, N. M., Cho, H., Wandinger-Ness, A. and Pierce, S. K. (1996). B cell antigen receptor signaling links biochemical changes in the class II peptide-loading compartment to enhanced processing. *Int. Immunol.* **8**, 1867–1876.

Xu, L., Nagai, Y., Kajihara, Y., Ito, G. and Tomita, T. (2021). The regulation of rab gtpases by phosphorylation. *Biomolecules* **11**, 1340.

Yamaguchi, Y., Sakai, E., Okamoto, K., Kajiya, H., Okabe, K., Naito, M., Kadowaki, T. and Tsukuba, T. (2018). Rab44, a novel large Rab GTPase, negatively regulates osteoclast differentiation by modulating intracellular calcium levels followed by NFATc1 activation. *Cell. Mol. Life Sci.* **75**, 33–48.

Yang, J. and Reth, M. (2010). Oligomeric organization of the B-cell antigen receptor on resting cells. *Nature* **467**, 465–469.

Yim, W. W. Y. and Mizushima, N. (2020). Lysosome biology in autophagy. *Cell Discov. 2020 61* **6**, 1–12.

Yokogawa, M., Takaishi, M., Nakajima, K., Kamijima, R., Fujimoto, C., Kataoka, S., Terada, Y. and Sano, S. (2014). Epicutaneous application of toll-like receptor 7 agonists leads to systemic autoimmunity in wild-type mice: A new model of systemic lupus erythematosus. *Arthritis Rheumatol.* **66**, 694–706.

Youd, M. E., Ferguson, A. R. and Corley, R. B. (2002). Synergistic roles of IgM and complement in antigen trapping and follicular localization. *Eur. J. Immunol.* **32**, 2328–2337.

Young, C. and Brink, R. (2021). The unique biology of germinal center B cells. *Immunity* **54**, 1652–1664.

Yuseff, M. I., Reversat, A., Lankar, D., Diaz, J., Fanget, I., Pierobon, P., Randrian, V., Larochette, N., Vascotto, F., Desdouets, C., et al. (2011). Polarized Secretion of Lysosomes at the B Cell Synapse Couples Antigen Extraction to Processing and Presentation. *Immunity* **35**, 361–374.

Yuseff, M. I., Pierobon, P., Reversat, A. and Lennon-Duménil, A. M. (2013). How B cells capture, process and present antigens: A crucial role for cell polarity. *Nat. Rev. Immunol.* **13**, 475–486.

Zerial, M. and McBride, H. (2001). Rab proteins as membrane organizers. *Nat. Rev. Mol. Cell Biol.* **2**, 107–117.

Zhang, M., Veselits, M., O'Neill, S., Hou, P., Reddi, A. L., Berlin, I., Ikeda, M., Nash, P. D., Longnecker, R., Band, H., et al. (2007). Ubiquitinylation of Igβ Dictates the Endocytic Fate of the B Cell Antigen Receptor. *J. Immunol.* **179**, 4435–4443.

Zhang, S., Readinger, J. A., DuBois, W., Janka-Junttila, M., Robinson, R., Pruitt, M., Bliskovsky, V., Wu, J. Z., Sakakibara, K., Patel, J., et al. (2011). Constitutive reductions in mTOR alter cell size, immune cell development, and antibody production. *Blood* **117**, 1228–1238.

Zhou, D., Li, P., Lin, Y., Lott, J. M., Hislop, A. D., Canaday, D. H., Brutkiewicz, R. R. and Blum, J. S. (2005). Lamp-2a facilitates MHC class II presentation of cytoplasmic antigens. *Immunity* **22**, 571–581.

Zhou, Z., Niu, H., Zheng, Y. Y. and Morel, L. (2011). Autoreactive marginal zone B cells enter the follicles and interact with CD4+T cells in lupus-prone mice. *BMC Immunol.* **12**,.

TURUN
YLIOPISTO
UNIVERSITY
OF TURKU

Painosalama, Turku, Finland 2022

ISBN 978-951-29-8921-8 (PRINT)
ISBN 978-951-29-8922-5 (PDF)
ISSN 0355-9483 (Print)
ISSN 2343-3213 (Online)